

**KINETIC MODELING OF THE HYDROTREATMENT OF LIGHT
CYCLE OIL/DIESEL**

A Dissertation

by

LUIS CARLOS CASTANEDA-LOPEZ

Submitted to the Office of Graduate Studies of
Texas A&M University
in partial fulfillment of the requirements for the degree of

DOCTOR OF PHILOSOPHY

December 2006

Major Subject: Chemical Engineering

**KINETIC MODELING OF THE HYDROTREATMENT OF LIGHT
CYCLE OIL/DIESEL**

A Dissertation

by

LUIS CARLOS CASTANEDA-LOPEZ

Submitted to the Office of Graduate Studies of
Texas A&M University
in partial fulfillment of the requirements for the degree of

DOCTOR OF PHILOSOPHY

Approved by:

Co-Chairs of Committee,	Gilbert F. Froment Rayford G. Anthony
Committee Members,	Kenneth R. Hall Abraham Clearfield
Head of Department,	N. K. Anand

December 2006

Major Subject: Chemical Engineering

ABSTRACT

Kinetic Modeling of the Hydrotreatment of Light Cycle Oil/Diesel.

(December 2006)

Luis Carlos Castaneda-Lopez, B.S., Instituto Tecnológico de Chihuahua, Mexico;

M.S. Instituto Tecnológico de Ciudad Madero, Mexico

Co-Chairs of Advisory Committee: Dr. Gilbert F. Froment
Dr. Rayford G. Anthony

A rigorous kinetic model of hydrodesulfurization (HDS) of complex mixtures such as light cycle oil (LCO) or diesel has been developed. An experimental setup was constructed to investigate the hydrotreatment of complex mixtures. The hydrodesulfurization of LCO on a commercial CoMo/Al₂O₃ (IMP) catalyst was investigated in a Robinson Mahoney perfectly mixed flow stationary basket reactor. An experimental investigation of the HDS of the dibenzothiophene (DBT) and substituted dibenzothiophenes in the LCO was carried out at temperatures between 290 and 330°C, space time for dibenzothiophene (W/F_{DBT}^0) between 1000 and 6500 kg_{cat}-h/kmol, and H₂/HC molar ratio constant of 2.8. To avoid having to deal with a huge number of parameters in the model, a methodology based on structural contributions was applied. DEN_σ and DEN_τ are the denominators of the Hougen-Watson rate expressions for hydrodesulfurization of dibenzothiophene (DBT) and methyl-substituted dibenzothiophenes contained in the LCO. Both denominators comprise the concentration

of all adsorbing species of the LCO multiplied by their adsorption equilibrium constants. The estimation of the denominators DEN_{σ} and DEN_{τ} was performed using the Levenberg-Marquardt algorithm and the results in terms of conversion for DBT, biphenyl and cyclohexylbenzene obtained in the hydrodesulfurization of the LCO. The evolution of DEN_{σ} and DEN_{τ} values with the composition was calculated for each LCO experiment.

Structural contributions were taken from Vanrysselberghe and Froment for hydrogenolysis and hydrogenation of methyl-substituted dibenzothiophenes with a significant reduction in the number of parameters to be estimated in the HDS of the LCO.

The multiplication factors, f_{sDBT} , which are products of structural contributions for hydrogenolysis and hydrogenation of the mono- and dimethyl-dibenzothiophenes were also taken from Vanrysselberghe and Froment. These multiplication factors are based on experimental results with model components such as DBT, 4-Methyl dibenzothiophene and 4,6-Dimethyl dibenzothiophene.

The results obtained in the modeling are in good agreement with the experimental data because the model reproduces very well the observed total conversions of DBT, conversions of DBT into biphenyl and conversions of DBT into cyclohexylbenzene as a function of temperature.

DEDICATION

This dissertation is dedicated to the memory of my unforgettable parents, Esteban and Maria, who both passed away in the first year of my doctoral studies at Texas A&M. They had been a light in my journey every day which helped me to reach the end of my objectives. They both always taught me to fight against adversities and to keep human principles, such as honor, truth, and respect, for everybody. God bless them forever.

This dedication is also to my lovely wife, Celia, because she has been not only a woman but a professional in the same major, Chemical Engineering. We both were working back-to-back on every step of our research to accomplish our objectives and our corresponding Ph.D.s. This experience has been unique for both.

Thanks to my brothers, sister and all relatives who have believed in me. Finally, thanks to my parents in law for your help and support.

ACKNOWLEDGMENTS

First of all, my sincere and respectful acknowledgement is to my research advisor Dr. Gilbert F. Froment for his wise guidance during my study at TAMU. Thanks to Dr. Rayford G. Anthony, the co-advisor who always encouraged me to struggle with the challenges I found during my stay in the Kinetics, Catalysis and Reaction Engineering group.

Special thanks to Dr. Kenneth Hall for being on my committee and for your support in the final step of my research when he was the department head. Thanks also to Dr. Abraham Clearfield for serving on my advisory committee and for his teaching as well. My appreciation to Dr. Perla Balbuena for the time she spent serving on my committee.

My deep gratitude goes to Mr. Charles Isdale, an MBA and retired faculty member, for his invaluable help in providing the level control loop and the required training to install and operate my experimental setup. Moreover, thanks for his advice and time he spent during the different stages in our experimental work and for his time off campus as well.

Thanks to my entire fellows in the Kinetics, Catalysis and Reaction Engineering group. My honest acknowledgement to the scientific instrument maker, Randy Marek, for the support, knowledge and availability he always showed us in our experimental setup.

I would like to thank the staff of the Department of Chemical Engineering, and mainly to Towanna Hobacek for your help in all paperwork I needed. I am grateful to Dr. Jose Sericano for his advice and fruitful discussions on the GC-MS operation. Thanks to Sassol, Agilent, Shimadzu, and St Gobain for providing free samples and other materials used in my research.

My appreciation goes to Jackie Franzen, the first and beloved friend I met my first day at Texas A&M.

I owe special thanks to my company, Instituto Mexicano del Petroleo (IMP), for honoring me with a scholarship to pursue a Ph.D. at Texas A&M University in College Station. In addition, thanks to Elva Arzate for sending me the feedstock I used in my experimental work, and to Lazaro Moises Garcia for his comments, communications and advice he provided during the construction of my experimental setup.

TABLE OF CONTENTS

	Page
ABSTRACT.....	iii
DEDICATION.....	v
ACKNOWLEDGMENTS.....	vi
TABLE OF CONTENTS.....	viii
LIST OF FIGURES.....	xi
LIST OF TABLES.....	xiv
 CHAPTER	
I INTRODUCTION.....	1
1.1 Motivation.....	1
1.2 Background.....	2
1.3 Research Objectives.....	3
II LITERATURE REVIEW.....	5
2.1 Hydrotreatment Process.....	5
2.2 Hydrodesulfurization	6
2.2.1 Thermodynamics.....	6
2.2.2 First-order Kinetics.....	7
2.2.3 Structural Contribution Approach.....	11
III EXPERIMENTAL APPARATUS AND METHODS.....	13
3.1 Materials.....	13
3.2 Experimental Setup.....	15
3.3 Characterization of Reaction Products.....	17
3.3.1 Gas Product.....	17
3.3.2 Liquid Product.....	21
3.4 Reaction Test.....	26
3.4.1 Loading of Catalyst and Start Up.....	26

CHAPTER	Page
VI CONCLUSIONS AND RECOMMENDATIONS FOR FUTURE WORK.....	99
NOMENCLATURE.....	101
LITERATURE CITED.....	105
APPENDIX A GALLERY OF EXPERIMENTAL WORK IN THE HDS OF THE LCO.....	111
APPENDIX B FUNDAMENTALS OF THE SULFIDING PROCESS.....	115
APPENDIX C HP MANUAL INJECTION TECHNIQUE FOR THE GC-MS ANALYSIS OF LCO SAMPLES.....	118
APPENDIX D REACTIONS OF SUBSTITUTED BENZO AND DIBENZO-THIOPHENES.....	119
APPENDIX E SEPARATOR OF REACTION PRODUCT (CYCLONE).....	121
APPENDIX F TYPICAL OUTPUT GENERATED IN THE ESTIMATION OF PARAMETERS DEN_{σ} AND DEN_{τ} USING TWMARM AND TWINVE SUBROUTINES (MARQUARDT).....	124
VITA.....	127

LIST OF FIGURES

FIGURE		Page
1.1	Estimated petroleum demand by end-use sector, 2004.....	2
2.1	Schematic of typical hydrotreatment (HDT).....	6
3.1	Schematic of high pressure experimental setup for hydrotreatment studies of LCO.....	16
3.2	Schematic of switching valve and loop sampling with backflush of an OV-101 column in H ₂ , CH ₄ , and H ₂ S gas analysis.....	19
3.3	Schematic of GC-TCD measuring the flow rate gas leaving the HDS setup.....	20
3.4	Typical total chromatogram of LCO using a GC-MS.....	23
3.5	Total chromatogram of reaction products for the HDS of LCO using a GC-MS.....	23
3.6	Procedure carried out for activating the CoMo/Al ₂ O ₃ catalyst, reaction test and shut down.....	27
3.7	Sulfidation of the HDS-1 catalyst. Concentration of H ₂ S in the gas phase as a function of time.....	36
3.8	Typical chromatogram of gas from reaction products H ₂ S, H ₂ and CH ₄ on the GC-TCD.....	37
3.9	Concentration of H ₂ S during the conversion test. (a) W/F _{DBT} ⁰ = 6262 kg _{cat} h/kmol (b) W/F _{DBT} ⁰ = 4815 kg _{cat} h/kmol.....	37
3.10	Concentration of H ₂ S during the conversion test. (a) W/F _{DBT} ⁰ = 3538 kg _{cat} h/kmol. (b) W/F _{DBT} ⁰ = 2857 kg _{cat} h/kmol.....	38
3.11	Concentration of H ₂ S as a function of W/F _{DBT} ⁰	39
3.12	Part of the total ion chromatogram of the LCO showing part of the peaks corresponding to the BT and C ₁ -BT desulfurization products.....	43

FIGURE	Page	
3.13	Part of the single ion chromatogram of the LCO showing part of the peaks corresponding to the C ₁ -BT desulfurization products.....	44
3.14	Part of the single ion chromatogram of the LCO showing part of the peaks corresponding to the naphthalene and C ₁ -BT desulfurization products.....	45
3.15	Part of the single ion chromatogram of the LCO showing part of the peaks corresponding to the C ₁ -BT desulfurization products.....	46
3.16	Part of the total ion chromatogram of the LCO showing the peaks corresponding to the C ₁ -DBT desulfurization products.....	49
3.17	Part of the single ion chromatogram of the LCO showing part of the peaks corresponding to the C ₁ -DBT desulfurization products and fluorene the internal standard.....	50
3.18	Part of the single ion chromatogram of the LCO showing part of the peaks corresponding to the C ₁ -DBT desulfurization products...	51
3.19	Part of the single ion chromatogram of the LCO showing part of the peaks corresponding to the C ₁ -BT desulfurization products.....	52
3.20	Part of the single ion chromatogram of the LCO showing part of the peaks corresponding to the C ₂ -BT desulfurization products.....	53
3.21	Total conversion of DBT as a function of operating time.....	54
3.22	Total conversion of DBT as a function of W/F_{DBT}^0	56
3.23	Conversions as a function of space time, W/F_{DBT}^0 and T=330°C ...	56
3.24	Conversions as a function of space time, W/F_{DBT}^0 and T=310°C ...	57
3.25	Conversions as a function of space time, W/F_{DBT}^0 and T=290°C ...	57
4.1	Reaction network for the HDS of dibenzothiophene into biphenyl (BPH), cyclohexylbenzene (CHB) and bicyclohexyl (BCH).....	59

FIGURE		Page
5.1	DEN _σ at 330°C as a function of the molar-averaged conversion of LCO.....	83
5.2	DEN _τ at 330°C as a function of the molar-averaged conversion of LCO.....	84
5.3	DEN _σ at 310°C as a function of the molar-averaged conversion of LCO.....	84
5.4	DEN _τ at 310°C as a function of the molar-averaged conversion of LCO.....	85
5.5	DEN _σ at 290°C as a function of the molar-averaged conversion of LCO.....	85
5.6	DEN _τ at 290°C as a function of the molar-averaged conversion of LCO.....	86
5.7	Comparison of conversions as a function of W/F _{DBT} ⁰ at 330°C.....	87
5.8	Comparison of conversions as a function of W/F _{DBT} ⁰ at 310°C.....	87
5.9	Comparison of conversions as a function of W/F _{DBT} ⁰ at 290°C.....	88
5.10	Comparison of experimental and calculated R _i as a function of W/F _{DBT} ⁰ for various s-DBT at 330°C.....	98

LIST OF TABLES

TABLE		Page
2.1	Typical Hydrotreating Process Conditions for Different Feedstocks.	5
2.2	Reactivities of Several Sulfur Compounds.....	9
2.3	Hydrogenolysis Rate Coefficients of Selected Methyl-Substituted Dibenzothiophenes.....	11
3.1	Typical Properties of Light Cycle Oil (LCO).....	14
3.2	Typical Purity of Gases.....	14
3.3	Gas Chromatograph Conditions for the Analysis of Hydrogen Sulfide, Hydrogen and Methane in the Desorbed Gas from Reaction Products.....	17
3.4	Operating Conditions Used in the GCD for Analysis of the LCO and Liquid Reaction Products of the Hydrodesulfurization Reaction	24
3.5	Parameters of Integration Used in the GCD for Analysis of the LCO and Liquid Reaction Products of the Hydrodesulfurization Reaction	25
3.6	Set of Experiments Carried Out in the Hydrodesulfurization of the LCO.....	29
3.7	Relative Retention Factors for Gases in the GC-TCD.....	31
3.8	Retention Times in Gas Chromatographic Analysis of Identified Methyl Substituted Benzothiophenes (BT's) for the Hydrodesulfurization of LCO.....	41
3.9	Retention Times in Gas Chromatographic Analysis of Identified Methyl Substituted Dibenzothiophenes (DBT's) for the Hydrodesulfurization of LCO.....	41
3.10	The C ₁ -BT Isomers and Their Corresponding C ₁ -BT Desulfurization Products.....	42

TABLE	Page	
3.11	The C ₂ -BT and C ₃ -BT Isomers and Their Corresponding C ₂ -BT and C ₃ -BT Desulfurization Products.....	42
4.1	Ways Hydrogen Can be Adsorbed on the Active Sites of Catalyst...	61
4.2	Total Number of Parameters for the Hydrodesulfurization of DBT and Methyl-Substituted Dibenzothiophene in the Classical Molecular Approach.....	64
4.3	Assumptions Comprised in the Hydrogenolysis Step of Structural Contributions.....	66
4.4	Total Number of Parameters for the HDS of DBT and MeDBTs Based on the Structural Contributions.....	70
5.1	Properties of the Catalysts Used in the HDS of LCO.....	77
5.2	Rate – and Adsorption Parameters for DBT Utilized in the Modeling of the HDS of the LCO.....	78
5.3	Analysis of Variance on DEN _σ and DEN _τ at 330 °C.....	81
5.4	Parameter Estimates, 95% Confidence Intervals and t-Values at 330°C.....	81
5.5	Parameter Estimates, 95% Confidence Intervals and t-Values at 310°C.....	81
5.6	Parameter Estimates, 95% Confidence Intervals and t-Values at 290°C.....	81
5.7	Value of the Products $k_{i,\sigma}K_{i,\sigma}K_{H,\sigma}$ and $k_{i,\tau}K_{i,\tau}K_{H,\tau}$ at 330°C.....	91
5.8	Value of the Products $k_{i,\sigma}K_{i,\sigma}K_{H,\sigma}$ and $k_{i,\tau}K_{i,\tau}K_{H,\tau}$ at 310°C.....	91
5.9	Value of the Products $k_{i,\sigma}K_{i,\sigma}K_{H,\sigma}$ and $k_{i,\tau}K_{i,\tau}K_{H,\tau}$ at 290°C.....	91
5.10	The Multiplication Factors $f_{sDBT,\sigma}$ and $f_{sDBT,\tau}$ for the Substituted Dibenzothiophenes Calculated from the Structural Contributions at 330°C.....	96

TABLE		Page
5.11	The Multiplication Factors $f_{sDBT,\sigma}$ and $f_{sDBT,\tau}$ for the Substituted Dibenzothiophenes Calculated from the Structural Contributions at 310°C.....	97
5.12	The Multiplication Factors $f_{sDBT,\sigma}$ and $f_{sDBT,\tau}$ for the Substituted Dibenzothiophenes Calculated from the Structural Contributions at 290°C.....	97

CHAPTER I

INTRODUCTION

1.1 Motivation

Sulfur has to be removed from oil fractions for technical and environmental reasons. The increasing petroleum demand from the transportation sector has focused the attention of refiners and environmental authorities on removal of sulfur compounds from fuels. Figure 1.1 shows the estimated demand by end-use in USA. Middle distillates fuels similar to diesel are being strictly regulated. Diesel exhaust is a hazardous substance that has been linked to cancer and respiratory disease, especially after repeated exposure (EPA, 2005). Trucks and buses consist of less than 2 percent of highway vehicles and cover less than 6 percent of the miles driven each year, but they are responsible for one-quarter of the smog-causing pollution from highway vehicles. The European Union has limited the sulfur content in diesel to 0.005 wt% since 2005 year (National Petroleum Refiners Association, 1998). In the United States the Environmental Protection Agency (EPA) has limited the sulfur content in diesel to 500 parts per million by weight (wppm) since 1993. For the year 2006 this content should be decreased to 15 wppm (EPA, 2001).

This dissertation follows the style and format of *Industrial & Engineering Chemistry Research Journal*.

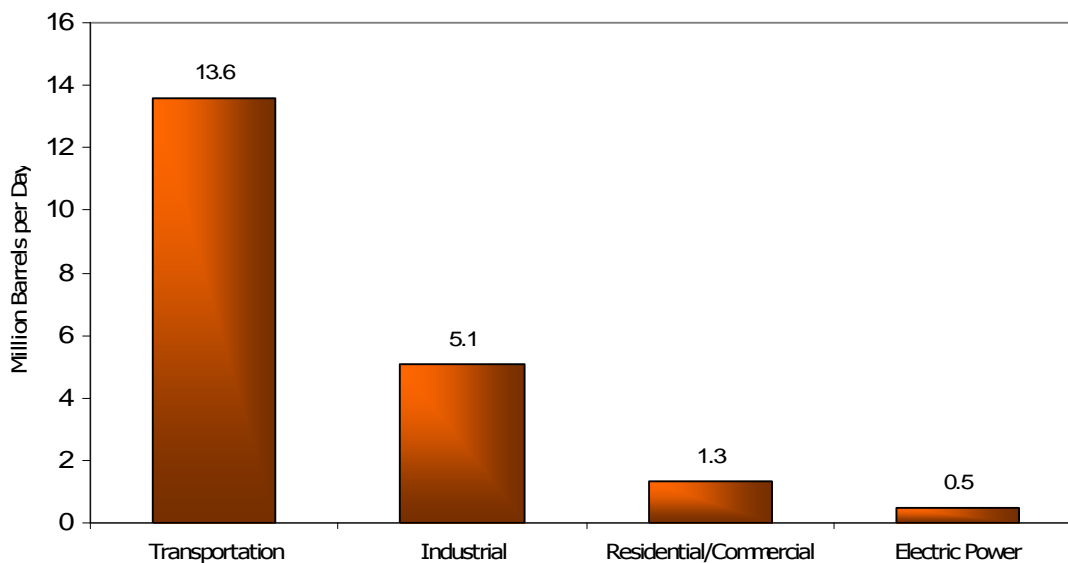


Figure 1.1 Estimated petroleum demand by end-use sector, 2004. (DOE 2004).

1.2 Background

Petroleum-derived Light Cycle Oil (LCO) typically has high sulfur and nitrogen content (Depauw and Froment, 1997; Tsonopoulos et al., 1986). LCO and diesel contain various methyl-substituted benzothiophenes, dihydrobenzothiophenes, dibenzothiophenes, dihydrodibenzothiophenes and naphthothiophenes which are relatively refractory to sulfur removal or hydrodesulfurization (HDS).

Until now the HDS of oil fractions has been studied in terms of lumps of sulfur components which were converted according to first-order or second-order kinetics. Deep HDS requires more accurate kinetic modeling, which includes individual

components and rate equations of the Hougen-Watson type accounting for the adsorption of the various species. If the kinetic modeling is based upon individual components, the number of rate parameters becomes awesome. A different approach is required to reduce this number. A methodology based upon structural contributions has been proposed by Froment et al. (1994). In this concept the rates of substituted S components are related to one of the unsubstituted head of family or parent molecule. The methodology can be applied for the HDS of oil fractions such as LCO (Vanrysselberghe and Froment, 1998b and Froment, 2004). In the present development that methodology was applied to the family of dibenzothiophenes, considering DBT as the parent molecule.

1.3 Research Objectives

A pioneer research program on catalytic hydrotreatment has started at the Department of Chemical Engineering-Texas A&M with the aim of gaining more basic understanding of the chemistry, catalysis and kinetics of the hydrotreatment (HDT). The basic philosophy of this program is to study not only important model sulfur-containing compounds but more complex systems such as petroleum fractions. The present work is an extension of Froment's studies. The emphasis is on applying a methodology of structural contributions to describe the kinetics of hydrodesulfurization in terms of individual sulfur components rather than classical lumping.

The main objectives of this project can be formulated as follows:

1. Build an experimental setup to investigate the hydrotreatment of complex feedstocks such as Light Cycle Oil (LCO) or gasoil.
2. Study the HDS of LCO/Diesel on a commercial CoMo/Al₂O₃ catalyst in a perfectly mixed reactor (Robinson-Mahoney).
3. Develop a rigorous kinetic model for predicting profiles of concentration of sulfur compounds and of sulfur removal in the HDS of the LCO.
4. Apply structural contributions methodology in order to restrict the number of independent parameters.

CHAPTER II

LITERATURE REVIEW

2.1 Hydrotreatment Process

Hydrotreatment has been part of refinery processing since the 1930's (Topsoe et al., 1996). Typical hydrotreatment reactions refer to the catalytic hydrodesulfurization (HDS), hydrodenitrogenation (HDN), hydrodeoxygenation (HDO), and hydrodearomatization (HDA) in presence of hydrogen. These reactions are typically carried out over a sulfided CoMo or NiMo catalyst at 350-450°C and 35-250 atm of hydrogen partial pressure. A summary of the hydrotreating process conditions for different feedstocks are shown in Table 2.1.

Table 2.1 Typical Hydrotreating Process Conditions for Different Feedstocks. (Adapted from Topsoe et al., 1996)

Feedstock	Temperature (°C)	Hydrogen partial pressure (atm)	LHSV (h ⁻¹)
Naphtha	320	10 – 20	3 – 8
Kerosene	330	20 – 30	2 – 5
Atmospheric gas oil	340	25 – 40	1.5 – 4
Vacuum gas oil	360	50 – 90	1 – 2
Atmospheric residue	370-410	80 – 130	0.2 – 0.5
Vacuum heavy gas oil	380-410	90 – 140	1 – 2
Vacuum residue	400-440	100 – 150	0.2 – 0.5

In the last two decades petroleum refining technology has significantly changed and the reactions of hydrotreatment, in particular, have risen to a level of economic importance (Gates et al., 1979; Ma et al., 1994). Hydrotreaters now have a central position in modern refineries as shown in Figure 2.1.

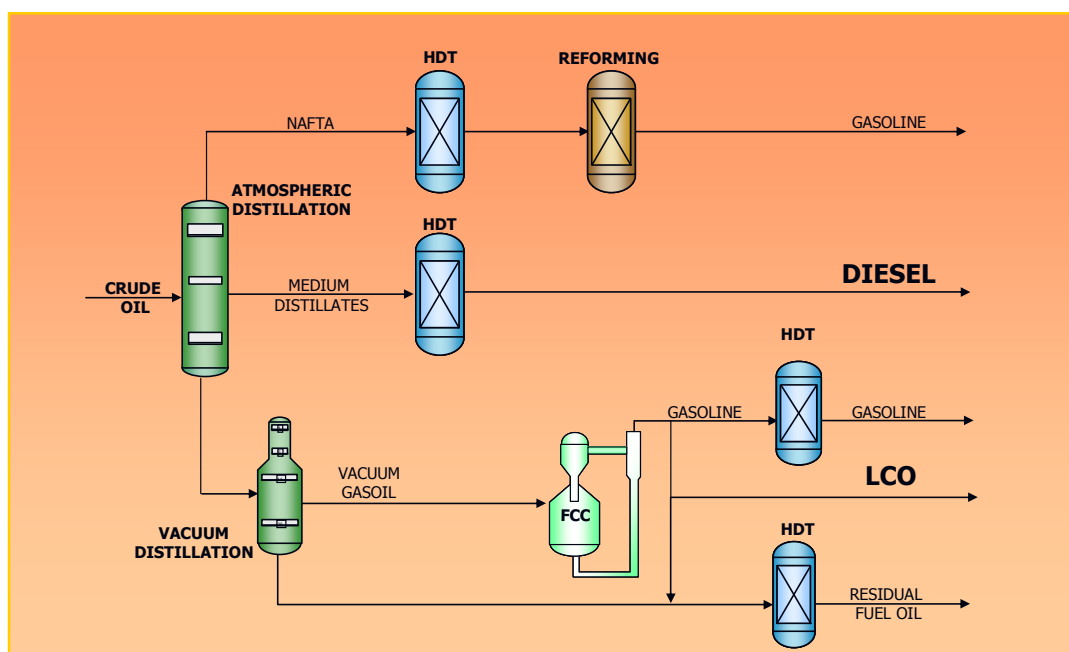


Figure 2.1 Schematic of typical hydrotreatment (HDT). (Adapted from Castaneda et al., 1999).

2.2 Hydrodesulfurization

2.2.1 Thermodynamics

The HDS of sulfur compounds is exothermic and fundamentally irreversible under the reaction conditions employed industrially (Gates et al., 1979; Speight, 1981; Vrinat,

1983). Actually, there is very little thermodynamics data available for sulfur compounds present in high boiling fractions. Vrinat (1983) shows data for dibenzothiophene HDS. According to these results the conversion of dibenzothiophene into biphenyl is favored at temperatures of industrial practice and is exothermic ($\Delta H^{\circ} = -11$ kcal/mol). Those results also suggest that the HDS of higher molecular weight sulfur compounds (e.g., benzonaphthothiophenes) are also favored.

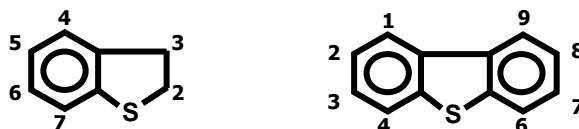
As will be discussed later, sulfur removal occurs along two parallel pathways, hydrogenolysis and hydrogenation (Froment, 2004). Since hydrogenation of the rings of sulfur compounds is equilibrium-limited at industrial HDS temperatures, the pathways concerning previous hydrogenation of the ring can be affected by thermodynamics (Girgis and Gates, 1991). Vrinat (1983) found that the equilibrium constant for hydrogenation of thiophene into tetrahydrothiophene is less than unity at temperatures above 350°C. Thus, sulfur-removal pathways via hydrogenated sulfur intermediates may be inhibited at low pressures and high temperatures because of the low equilibrium concentrations of the latter species.

2.2.2 First-order Kinetics

The most important hydroprocessing application in a refinery is hydrodesulfurization (HDS), which comprises reactions leading to removal of sulfur from petroleum fractions by their conversion into hydrocarbon products and hydrogen sulfide (H_2S). The literature on hydrodesulfurization of oil fractions and sulfur-

containing model compounds has been reviewed by Gates et al. (1979), Vrinat (1983), Vanrysselberghe and Froment (2003) and Froment (2004). The kinetics for the decomposition of substituted benzothiophenes and dibenzothiophenes in complex mixtures has been published by Kabe et al. (1992) in the study of hydrodesulfurization of a light oil on a CoMo/Al₂O₃ catalyst, and Ma et al. (1994) in the study on hydrodesulfurization in a diesel fuel, a gas oil, and a vacuum gas oil, on CoMo/Al₂O₃.



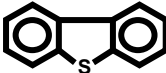


The numbering of the carbon atoms in benzothiophene and dibenzothiophene is as follows:



First-order kinetics for the removal of substituted benzothiophenes and dibenzothiophenes in complex mixtures prevail in the literature. Studies of hydrodesulfurization of a light oil (245-374°C) on a CoMo/Al₂O₃ catalyst found that benzothiophenes with substituents in positions 2, 3, and/or 7 were less reactive than BT (Kabe et al., 1992). The most refractive methylsubstituted-BT was 2,3,7-trimethyl-BT (2,3,7-TriMeBT). Dibenzothiophenes with substituents in positions 4 and/or 6 were less reactive than other substituted dibenzothiophenes. Similar results were obtained by Ma et al. (1994, 1995a, 1996) in the HDS of substituted BT's and dibenzothiophenes in oil fractions such as diesel fuel, gasoil, and vacuum gasoil, on CoMo/Al₂O₃ and NiMo/Al₂O₃ catalysts. In addition, methyl substituents in positions 2, 3, and/or 7 reduce

the hydrodesulfurization rate (Kilanowski et al., 1978). The reactivities of a set of sulfur compounds, reported as the pseudo-first-order rate constants at 300°C and 71 atm, are shown in Table 2.2.

Table 2.2 Reactivities of Several Sulfur Compounds. (Adapted from Nag et al., 1979)

Reactant	Structure	Pseudo-first-order rate constant L/ (g _{cat} s)
Thiophene (T)		1.38×10^{-3}
Benzothiophene (BT)		8.11×10^{-4}
Dibenzothiophene (DBT)		6.11×10^{-5}
Benzo[b]naphtho-[2,3-d]thiophene		1.61×10^{-4}
7,8,9,10-Tetrahydrobenzo[b]naphtho-[2,3-d]thiophene		7.78×10^{-4}

(a) Experimental conditions: batch reactor, n-C₁₆ solvent, 300°C, 71 atm, CoMo/Alumina catalyst.

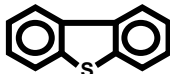
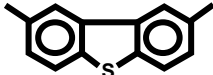
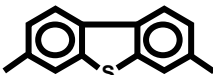
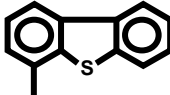
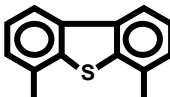
The operating conditions of data presented in Table 2.2 can be considered as representative of industrial conditions. From this Table it can be inferred that DBT is one of the most representative sulfur compounds comprised in higher boiling fractions of oil.

Because DBT is readily available commercially, it has been used as model compound or parent molecule for investigating the HDS of organic sulfur compounds.

The hydrogenation rate of 2-methyl-, 3-methyl-, and 2,3-dimethylbenzothiophene was less than benzothiophene (Geneste et al. (1980) and Levache' et al. (1981)). Hydrogenolysis reactions were not considered by these researchers.

Vanrysselberghe & Froment (1998b) obtained similar results in a study of hydrodesulfurization of Light Cycle Oil (LCO). Benzothiophenes with substituents in positions 2, 3, and/or 7 were less reactive than benzothiophene. Dibenzothiophenes with substituents in positions 4 and/or 6 were even less reactive. Methyl groups in other positions led to hydrodesulfurization rates higher than that of dibenzothiophene. Opposite to this, Kabe et al. (1992, 1997) and Ma et al. (1994, 1995a, 1996) found that methyl groups in positions 1, 2, and/or 3 had no influence on the hydrodesulfurization rate. Houalla et al. (1980) established that the first-order rate coefficient for the HDS of DBT is almost identical with that of 2,8-DiMeDBT (dimethyldibenzothiophene) and is about 2 times larger than that of 3,7-DiMeDBT. The HDS of the reactants shown in Table 2.3 is described by pseudo-first order kinetics as determined by this investigator.

Table 2.3 Hydrogenolysis Rate Coefficients of Selected Methyl-Substituted Dibenzothiophenes^(a). (Adapted from Houalla, 1980)

Reactant	Structure	Pseudo-first-order rate constant $\text{m}^3/(\text{kg}_{\text{cat}} \text{s})$
Dibenzothiophene (DBT)		6.11×10^{-5}
2,8-dimethyl-dibenzothiophene (2,8-DMDBT)		6.72×10^{-5}
3,7-dimethyl-dibenzothiophene (3,7-DMDBT)		3.53×10^{-5}
4-methyl-dibenzothiophene (4-MDBT)		6.64×10^{-6}
4,6-dimethyl-dibenzothiophene (4,6-DMDBT)		4.92×10^{-6}

(a) Experimental conditions: batch reactor, $n\text{-C}_{16}$ solvent, 300°C , 102 atm, CoMo/Alumina catalyst.

2.2.3 Structural Contribution Approach

First-order rate coefficients for the HDS of sulfur components such as benzothiophenes and dibenzothiophenes in oil fractions reported in the previous section contain the hydrogen concentration and the adsorption group on both types of active sites σ and τ . Therefore, it is necessary recognize that those coefficients vary with the

feedstock composition and that an extensive experimental program is required for every new feedstock. Also, to come to invariant parameters, it is necessary in the first place to distinguish between hydrogenolysis and hydrogenation reactions. Deep HDS requires more accurate kinetic modeling considering rate equations of the Hougen–Watson type accounting for the adsorption of the various species. If the kinetic modeling is based upon individual components the number of rate parameters becomes awesome. Therefore, Froment et al. (1994) developed a methodology based upon structural contributions for the kinetic modeling of hydrodesulfurization of oil fractions. This methodology considers the Hougen-Watson concepts, i.e. accounting for the adsorption of the reacting species and individual components instead of lumping for the sulfur components. Moreover, structural contributions account for the electronic effects and the steric hindrance of the substituents on the rate coefficients and the adsorption equilibrium constants (Vanrysselberghe & Froment (1998b)). In the project developed here the structural contributions methodology was applied to determine the kinetic modeling of the HDS of the LCO. This methodology is further described in the formulation of the kinetic model.

CHAPTER III

EXPERIMENTAL APPARATUS AND METHODS

The experimental setup used in these catalytic hydrotreating experiments was constructed starting from the one described by Vanrysselberghe and Froment (1996). Some modifications were done in the new equipment such as the volume of the reactor, which in this project was 1.0 liter. A demister was placed after the cyclone separator as a second step of gas-liquid separation to avoid the liquid entrainment to the gas chromatograph.

3.1 Materials

The feedstock was a Mexican Light Cycle Oil (LCO) containing 2.94 wt% of total sulfur, determined by neutron activation analysis (Nadkarni, 1984). The LCO was supplied by the Instituto Mexicano del Petroleo (IMP). The activating agent for the catalyst was a mixture of 15 vol% of hydrogen sulfide (H_2S) in H_2 acquired from Praxair. Hydrogen and methane used were from Brazos Valley Welding Supply Company. The physical properties of the LCO, H_2S , CH_4 and H_2 are listed in Tables 3.1 and 3.2 respectively.

Carrier gas used in the GC-TCD was a special mixture of 8.5 vol% H_2 in Helium according to Vanrysselberghe and Froment (1996) and Altgelt and Gouw (1979).

Helium ultra pure grade was used as carrier in the gas chromatograph coupled to a mass spectrometer (GC-MS). Both carrier gases were from Praxair.

The catalyst used in all experiments was CoMo/Al₂O₃ here identified as HDS-1 also supplied by IMP. It contains 13.1-16.1 wt% MoO₃, 3.2-3.8 wt % CoO. A physical analysis of this catalyst shows a pore volume of 0.5 cm³/g and BET surface area of 215 m²/g. The catalyst was crushed to the required particle size (750-820 μ) to avoid diffusional limitations. (Vanrysselberghe and Froment (1996)).

Table 3.1 Typical Properties of Light Cycle Oil (LCO).

Molecular Weight	188.5
Specific Gravity	0.9096
Initial Boiling Point, °C	182
Final Boiling Point, °C	399
Total Sulfur, wt %	2.94

Table 3.2 Typical Purity of Gases.

	Hydrogen Sulfide mixture	Hydrogen	Methane
Purity (From Manufacturer)	15 %	>99.95%	>99.995%
Balance	H ₂ (85%)	-	-
Molecular Weight	6.83	2.016	16.04

3.2 Experimental Setup

A flow diagram of the experimental equipment is shown in Figure 3.1 and a photograph of this setup is found in Appendix A. The setup was built according to the design of the equipment constructed and used by Vanrysselberghe and Froment (1996). In fact, this setup was built by the author of this dissertation in combination with Marin (2006) who used the setup in testing of catalysts. The experiments were performed in a 1.0 L Robinson-Mahoney stationary catalyst basket reactor with complete mixing of the gas and the liquid phases, and it was provided by Texaco. The fixed annular catalyst basket has baffles inside and outside to control vortexes. The rotating shaft is equipped with two impellers that lead fluid into the center of the annulus at the top and bottom and through the catalyst bed. Appendix A comprises illustrations of the basket and shaft. The reactor is made of stainless steel and can operate at pressures up to 140 bars and temperatures up to 450°C. Pictures of this reactor are shown in Appendix A. The temperature was measured by using thermocouples and controlled by temperature controllers. All the controllers in this setup were installed on one panel. The pressure was controlled by a back pressure regulator. The effluent of the reactor consisting of gas and liquid phases at high pressure and high temperature was separated under the same conditions by means of a cyclone coupled with a demister. This separator was designed according to Perry and Green (1995), Castaneda (2000), and Gonzalez et al. (1986) and it was constructed in the workshop of the Department of Chemical Engineering. The gas phase was analyzed on-line by means of a gas chromatograph (GC) with a TCD detector. The remaining phase was cooled, for condensing heavy fractions and then was scrubbed

by means of a 20 wt% sodium hydroxide solution to remove hydrogen sulfide. The liquid product was cooled and flashed under ambient conditions. The light gases, dissolved in the liquid phase, were desorbed and collected in a glass burette. The GC-TCD was used to analyze and quantify light gases such as H_2 , H_2S , and methane. The liquid product was measured and analyzed off-line by means of a GC-MS. A picture of this analyzer is shown in Appendix A.

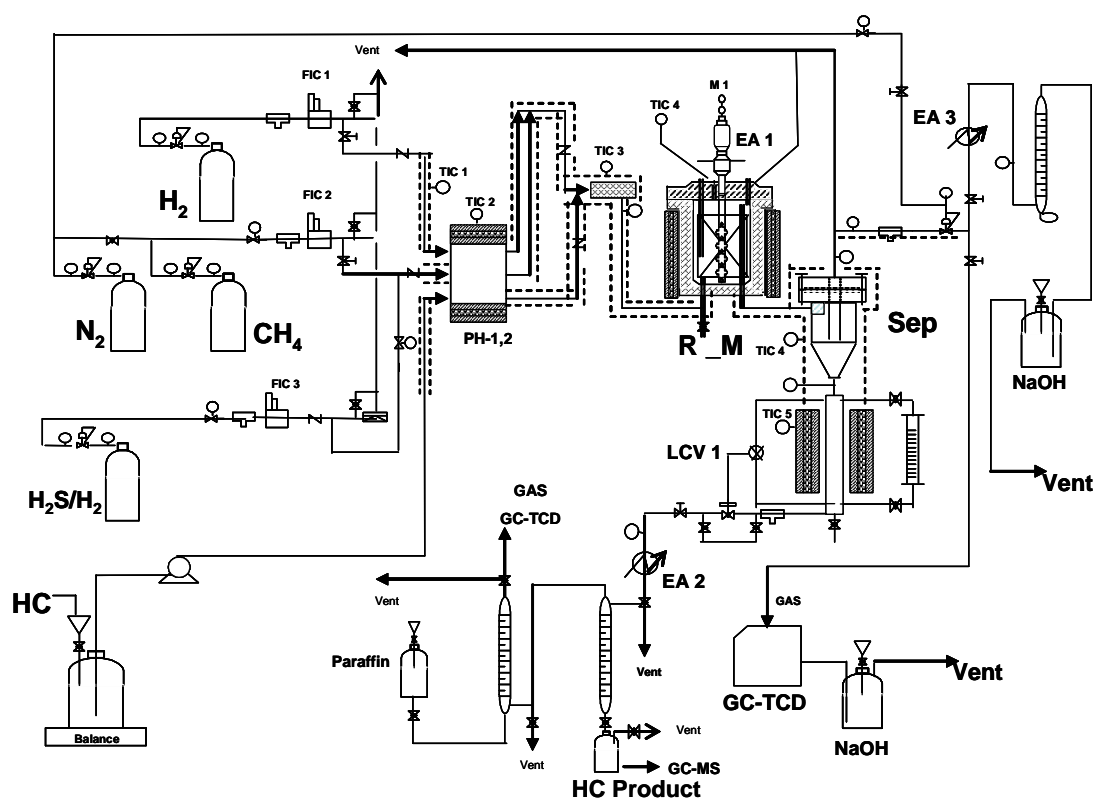


Figure 3.1 Schematic of high pressure experimental setup for hydrotreatment studies of LCO. Robinson-Mahoney reactor (R_M).

3.3 Characterization of Reaction Products

3.3.1 Gas Product

The gas samples were analyzed on line by a Shimadzu model 17A gas chromatograph equipped with a Hayesep D column to separate H₂, CH₄, and H₂S, and an OV-101 column to retain heavier hydrocarbons and backflushing after each analysis. The features of the GC and the operating conditions are shown in Table 3.3.

Table 3.3 Gas Chromatograph Conditions for the Analysis of Hydrogen Sulfide, Hydrogen and Methane in the Desorbed Gas from Reaction Products.

Chromatograph:	Shimadzu model 17A
Columns	<ul style="list-style-type: none"> • 20% OV-101 CHROM P-AW 80/100 6' x 1/8" x 0.085" SS OV-101; • 30' x 1/8" x 0.085 SS Hayesep D 100/120
Column Temperature	110 °C Isothermal
Carrier gas	8.5% H ₂ /Helium balance at 20 ml/min
Detector Temperature	120 °C
Injection port Temperature	120 °C
Switching valve Temperature	120 °C
Current in TCD	100 mA
Range / Polarity	1 / 1
Integration	Sensitivity: 90%; Baseline: 60%
Auxiliary pressure controller	78 kPa

The GC columns were conditioned prior to the injection of gas samples to test the resolution of these columns. Samples were injected by using a 10-port switching valve

with a 98.5 μl sample loop. The switching valve is remote actuated from a personal computer connected to a PeakSimple Chromatography Data System.

The configuration of GC packed columns, 10-ports switching valve and sample loop is shown in Figure 3.2. In this configuration the carrier gas is split in three different lines. In the first line, labeled on the GC as auxiliary, the flow rate is controlled by using a pressure regulator allowing the carrier to flow directly to the TCD. The carrier in the analysis line is controlled by a mass flow controller to flow through the injection port, switching valve, packed columns and finally to the TCD. A pressure regulator controls the carrier in the third line to flow through the switching valve and the OV-101 column. The latter column is backflushed after each analysis.

In the Load position of the switching valve the gas leaving the experimental setup flows through the sample loop of 98.5 μl . The OV-101 column is back flushed with the same carrier gas whereas the Hayesep D column is waiting for the sample. When the valve is switched to Inject position, the carrier takes the sample from the loop, then flows through OV-101 and Hayesep D columns and gets to the TCD. After the analysis is complete the valve switches back closing the cycle.

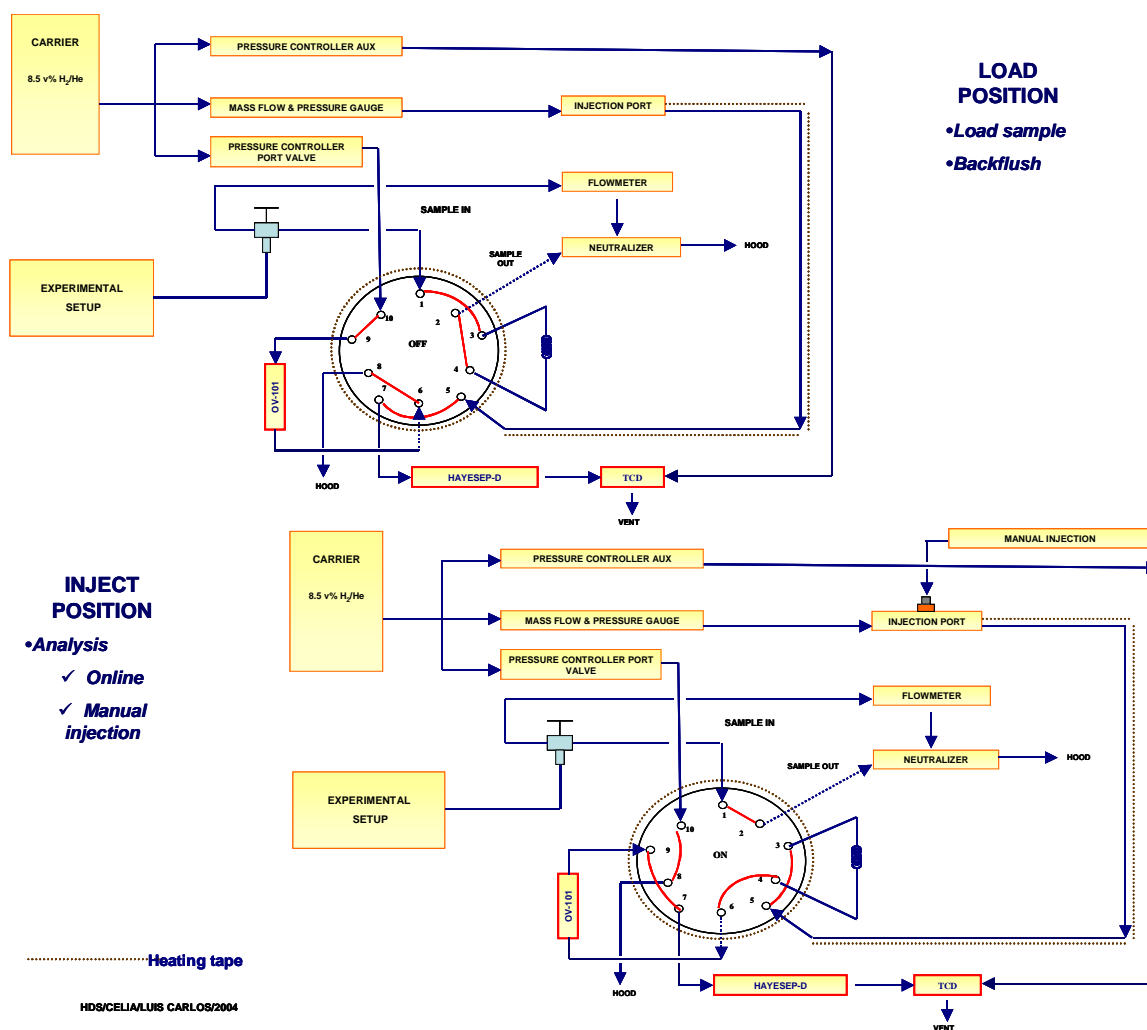


Figure 3.2 Schematic of switching valve and loop sampling with backflush of an OV-101 column in H_2 , CH_4 , and H_2S gas analysis.

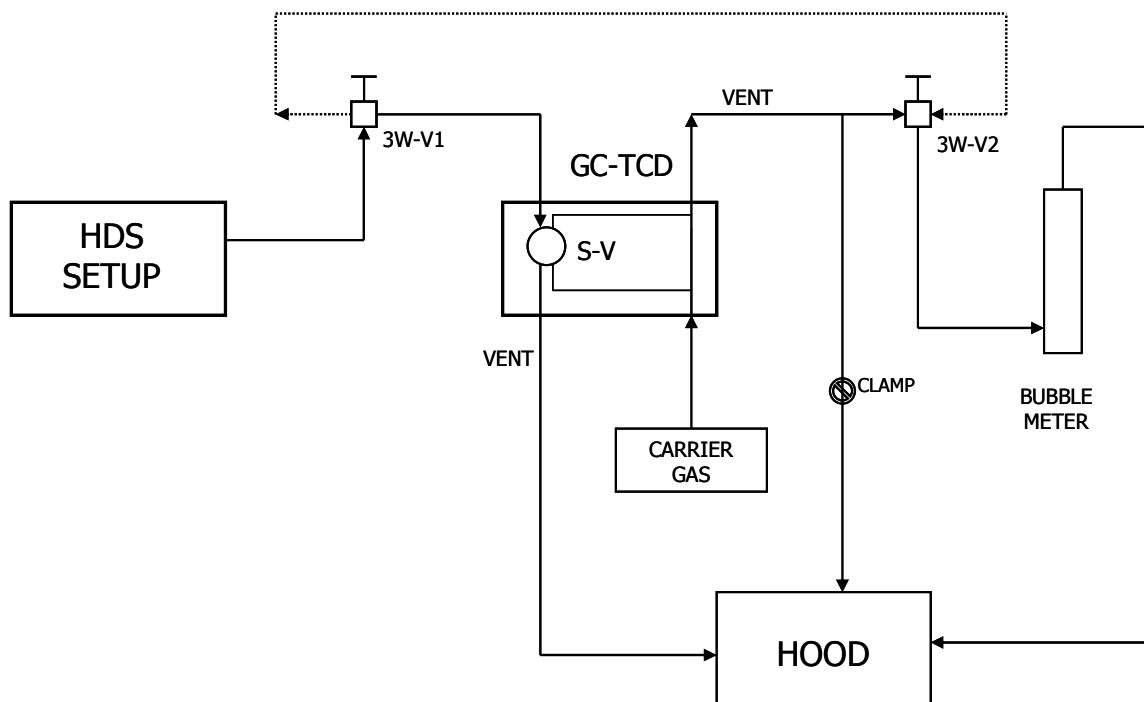


Figure 3.3 Schematic of GC-TCD measuring the flow rate gas leaving the HDS setup.

Figure 3.3 shows a diagram of the online configuration used to measure the flow rate of the gas product of the experimental setup. In normal operation, the gas leaving the setup goes through the 3 way valve (3W-V1) and goes to the GC-TCD to be analyzed. Once the analysis is completed the gas is vent to the hood. The carrier gas leaving the GC-TCD (VENT) goes through the 3W-V2 valve to the bubble meter and finally is sent to the hood. The auxiliary line between the GC and 3W-V2 is closed by means of a clamp. On the other hand, if the gas product from the setup needs to be measured, both 3 way valves (3W-V1 and 3W-V2) are switched to the opposite direction and the clamp is released from the auxiliary line sending the vent gas to the hood. Since the risk of

handling H₂S is high and because this section is out of the hood, special care should be taken in the right position of the 3W-V valves and the clamp as well. This will avoid eventual blocking of lines and consequently gas leaks.

3.3.2 Liquid Product

The liquid samples were analyzed by a Hewlett-Packard G1800A GCD gas chromatograph equipped with a 0.5 µm thickness x 0.2 mm I.D. x 50 m long capillary column (HP PONA) and an Electron Ionization detector (EID). The operating conditions are shown in Table 3.4.

In the HP-GCD, the compounds in the sample are separated in the HP-PONA column, before reaching the detector. Once the compounds exit the column, they are bombarded with a stream of electrons, which causes reproducible fragmentation of the molecules also called electron impact ionization. Once the fragmentation has occurred, the mixture of ions created can be detected in two distinct modes Scan and SIM (Selected Ion Monitoring).

For all analysis a mode Scan was selected. In this mode the EID scans from high to low across a set range of atomic mass units (amu) or mass-to charge ratios (m/z). When one scan is complete, the system resets and immediately scans the range again. This process is repeated continuously during the run (except for during the Solvent Delay time at the start of the run when the detector is off). Ideally the system should take 5-10 scans across each compound (peak) that elutes from the column to fully define the peak shape, especially for quantitative analysis. At the end of the run, the data is recorded in a

file as scan numbers and abundances of individual ions detected at each scan. The full scan range on the GCD was 10-425 amu. This range produces standard mass spectra that can be searched in spectral libraries and is recommended to be used for unknown samples (Hsu and Drinkwater, 2001). The GC parameters and report options edited are shown in Table 3.4.

Manual injection was selected because of the lack of an auto sampler. Furthermore, the HP injection technique described in Appendix C was applied since it produces reliable results when executed carefully and reproducibly for each injection.

Figure 3.4 shows a typical total chromatogram of LCO feed and Figure 3.5 shows a total chromatogram of reaction products analyzed at the same LCO conditions. From the figures it can be easily observed how the composition is displaced from the heavy components in the feed to lighter components in the product due to HDS.

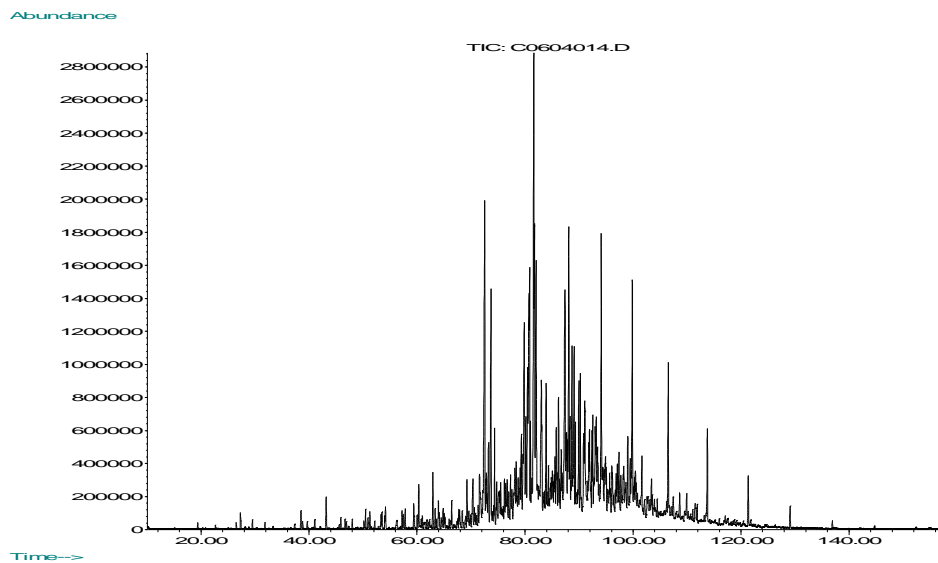


Figure 3.4 Typical total chromatogram of LCO using a GC-MS.

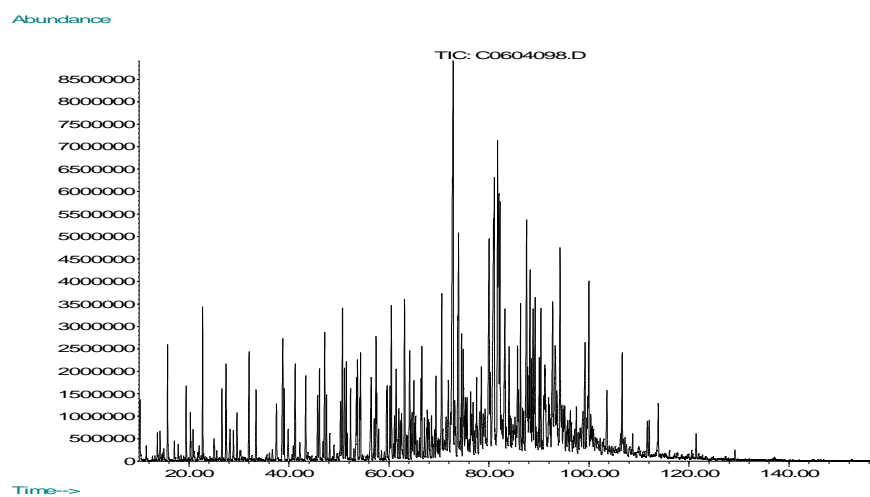


Figure 3.5 Total chromatogram of reaction products for the HDS of LCO using a GC-MS. Experimental conditions: $T=330^{\circ}\text{C}$, $P_t=65.5$ bar, $W/F_{\text{DBT}}^0=3672$ kg_{cat} h/kmol

Table 3.4 Operating Conditions Used in the GCD for Analysis of the LCO and Liquid Reaction Products of the Hydrodesulfurization Reaction.

Chromatograph		Hewlett-Packard model G1800A GCD		
Column	50 m x 0.2 mm fused-silica capillary column coated with a 0.5 μm film of cross-linked 100% dimethylsiloxane (HP-PONA).			
Inlet	250 $^{\circ}\text{C}$			
Detector	270 $^{\circ}\text{C}$			
Injection	Splitless			
Oven information				
Column max temperature	325			
Initial temperature	35			
Initial time	5			
	Rate, $^{\circ}\text{C}/\text{min}$	Final, $^{\circ}\text{C}$	Time, min	
Level 1	2.5	80	15	
Level 2	2.0	200	5	
Level 3	1.0	250	5	
Total time	158 min			
Injection parameters				
Injection mode	Manual			
Sample volume	2 μl ; 50 times diluted			
Constant flow				
Gas	Helium			
Program Flow	0.643 ml/min (pulseless constant flow)			
Pressure at oven temp 35 $^{\circ}\text{C}$	20 psi			
Pressure at oven temp 250 $^{\circ}\text{C}$	39.9 psi			
Detector Parameters				
Solvent Delay	10.0 min			
Mass Range	10-450 m/z			
Specific reports	Area percent, Quantification			

The GCD software was used to review data acquired in the following ways:

- Display total ion chromatograms
- Customize integrating parameters

- View and interpret spectral data
- Compare data acquired at different times
- Reviewing integration results.

To identify components, spectral data of the samples were compared to databases of reference called spectral libraries (Wiley 138K mass spectral database). To reintegrate chromatograms a ChemStation integrator was used. Table 3.5 shows the parameters of integration.

Table 3.5 Parameters of Integration Used in the GCD for Analysis of the LCO and Liquid Reaction Products of the Hydrodesulfurization Reaction.

Integration Events	Value	Time
Initial Area Reject	1	Initial
Initial Peak Width	0.02	Initial
Shoulder Detection	On	Initial
Initial Threshold	14.0	Initial
Integrator OFF	--	0.001
Threshold	0.1	--
Integrator ON	--	11.3

Using these integration events when reviewing data of liquid samples analysis, around 600 peaks are successfully integrated, and a few interesting peaks corresponding to sulfur compounds have been manually integrated.

3.4 Reaction Test

3.4.1 Loading of Catalyst and Start Up

A homogeneous solid mixture was prepared using 7.7 g of crushed catalyst (10 ml) diluted with 72.6 g of alpha alumina (71 ml) to yield a total volume of 81 ml. The latter is the corresponding volume in the annular basket for the catalyst. The particle size of the catalyst and the alumina was between 710 and 850 μm (-20, +25 mesh). The diluted catalyst mixture was carefully loaded into the basket then the basket was placed in the reactor. The reactor was safety closed according to the torque specified by the manufacturer (60-90 ft-lb). The reactor was pressurized up to 76 bar (1100 psi) with N_2 and leaks were checked and corrected. The nitrogen valve was closed and then the reactor and process lines were flushed with hydrogen for 2 hours at 28 liters @ STP/h (Maximum flow rate on the H_2 mass flow meter) before the activation step. Standard conditions (STP) in this work are 25°C and 1 atm.

3.4.2 Catalyst Activation

The presulfided HDS-1 catalyst was activated with 15 vol % $\text{H}_2\text{S}/\text{H}_2$ balance gas mixture. The activation was carried out at 1 bar and 330°C and no methane was fed during this stage. The procedure is shown in Figure 3.6 and in Appendix B.

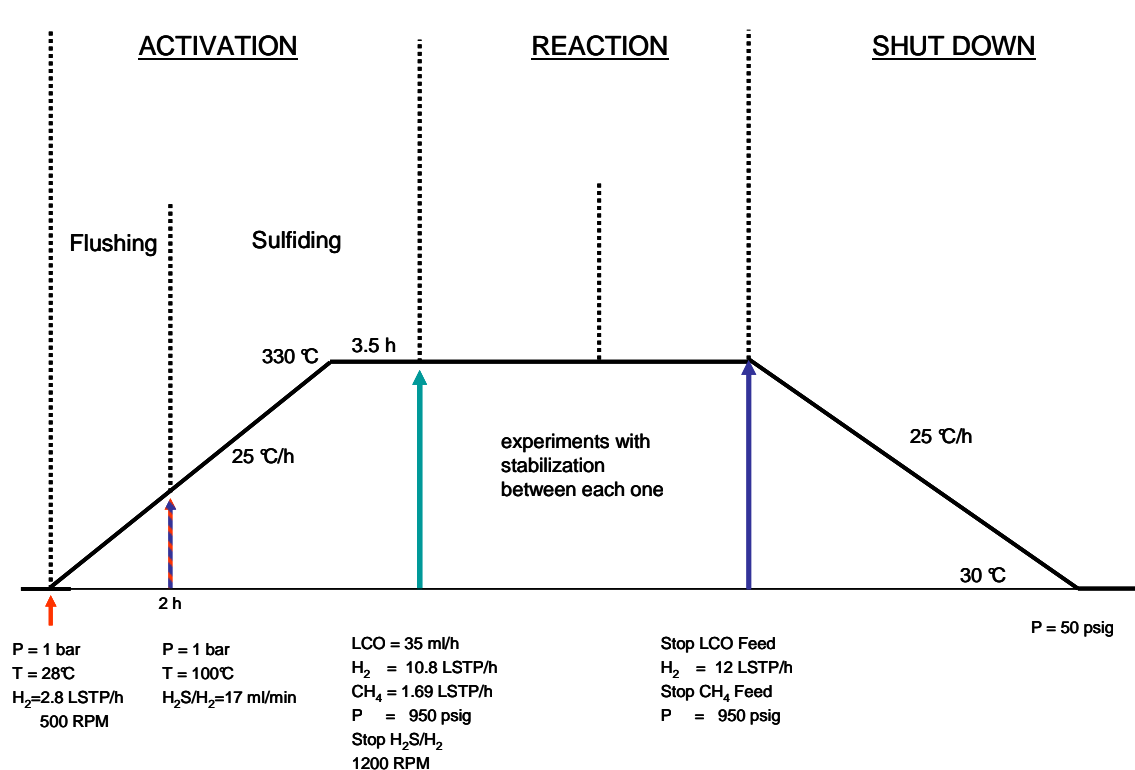


Figure 3.6 Procedure carried out for activating the CoMo/Al₂O₃ catalyst, reaction test and shut down.

The pressure in the setup was decreased to 1 bar and H₂ flow rate was set to 2.8 LSTP/h. The temperature of reactor was increasing at 25°C/h until 330°C was reached. The agitation started at 500 RPM and the temperature of preheater, mixer, separator and demister was increased in steps of 50°C/h when the reactor reached 50, 100, 150, 200, 250 300 and 330°C, respectively. When the reactor temperature was 50°C gas samples were analyzed in the GC-TCD to verify if N₂ was still present in the gas. After two hours of hydrogen flushing through the reactor, H₂ flow was stopped and the flow rate of the sulfiding gas mixture (H₂S/H₂) was set to 17 ml/min. This flow rate was maintained

constant for all the sulfidation. The amount of H₂S required for sulfidation was calculated according to the catalyst metal content and its reaction stoichiometry. When the reactor reached every increment of 50°C, gas samples were analyzed in the GC-TCD.

3.4.3 HDS Reaction

Once the activation of the catalyst was completed the H₂S/H₂ flow was stopped. The backpressure was set at 65.5 bar, H₂ flow rate was set to 10.8 LSTP/h, the methane flow rate was 1.69 LSTP/h and the LCO flow rate 35 ml/h. The agitation for the reacting mixture was set to 1200 rpm. The temperature of the reactor was increased to 330°C at 25°C/h. Operating conditions were maintained for 13-29 h for stabilizing and 8 h for the conversion test. Readings were taken every 30 min of temperature controllers (TIC), mass flow controllers (FIC), temperature indicators (TI), pressure gauges and balance. Gases leaving the separator were analyzed on line in the GC-TCD and liquid samples were recovered and analyzed off line in the GC-MS.

Additional experiments varying W/F_{DBT}^0 (kg_{cat}/kmol/h) and temperature were performed to determine if the steady state is reached between 1 and 5 reactor volumes of liquid leaving the reactor.

The complete set of experiments performed at varying W/F_{DBT}^0 (kg_{cat}/kmol/h) and temperature are shown in Table 3.6.

Table 3.6 Set of Experiments Carried Out in the Hydrodesulfurization of the LCO.

LCO flow rate, ml/h	W/F ⁰ _{DBT} , kg _{cat} h/kmol	330°C T1	(*)	310°C T2		290°C T3
35	6228	(W/F) ₁ -T1	{1}→	(W/F) ₁ -T2	{2}→	(W/F) ₁ -T3
45	4848	(W/F) ₂ -T1	←{6}	(W/F) ₂ -T2	↑	(W/F) ₂ -T3
62	3556	(W/F) ₃ -T1	{7}	(W/F) ₃ -T2	↑{5}	(W/F) ₃ -T3
77	2881	(W/F) ₄ -T1	↓	(W/F) ₄ -T2	←{4}	(W/F) ₄ -T3
62	3550	(W/F) ₁ -T1	{8}	(W/F) ₁ -T2	↑	(W/F) ₁ -T3
81	2700	(W/F) ₂ -T1	↓	(W/F) ₂ -T2	↑	(W/F) ₂ -T3
119	1850	(W/F) ₃ -T1	↓	(W/F) ₃ -T2	↑	(W/F) ₃ -T3
219	1000	(W/F) ₄ -T1	↓	(W/F) ₄ -T2	{9}	(W/F) ₄ -T3

(*) Arrows point out the sequence and direction that experiments were conducted.

The molar hydrogen to hydrocarbon (LCO) ratio was 2.9, and the hydrogen to methane molar ratio was 6.4 for all experiments. As mentioned before gas samples were analyzed online in the GC-TCD. Methane was used as an internal standard for the on-line analysis. A ten-port switching valve was used with a sample loop of 98.5 μ l to take samples every hour. The valve is electronically actuated from a personal computer. The carrier gas was 8.5 % H₂/ Helium balance at 20 ml/min. Conditions of the GC-TCD were shown in Table 3.3.

Liquid product samples were collected in labeled vials and refrigerated until they were analyzed off-line in the GC-MS (GCD). Because direct samples of LCO cannot be well resolved in the GC-MS, every liquid sample was diluted 50 times with dichloromethane, then 2 μ l of each diluted sample was injected using a 10 μ l syringe. Conditions of the GC-MS were shown in Table 3.4.

3.4.4 Functionality Test

The most essential information for kinetic analysis in terms of conversion is in the range far away from the asymptotic behavior; therefore, experiments in the range of low conversions of DBT at the same H₂/HC ratio required increasing the flow rate of LCO and H₂. Because the mass flow controller (FIC-H₂) originally installed in the setup was limited the H₂/HC molar ratio was varied from 2.8 to 2.4. At these operating conditions, coking occurred, leading to operating problems such as blocking of valves, filters and lines. The mass flow meters of H₂ and CH₄ were showing big variations in their displays while an increasing delay in opening the valve actuated for the liquid controller confirmed this problem. Evidence of the presence of coke is illustrated in Appendix A. This problem was overcome by replacing the H₂ mass flow meter and running the experiments in the interval of W/F_{DBT}^0 1000- 2800 kg_{cat}-h/kmol corresponding to H₂/HC molar ratio greater than 2.4.

3.5 Data Treatment

3.5.1 Sulfiding Step

Because no methane was used in the activation step, the Internal Normalization method was applied to quantify H₂S. The internal normalization method via peak areas does not require knowing the exact amount of sample injected for quantification

(Schomburg, 1990). In this procedure, the sum of the amounts of each sample component is determined via the area of all peaks. From the ratios of the amounts of each individual component to the total amount of all sample components, the percentage composition of the sample is obtained.

The method of internal normalization requires the determination of the areas of all the peaks in a chromatogram. The determination of the peak area can be performed by integration using the PeakSimple integrator software. The corrected peak areas of individual peaks are related to the total peak area of the chromatogram as follows:

$$C_i = \frac{RRF_i * A_i}{\sum RRF_i * A_i} \quad (3.1)$$

where A_i is the peak-area of component i and RRF_i , the corresponding relative response factor. Table 3.7 shows the relative retention factor for H₂S, H₂ and methane.

Table 3.7 Relative Retention Factors for Gases in the GC-TCD.

Component	RRF_i
H ₂ S	2.486
H ₂	0.111
CH ₄	1.000

3.5.2 HDS Reaction

3.5.2.1 Gases

The quantification of H₂S, H₂ and CH₄ from the reaction products was carried out using the internal standard method via peak areas. This method is important to obtain data of high precision and accuracy for the individual components even in complex mixtures (Dzidic et al., 1992; Wadsworth and Villalanti, 1992). The internal standard methane was added to the original sample through the experimental setup at known concentrations determined by a mass flow meter.

The procedure can be followed for the determination of the weight G_i applied to the components *i* according to the equation

$$G_i = G_{st} \frac{A_i * RRF_i}{A_{st} * RRF_{st}} \quad (3.2)$$

The sum of all G_i must be equal to G_p, hence, the G_i data are converted into concentration data with the equation:

$$C_i = 100 \frac{G_i}{G_p} \quad (3.3)$$

3.5.2.2 Liquids

Calculations of conversions for LCO from the peak areas were carried out using Excel. The mixture composition was expressed in terms of a molar-averaged conversion defined as follows:

$$\bar{x} = \frac{1}{\sum_{i=1}^8 y_i} \sum_{i=1}^8 x_i y_i^{LCO} \quad (3.4)$$

with x_i the conversions of a set of the identified sulfur components in LCO and reaction products DBT, 4-MeDBT, 3-MeDBT, 3-ethylDBT, 4,6-DMDBT, 3,6-DMDBT, 2,8-DMDBT, 4,9 DMeNaphtho[2,3-b]thiophene, and y_i^{LCO} the corresponding mole fractions of i in the LCO. Peak areas from chromatograms were obtained from a ChemStation and total conversions for every selected compound were calculated using Fluorene as internal standard as follows:

$$x_i = 1 - \left[\frac{A_i}{A_f} \right]^{Prod} \times \left[\frac{A_f}{A_i} \right]^{LCO} \quad (3.5)$$

where A_i is the peak-area of component i and A_f , the peak-area of fluorene. This molecule is present in the LCO feed and is not produced nor hydrogenated or significantly evaporated under reaction conditions (Depauw and Froment 1997). In addition, it does not co-elute with other components with the same mass. The most important fragment of fluorene with m/z ratio of 166 was used for the calculations.

The conversions of every selected compound into the corresponding product were calculated using fluorene in a similar manner as follows:

$$x_{i \rightarrow j} = \left[\frac{A_j}{A_f} \right]^{Prod} \times \left[\frac{A_f}{A_i} \right]^{LCO} - \left[\frac{A_j}{A_i} \right]^{LCO} \quad (3.6)$$

where A_i is the peak-area of component i and A_j , the peak-area of its corresponding product. A_f is the peak-area of fluorene. For instance, the conversion of DBT into biphenyl ($x_{DBT \rightarrow BPH}$) can be expressed in this fashion:

$$x_{DBT \rightarrow BPH} = \left[\frac{A_{BPH}}{A_f} \right]^{Prod} \times \left[\frac{A_f}{A_{DBT}} \right]^{LCO} - \left[\frac{A_{BPH}}{A_{DBT}} \right]^{LCO} \quad (3.7)$$

3.6 Experimental Results and Discussion

3.6.1 Catalyst Activation

The variation of hydrogen sulfide concentration in the produced gas during the activation of the catalyst is shown in Figure 3.7. Monitoring of the H₂S concentration in the gas leaving the separator was followed from 153 to 330°C. In this interval the concentration in the gas decreased from 15 mol% to around 6.4 mol%. Prior to the sulfiding temperature reaching 330°C the H₂S concentration observed in the gas was the minimum value in this step. This concentration was similar to the value obtained during 3.5 hours that sulfiding conditions were maintained. After this point the gas concentration increased again so that the catalyst was considered to be activated and ready for the HDS experiments.

It is assumed that the H₂S concentration observed at the beginning of the sulfiding results from the oxysulfides present in the catalyst decompose to form H₂S, which converts the metal oxides into metal sulfides.

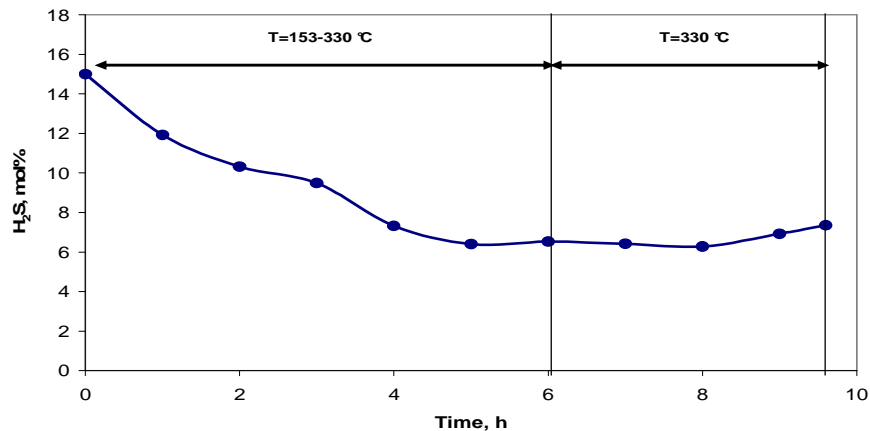


Figure 3.7 Sulfidation of the HDS-1 catalyst. Concentration of H₂S in the gas phase as a function of time. Pressure: P= 1 bar.

3.6.2 Gas Analysis Using CH₄ as Internal Standard

A typical chromatogram obtained for hydrogen, methane and hydrogen sulfide is shown in Figure 3.8. Retention times for H₂, CH₄ and H₂S were 6.28, 8.40 and 26.77 min respectively. Flow rate of carrier gas was 20 ml/min, temperature of TCD was 120°C and the remaining conditions for the analysis were shown in Table 3.3.

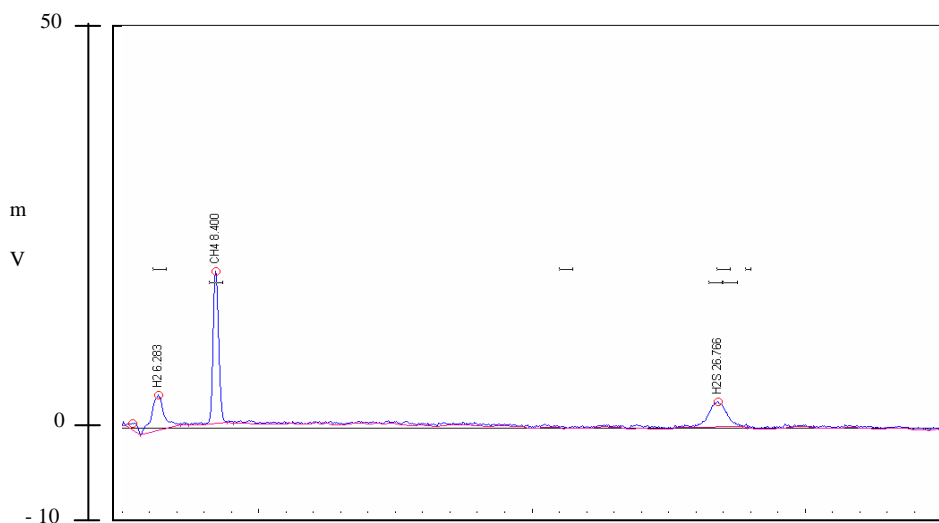


Figure 3.8 Typical chromatogram of gas from reaction products H_2S , H_2 and CH_4 on the GC-TCD.

For all the investigated space times (W/F_{DBT}^0) the variation in concentration of H_2S in the gas product as a function of time and temperature is between 10 and 15 mol%, as is shown in Figures 3.9 and 3.10.

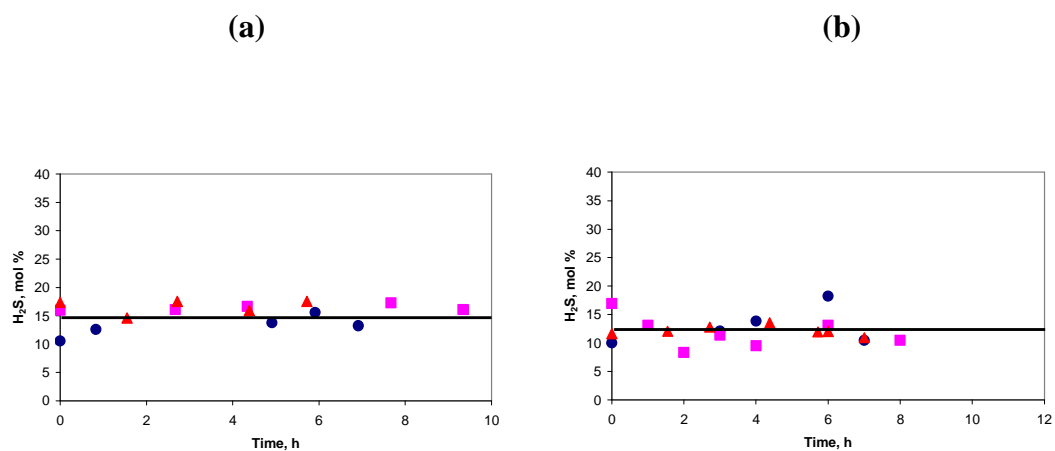


Figure 3.9 Concentration of H_2S during the conversion test. (a) $W/F_{\text{DBT}}^0 = 6262 \text{ kg}_{\text{cat}} \text{ h/kmol}$ (b) $W/F_{\text{DBT}}^0 = 4815 \text{ kg}_{\text{cat}} \text{ h/kmol}$. Conditions: $P = 65.5 \text{ bars}$, (\bullet) $T = 330^\circ\text{C}$; (\blacksquare) $T = 310^\circ\text{C}$; (\blacktriangle) $T = 290^\circ\text{C}$.

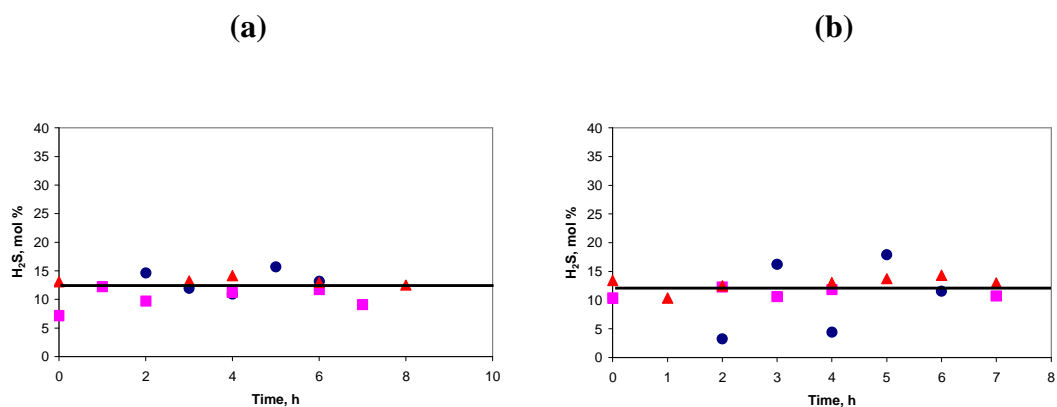


Figure 3.10 Concentration of H₂S during the conversion test. (a) $W/F_{DBT}^0 = 3538 \text{ kg}_{\text{cat}} \text{ h/kmol}$. (b) $W/F_{DBT}^0 = 2857 \text{ kg}_{\text{cat}} \text{ h/kmol}$. Conditions: $P = 65.5 \text{ bars}$, (●) $T = 330^\circ\text{C}$; (■) $T = 310^\circ\text{C}$; (▲) $T = 290^\circ\text{C}$.

The variation in concentration of H₂S in the product gas as a function of W/F_{DBT}^0 is shown in Figure 3.11.

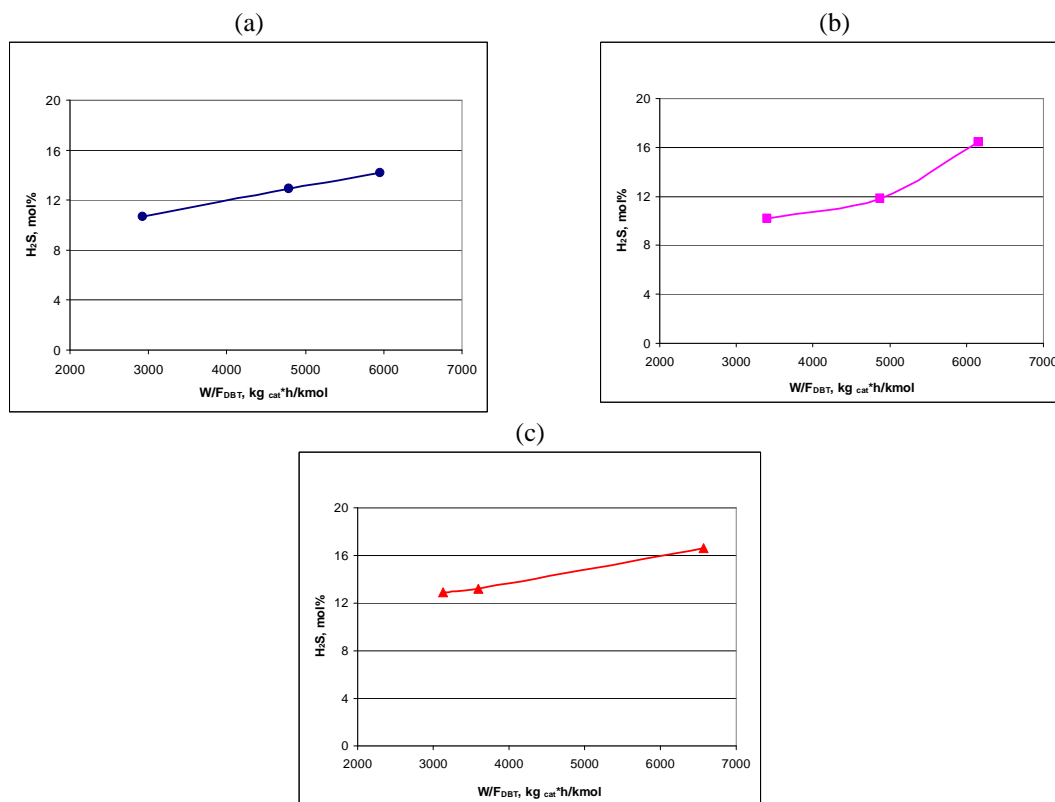


Figure 3.11 Concentration of H_2S as a function of W/F_{DBT}^0 . Experimental conditions: $P = 65.5$ bar, $H_2/HC = 2.8$. (a) $T=330^\circ C$, (b) $T=310^\circ C$, (c) $T=290^\circ C$.

The plots show that at all temperatures the H_2S concentration in the gas product increases with space time (from 1000 to 6500 kg_{cat} h/kmol). In this interval the variation of H_2S concentration was 40, 60 and 23% for 330, 310 and 290°C respectively. These values confirm that the rate of reaction increases with temperature.

3.6.3 Liquid Analysis

The peaks of a LCO were previously identified by Depauw & Froment (1997) using a GC-AED. Other researchers have taken advantage of this information in their investigations with LCO (Chen et al., 2003; Turaga and Song, 2000). As in previous reports the identification of sulfur compounds was carried out here following every single compound on the GC-MS chromatogram. Chemstation together with a Wiley Library of chemical compounds were used to identify selected compounds. In Table 3.8 methyl substituted benzothiophenes are shown and Table 3.9 shows methyl substituted dibenzothiophenes. Fluorene was used as an internal standard. Some compounds such as cyclohexylbenzene (CHB) and bicyclohexyl (BCH) were co-injected in separate samples of liquid products to confirm their identification. Because of the disappearance of sulfur compounds in the HDS, the samples of reaction products were more difficult to identify and quantify. Thus, some peaks were manually integrated when Chemstation ignored these compounds or when they were integrated together with others.

Table 3.8 Retention Times in Gas Chromatographic Analysis of Identified Methyl Substituted Benzothiophenes (BT's) for the Hydrodesulfurization of LCO^[a].

Peak No.	Compound	LCO feed Retention Time, min	Reaction Products Retention Time, min
1	Benzothiophene	63.62	63.58
2	2-methyl-benzothiophene	71.89	71.97
3	5-methyl-benzothiophene	73.22	73.24
4	6-methyl-benzothiophene	73.22	73.24
5	3-methyl-benzothiophene	73.63	73.41
6	4-methyl-benzothiophene	73.63	73.41
7	3,6-dimethyl-benzothiophene	79.31	79.42
8	2,5-dimethyl-benzothiophene	80.47	---
9	2,7-dimethyl-benzothiophene	81.01	81.21
10	2,3,7-trimethyl-benzothiophene	86.71	---

^[a] Carrier gas flow rate was 0.643 ml/min. Complete operating conditions for the GC-MS and the HP-PONA column were shown in Table 3.4.

Table 3.9 Retention Times in Gas Chromatographic Analysis of Identified Methyl Substituted Dibenzothiophenes (DBT's) for the Hydrodesulfurization of LCO^[a].

Peak No.	Compound	LCO feed Retention Time, min	Reaction Products Retention Time, min
1	Dibenzothiophene	102.02+102.18 ^[c]	101.83
2	4-methyldibenzothiophene	109.20	108.89
3	3-methyldibenzothiophene	110.54	110.15
4	3-ethyldibenzothiophene	115.69	115.47
5	4,6-dimethyldibenzothiophene	115.26+116.47 ^[c]	116.24
6	3,6-dimethyldibenzothiophene	117.58	117.31
7	2,8-dimethyldibenzothiophene	118.05	117.80
8	4,9-dimethylnaphtho[2,3-b]thiophene	119.25	119.04
9	3,4-dimethyldibenzothiophene	120.30	120.10
10	9H-Fluorene ^[b]	92.28	92.04

^[a] Carrier gas flow rate was 0.643 ml/min.

^[b] Internal Standard.

^[c] The area peaks at these two retention times were added.

The desulfurization of the six C₁-BT isomers results in the five C₃-benzenes shown in Table 3.10 and in Appendix B. The most refractive C₂-BT and C₃-BT isomers in the HDS and the corresponding desulfurization products are shown in Table 3.11.

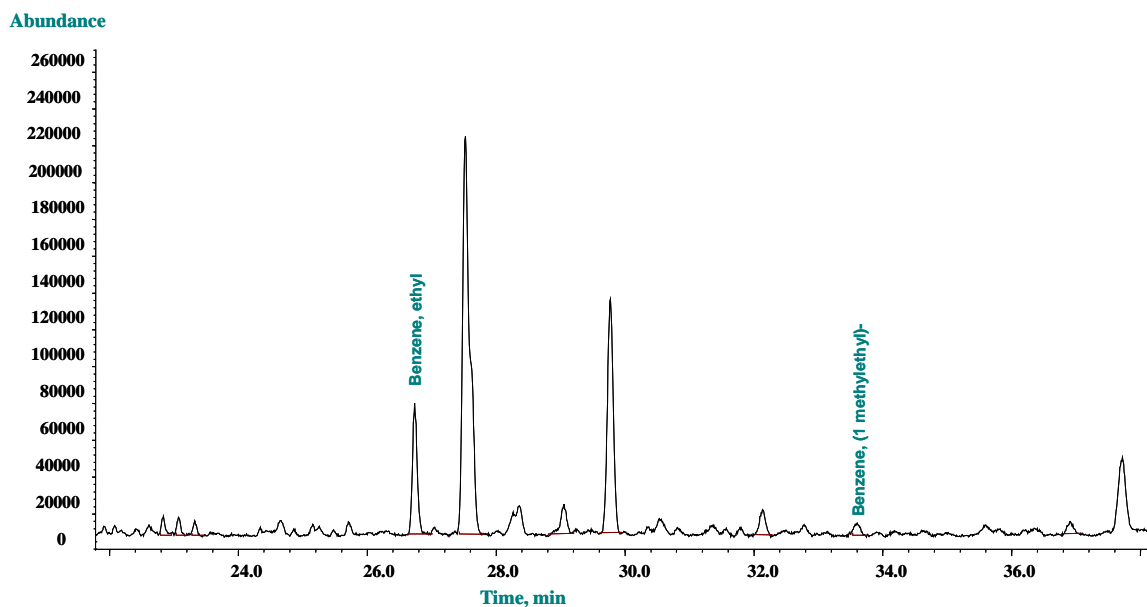
Table 3.10 The C₁-BT Isomers and Their Corresponding C₁-BT Desulfurization Products

C ₁ -BT isomer	HDS reaction products of the HDS of C ₁ -BT isomers
2-methyl-benzothiophene (2-MeBT)	n-Propyl-Benzene
3-methyl-benzothiophene (3-MeBT)	iso-Propyl-Benzene
4-methyl-benzothiophene (4-MeBT)	1-Et-2-Me-Benzene
5-methyl-benzothiophene (5-MeBT)	1-Et-3-Me-Benzene
7-methyl-benzothiophene (7-MeBT)	1-Et-3-Me-Benzene
6-methyl-benzothiophene (6-MeBT)	1-Et-4-Me-Benzene

Table 3.11 The C₂-BT and C₃-BT Isomers and Their Corresponding C₂-BT and C₃-BT Desulfurization Products

C ₂ -BT and C ₃ -BT isomer	reaction products of the HDS of C ₂ -BT and C ₃ -BT isomers
2,3-dimethyl-benzothiophene (2,3-DiMeBT)	1-methyl-Propyl-Benzene
2,5-dimethyl-benzothiophene (2,5-DiMeBT)	1-methyl-3-Propyl-Benzene
2,7-dimethyl-benzothiophene (2,7-DiMeBT)	1-Propyl-3-Me-Benzene
3,6-dimethyl-benzothiophene (3,6-DiMeBT)	1-methyl-Propyl-4-Me-Benzene
2,3,7-trimethyl-benzothiophene (2,3,7-TriMeBT)	1-methyl-Propyl-3-Me-Benzene

a) LCO0605013.D



b) PDT0405010.D

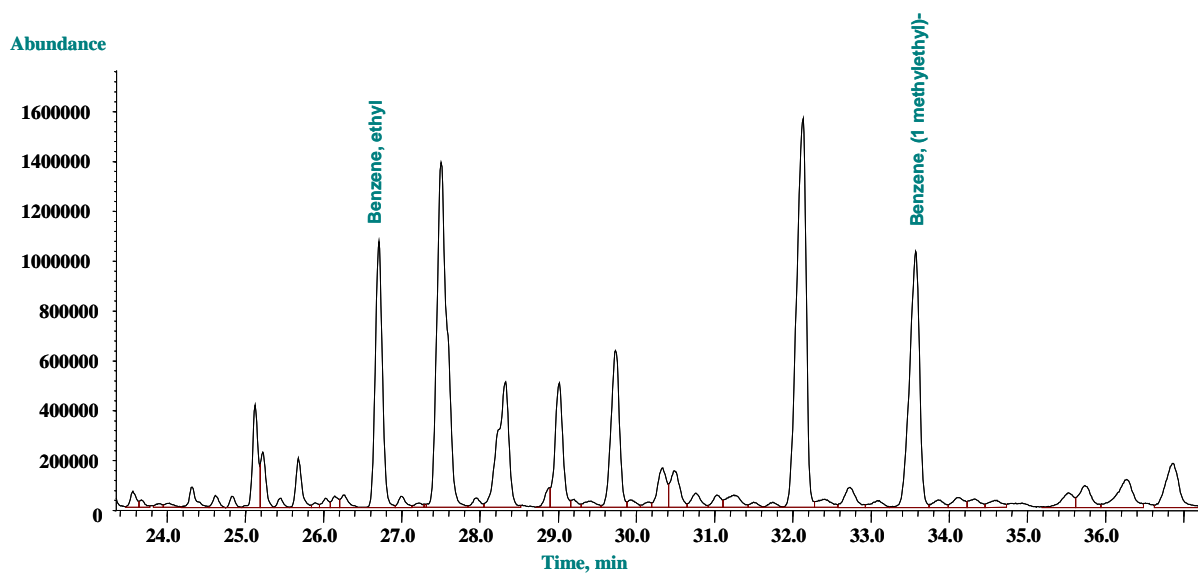


Figure 3.12 Part of the total ion chromatogram of the LCO showing part of the peaks corresponding to the BT and C₁-BT desulfurization products. a) before and b) after hydrodesulfurization.

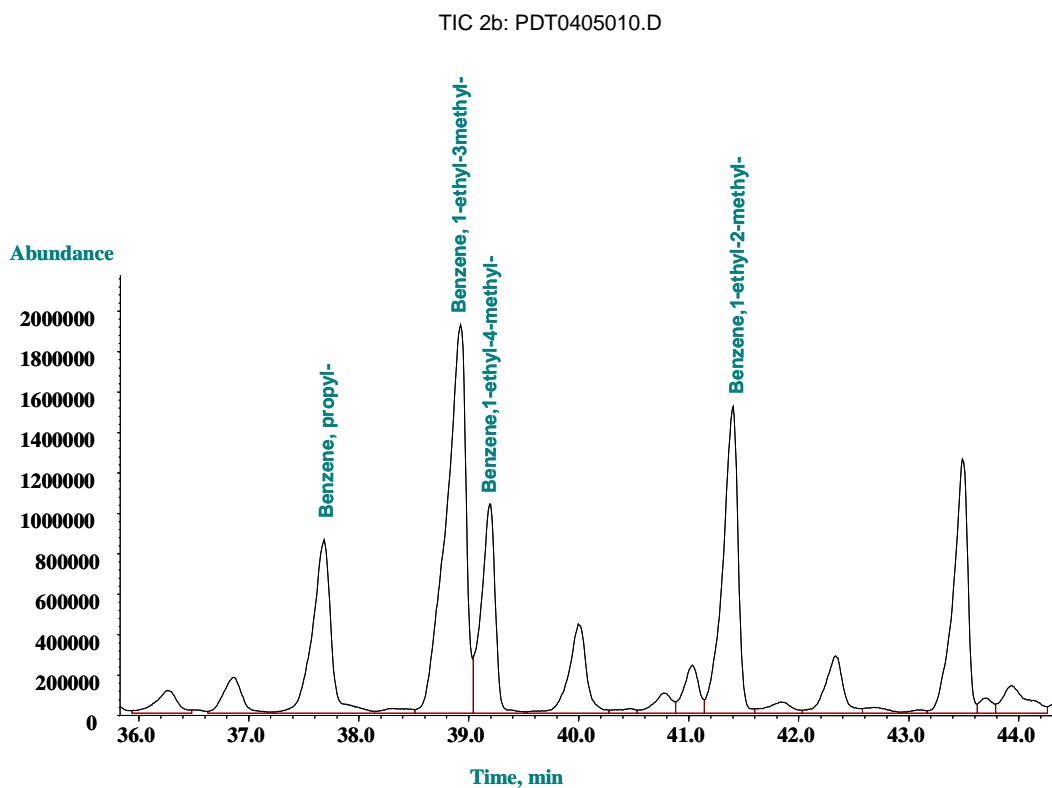
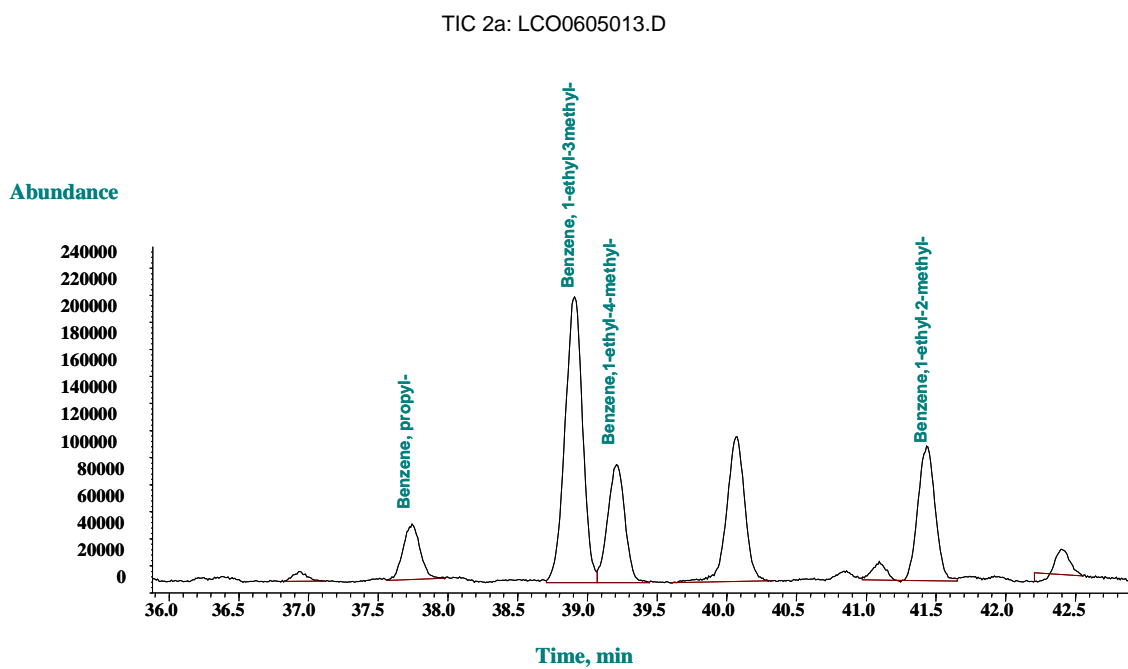
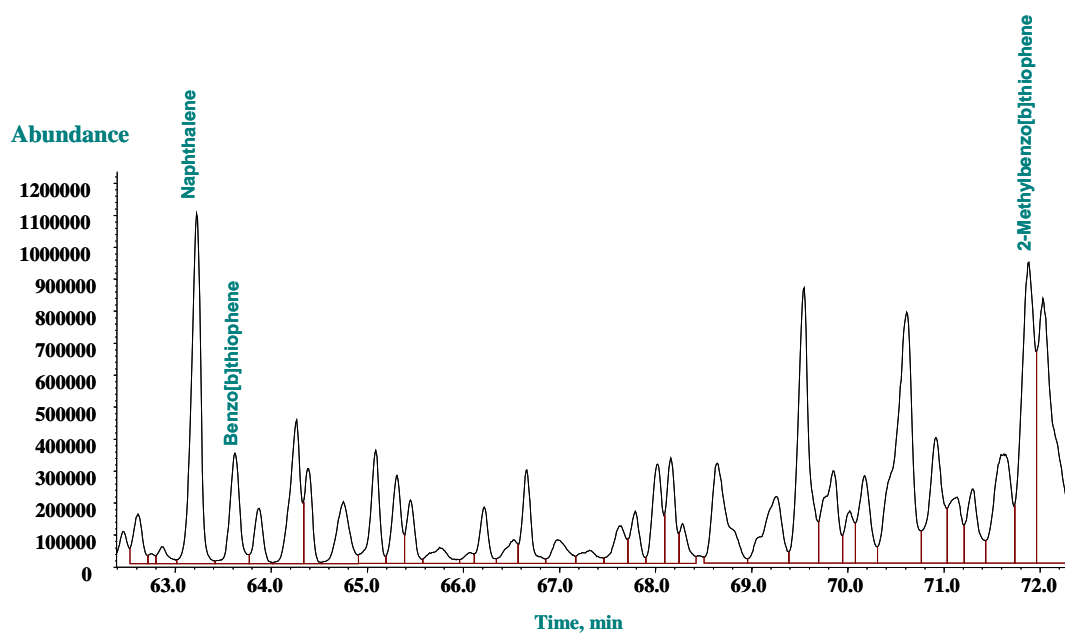


Figure 3.13 Part of the single ion chromatogram of the LCO showing part of the peaks corresponding to the C_1 -BT desulfurization products. a) before and b) after hydrodesulfurization.

a) LCO0605013.D



TIC 3b: PDT0405010.D

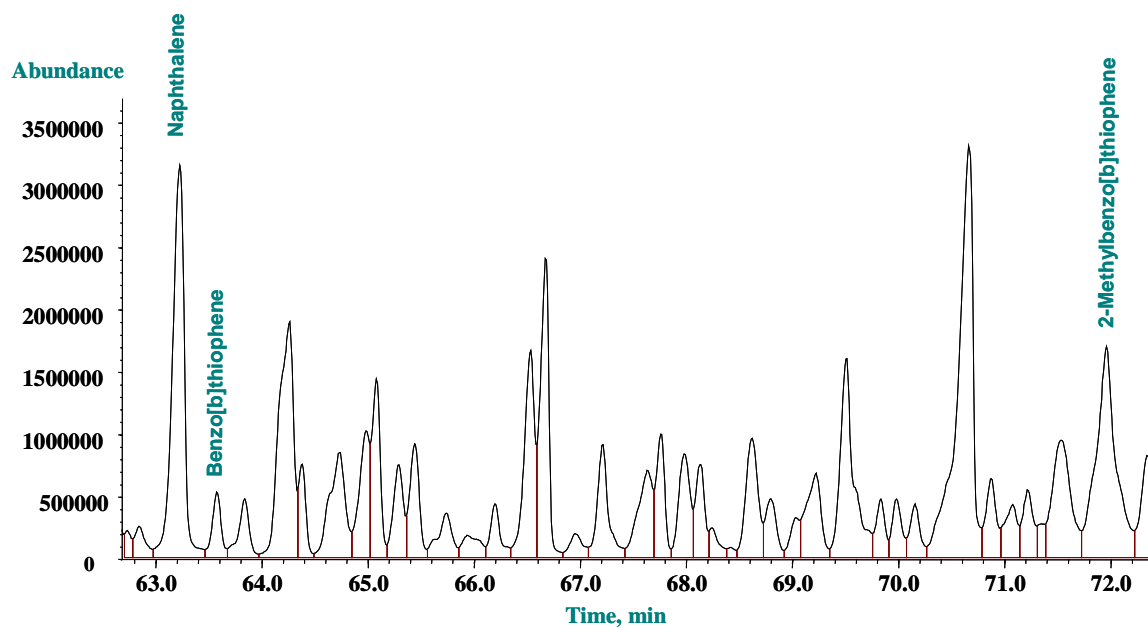
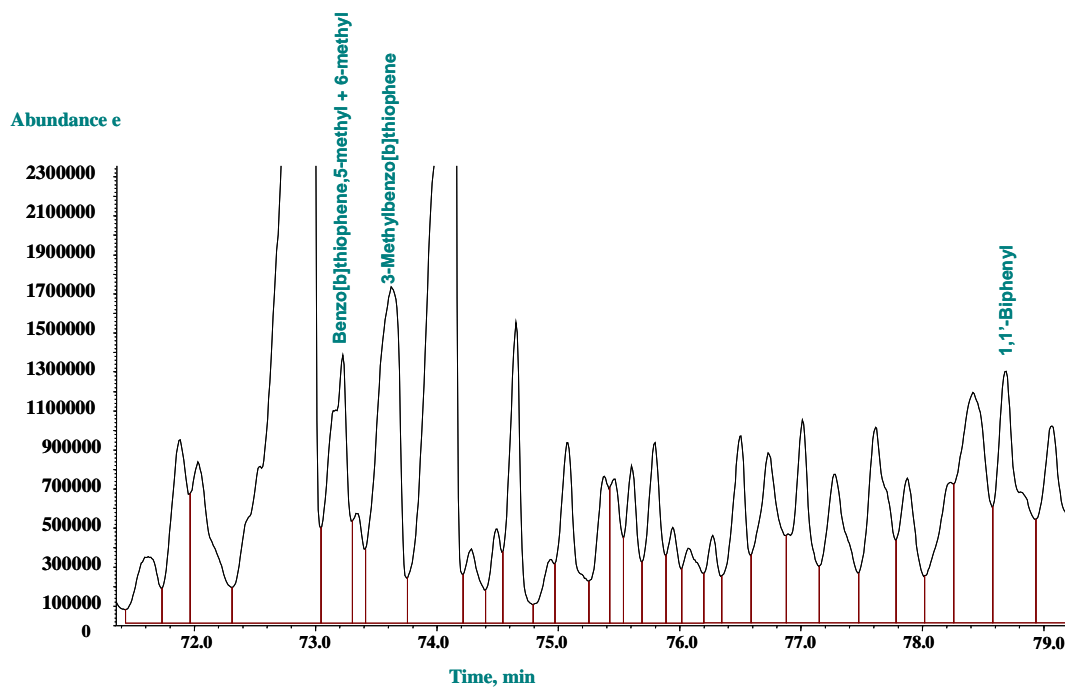


Figure 3.14 Part of the single ion chromatogram of the LCO showing part of the peaks corresponding to the naphthalene and C_1 -BT desulfurization products. a) before and b) after hydrodesulfurization.

a) LCO0605013.D



b) PDT0405010.D

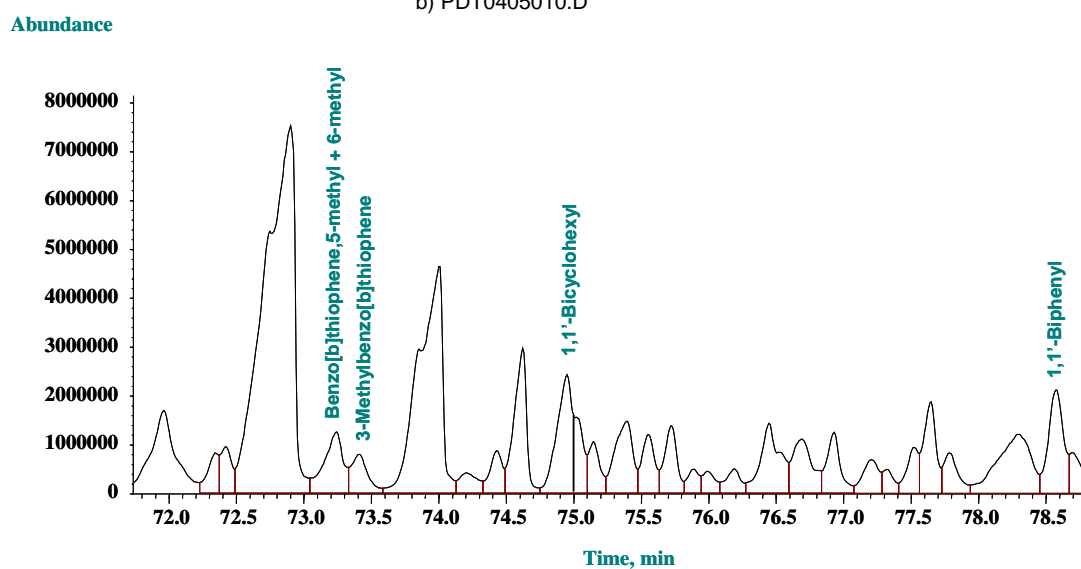


Figure 3.15 Part of the single ion chromatogram of the LCO showing part of the peaks corresponding to the C1-BT desulfurization products. a) before and b) after hydrodesulfurization.

Part of a total ion chromatogram of the LCO with the peaks corresponding to the C₁-BT desulfurization products of the mentioned sulfur compounds before and after HDS on a CoMo/Al₂O₃ catalyst in a completely mixed flow reactor at 330°C, 65.5 bar and a space time of 3550 kg_{cat}-h/kmol DBT are shown from Figure 3.12 to Figure 3.15. The C₁-BT isomers were completely converted under these conditions.

The Figure 3.15 also shows the peak of biphenyl which is the product of hydrogenolysis of DBT and the peak of bicyclohexyl which is the fully hydrogenated component in the hydrodesulfurization of DBT. In Figures 3.16 to Figure 3.20 part of a total chromatogram of the LCO with the peaks corresponding to the C₂-DBT desulfurization products of the referenced sulfur compounds before and after HDS are illustrated.

Figure 3.16 shows the peak of 1,1-biphenyl,3-methyl which is the product of hydrogenolysis of 4-MeDBT. Figure 3.17 shows the peak of 1,1-biphenyl,3,3'-dimethyl which is the product of hydrogenolysis of 4,6-DiMeDBT and the peak of fluorene the internal standard in the GC-MS analysis.

In Figure 3.18 is shown a pair of peaks corresponding to DBT. The Chemstation software integrated the DBT as two separated peaks because inflections in the upper level of the peak, however, both peaks were confirmed as DBT with the database of the GC-MS. The peak of phenanthrene is identified in this figure as well. Figure 3.19 shows the peaks of 4-Me-DBT and 3-MeDBT while the Figure 3.20 shows the other C₁-DBT, C₂-DBT presented in Table 3.10.

Some parts of these chromatograms show poor resolution for the identified and selected sulfur compounds. This is because of the complexity of the samples for a MS detector. More than 500 compounds are separated in every analysis. Moreover, the important peaks corresponding to those sulfur compounds are in the level of low abundances.

Even if the identification and quantification is an exhausting assignment, the sets of representative sulfur compounds shown in Tables 3.9 and Table 3.10 are in good agreement with the expected behavior that is shown by Vanrysselberghe & Froment (1996), for calculating conversions of BT, DBT in the HDS of the LCO.

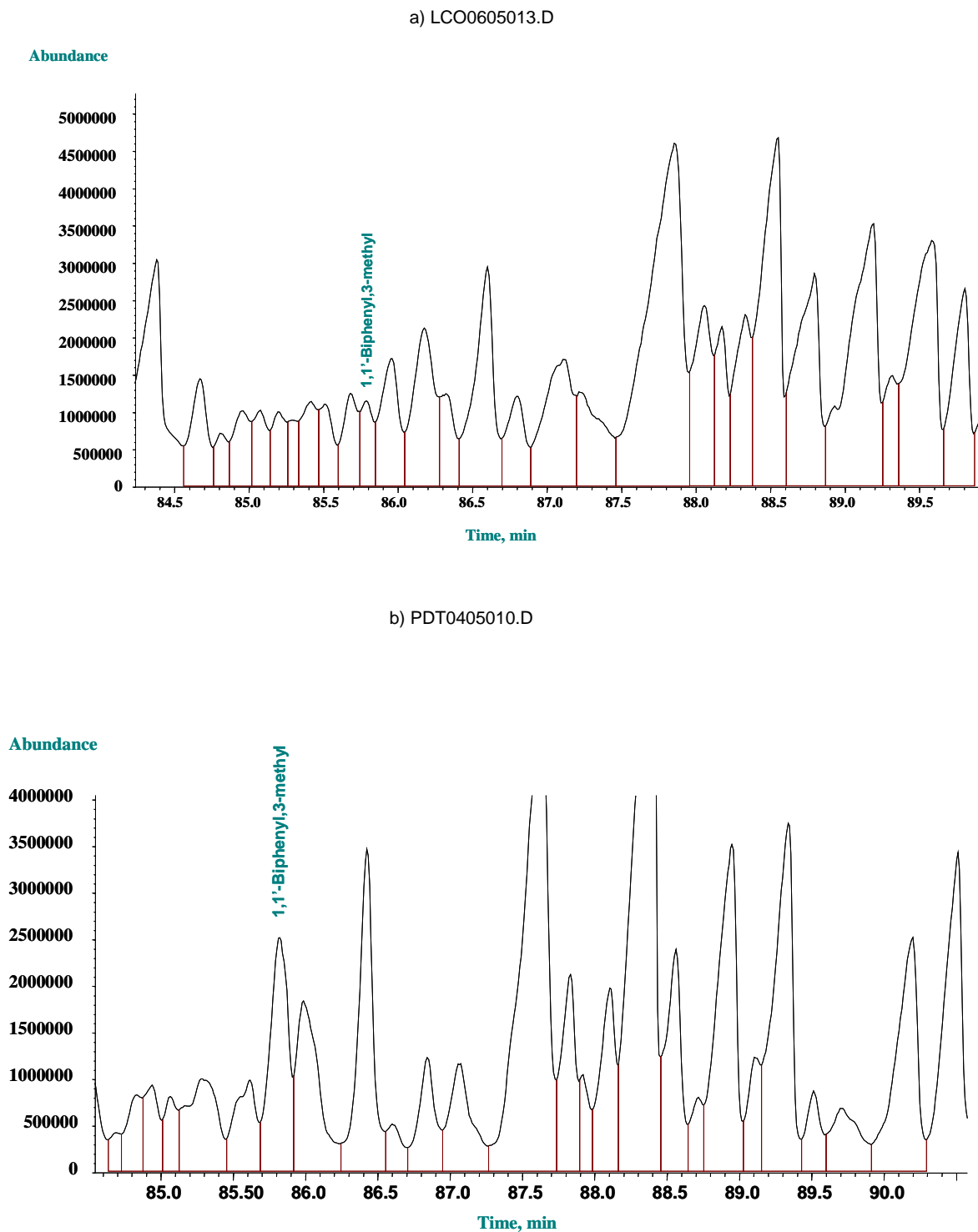
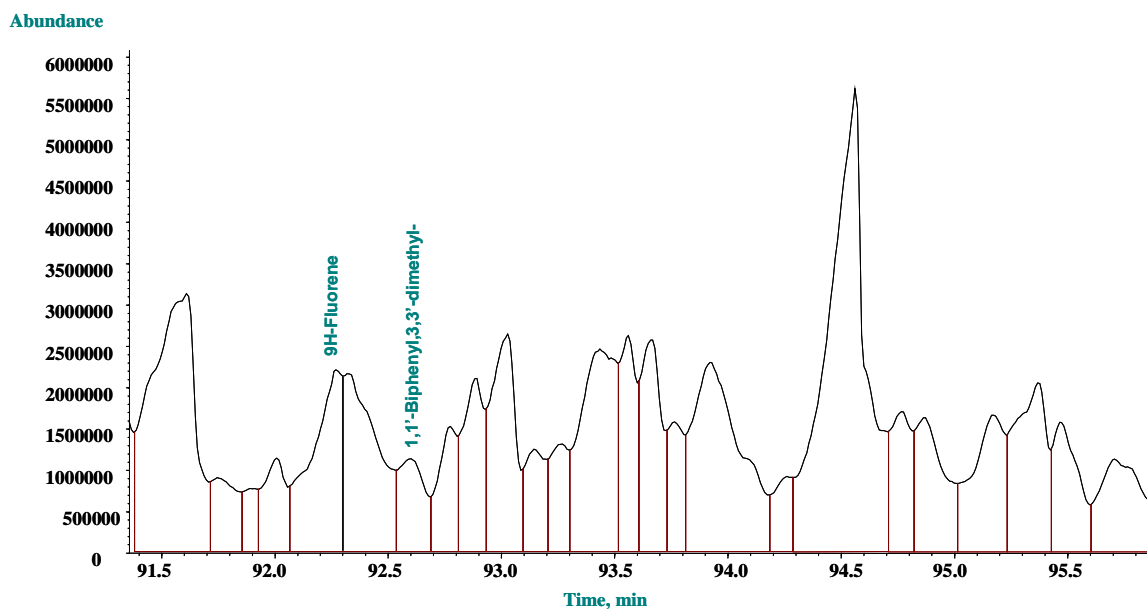


Figure 3.16 Part of the total ion chromatogram of the LCO showing the peaks corresponding to the C₁-DBT desulfurization products. a) before and b) after hydrodesulfurization.

a) LCO0605013.D



b) PDT0405010.D

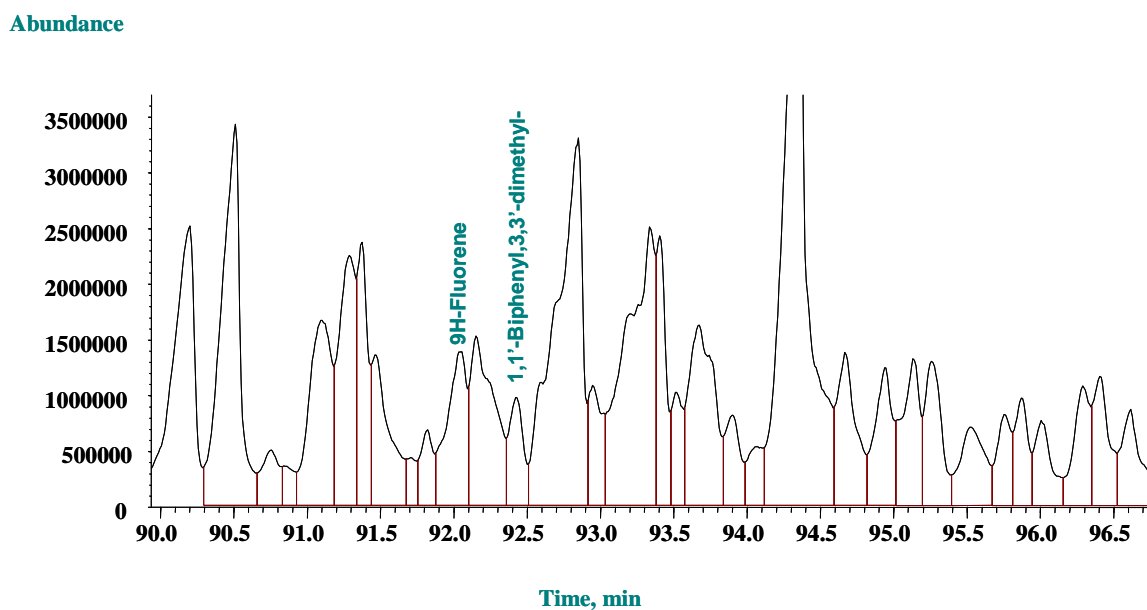


Figure 3.17 Part of the single ion chromatogram of the LCO showing part of the peaks corresponding to the C₁-DBT desulfurization products and Fluorene the internal standard. a) before and b) after hydrodesulfurization.

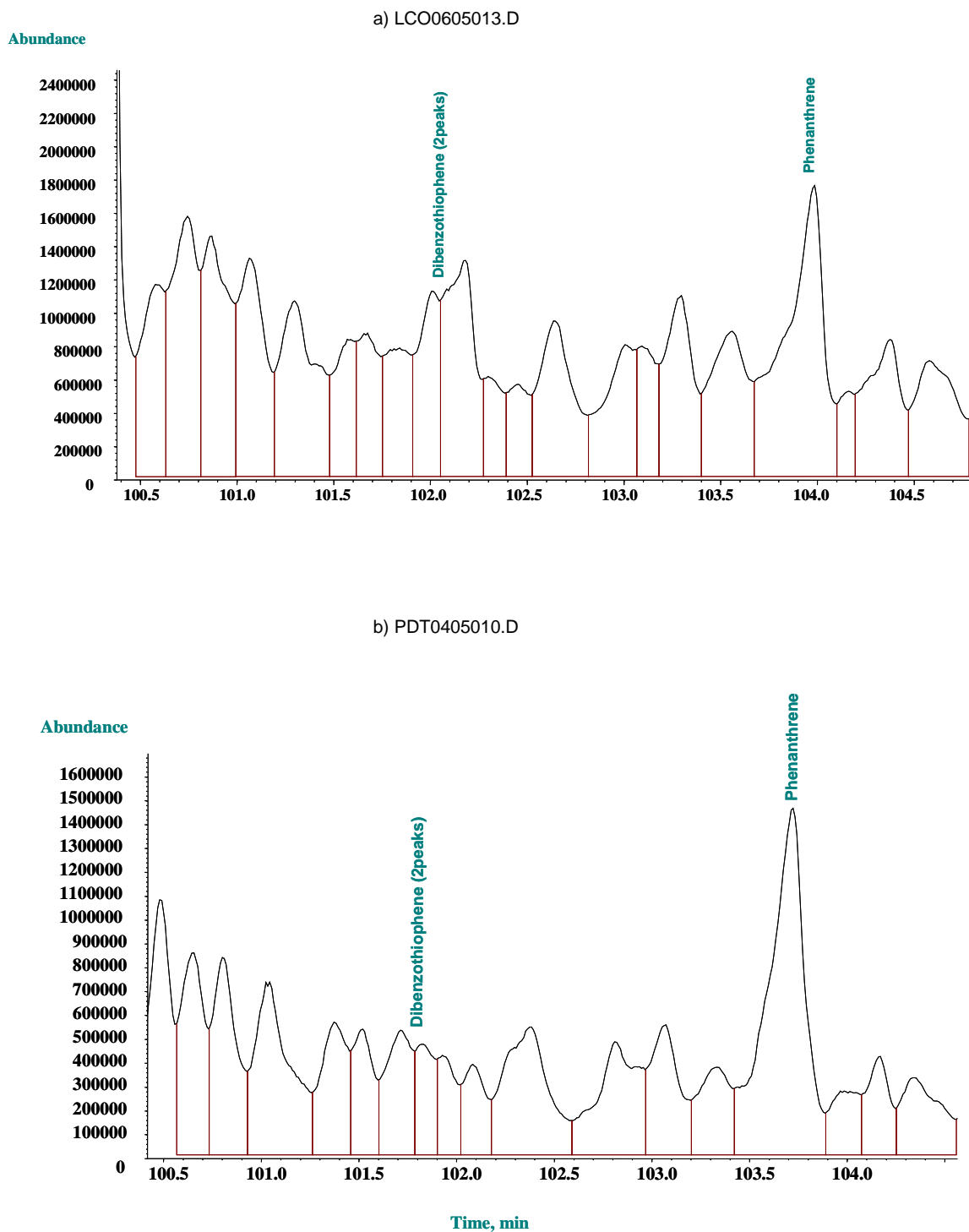
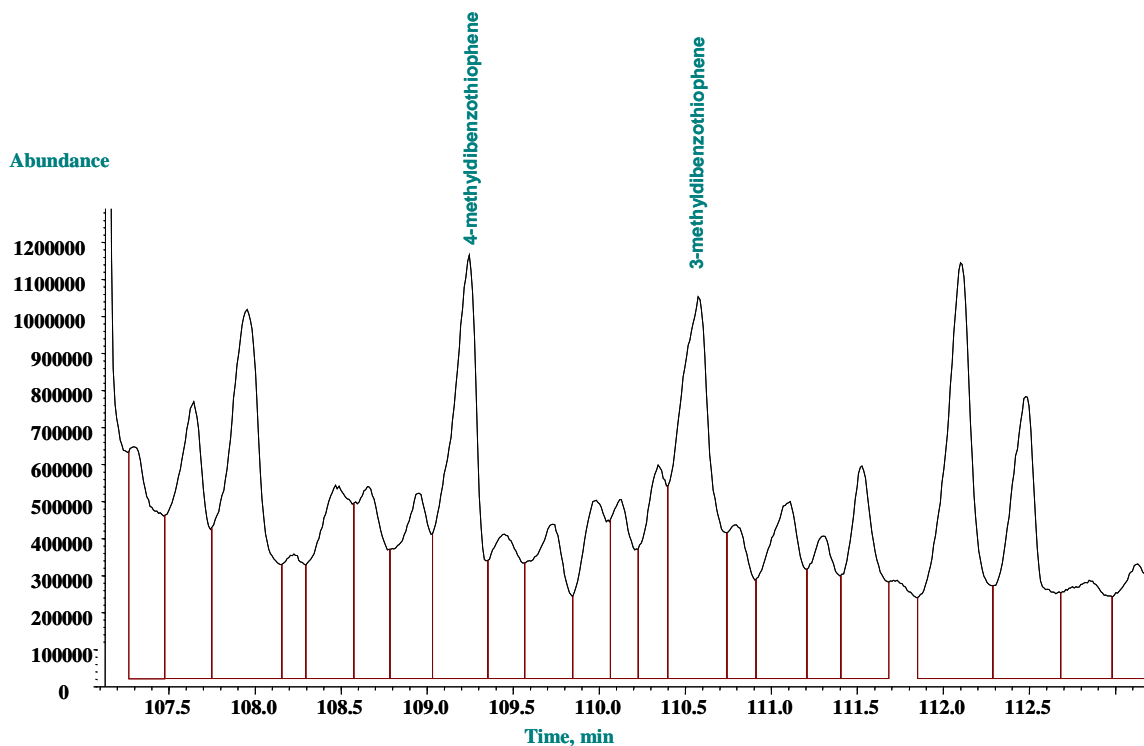


Figure 3.18 Part of the single ion chromatogram of the LCO showing part of the peaks corresponding to the C_1 -DBT desulfurization products. a) before and b) after hydrodesulfurization.

a) LCO0605013.D



b) PDT0405010.D

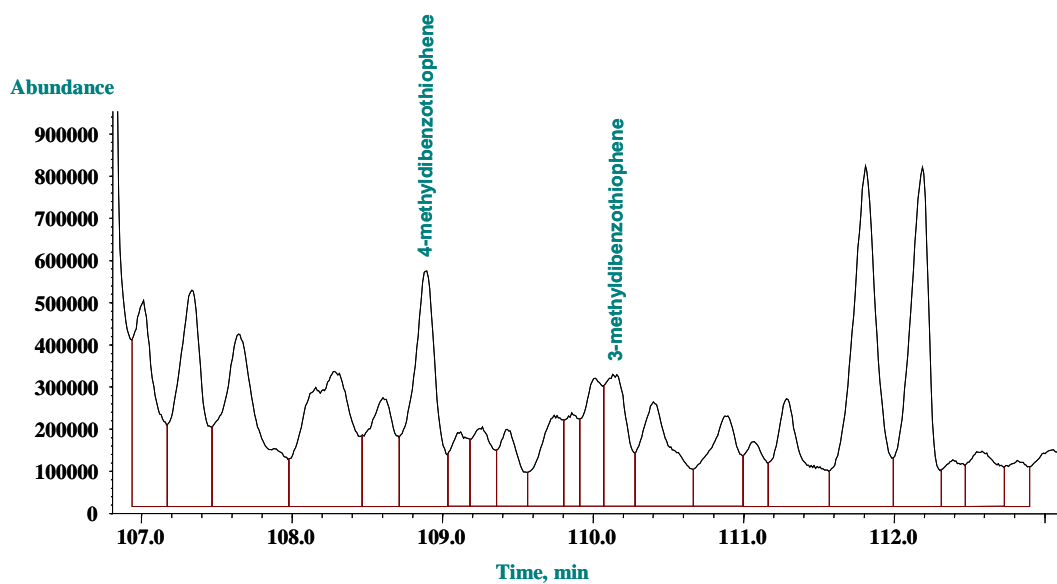


Figure 3.19 Part of the single ion chromatogram of the LCO showing part of the peaks corresponding to the C₁-BT desulfurization products. a) before and b) after hydrodesulfurization.

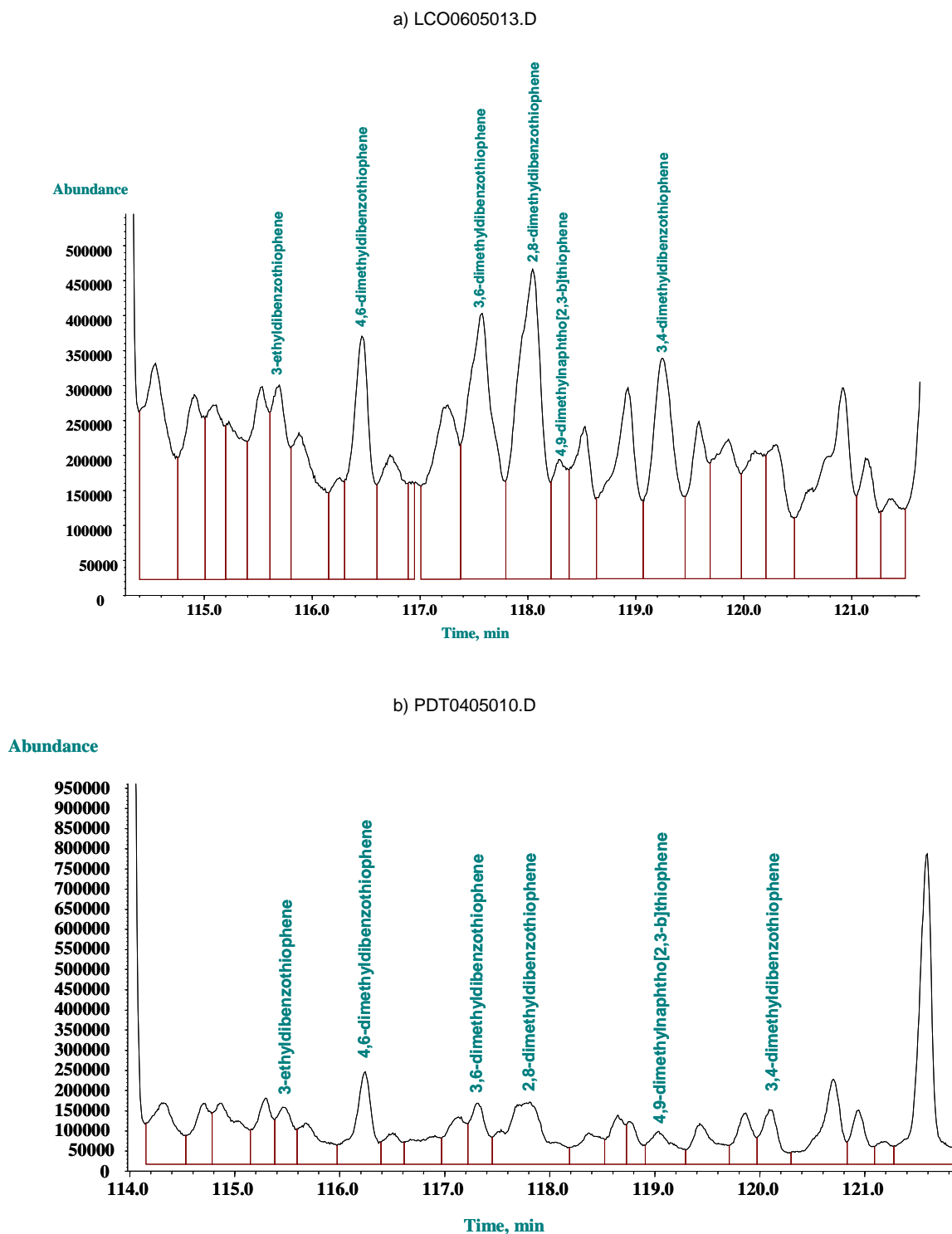


Figure 3.20 Part of the single ion chromatogram of the LCO showing part of the peaks corresponding to the C₂-BT desulfurization products. a) before and b) after hydrodesulfurization.

3.6.4 Conversions

3.6.4.1 Steady State Test

In order to assure the steady state was reached, an experiment was run to determine the required volume of reacting mixture that have to flow through the reactor before the conversion becomes constant. The plot of total conversion of DBT as a function of the operation time is shown in Figure 3.21. In this test one volume of reacting mixture is leaving the reactor after 19 hours while 5 volumes of the same reacting mixture are displaced after 81 hours. These times are relatively long because the reactor volume in this setup is 1.0 liter.

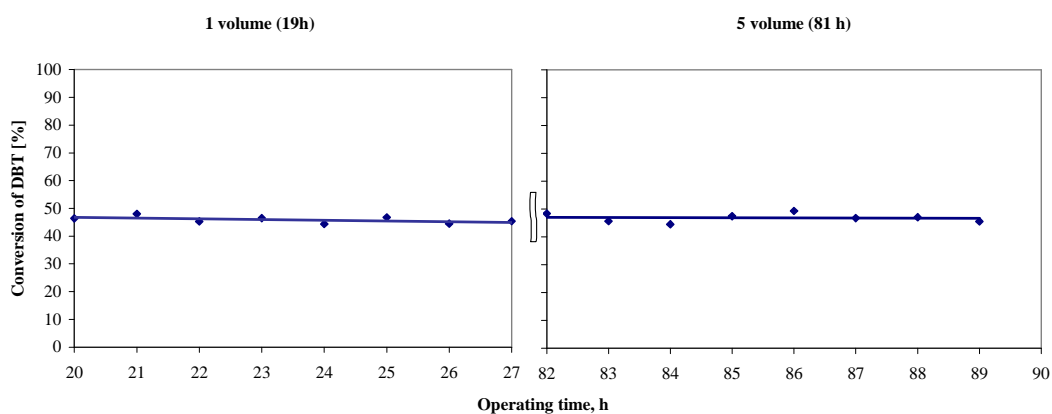


Figure 3.21 Total conversion of DBT as a function of operating time. Experimental conditions. $P=65.5$ bar, $T=330^{\circ}\text{C}$, $W/F_{\text{DBT}}^0=3550$ $\text{kg}_{\text{cat}}\text{-h/kmol}$, $\text{H}_2/\text{HC}=2.8$ mol ratio.

The conversion of DBT after one volume displaced is essentially the same compared with the conversion of DBT after one and 5 volumes. This test was important in order to define when the steady state is reached and consequently a reduction in time of every run was obtained. Because the conversion of DBT obtained after 1 volume is enough to determine the steady state, 1.5 volumes were chosen to run the set of experiments.

3.6.4.2 Total Conversion of DBT in the HDS of the LCO

Figure 3.22 shows the total conversion of DBT as function of space time (W/F_{DBT}^0) measured at 290°C, 310°C and 330°C respectively. The results shown in this and further figures correspond to the experiments considering steady state as defined in the latter section (3.6.4.1). The conversion of DBT increased with space-time and temperature. The maximum conversion (62%) is observed at 6110 $\text{kg}_{\text{cat}} \text{ h/kmol}$ and 330°C.

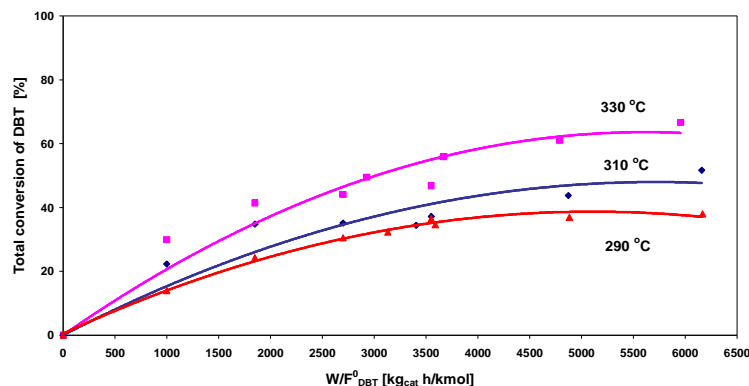


Figure 3.22 Total conversion of DBT as a function of W/F^0_{DBT} . Experimental conditions. $P=65.5$ bar, $H_2/HC=2.8$ mol ratio. Symbols: experimental. Curves: visual fit.

3.6.4.3 Conversions of DBT into BPH and CHB in the HDS of the LCO

The results on the total conversion of DBT, conversion of DBT into BPH and the conversion of DBT into cyclohexylbenzene (CHB) as a function of W/F^0_{DBT} are shown in figures 3.23, 3.24 and 3.25 for temperatures of 330°, 310° and 290°C respectively.

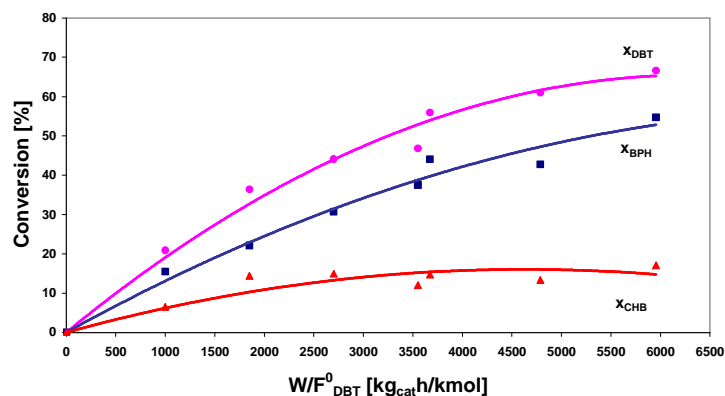


Figure 3.23 Conversions as a function of space time, W/F^0_{DBT} and $T=330^\circ\text{C}$. (x_{DBT})= total conversion of DBT, (x_{BPH})= conversion of DBT into biphenyl, (x_{CHB})= conversion of DBT into cyclohexylbenzene. Experimental conditions: $P= 65.5$ bar, $H_2/HC= 2.8$ mol ratio. Symbols: experimental. Curves: visual fit.

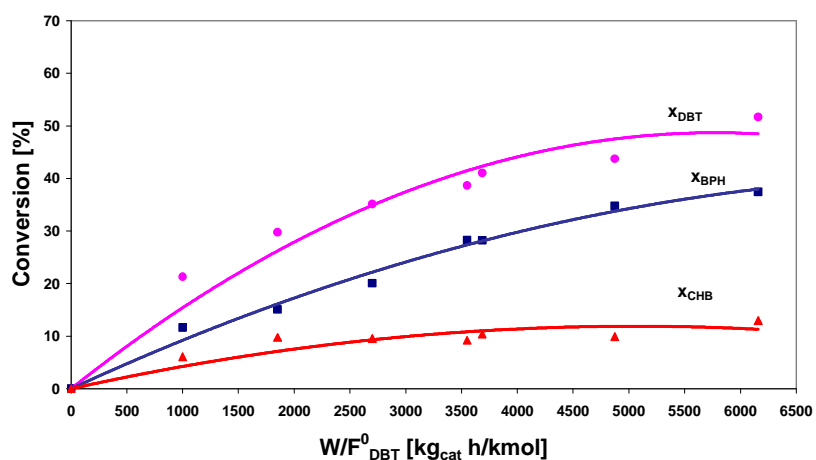


Figure 3.24 Conversions as a function of space time, W/F_{DBT}^0 and $T=310^\circ\text{C}$. (x_{DBT})= total conversion of DBT, (x_{BPH})= conversion of DBT into biphenyl, (x_{CHB})= conversion of DBT into CHB. Experimental conditions: $P= 65.5$ bar, $H_2/HC= 2.8$ mol ratio. Symbols: experimental. Curves: visual fit.

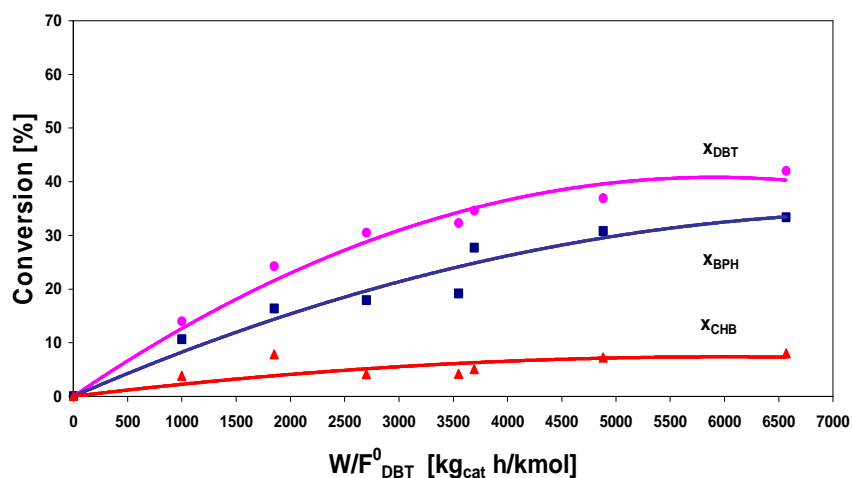


Figure 3.25 Conversions as a function of space time, W/F_{DBT}^0 and $T=290^\circ\text{C}$. (x_{DBT})= total conversion of DBT, (x_{BPH})= conversion of DBT into biphenyl, (x_{CHB})= conversion of DBT into CHB. Experimental conditions: $P= 65.5$ bar, $H_2/HC= 2.8$ mol ratio. Symbols: experimental. Curves: visual fit.

CHAPTER IV

FORMULATION OF THE KINETIC MODEL

4.1 Previous Work

The development of kinetic modeling for the hydrotreatment of oil fractions has been extensively explored; however, most of the researchers have studied the HDS of oil fractions in terms of lumps of sulfur components converted according to first-order or second-order kinetics (Diaz et al., 1993; Kumar et al., 2001; Lecrenay et al., 1997; Marroquin and Ancheyta, 2001).

Very few of these studies dealt with sulfur removal in terms of individual sulfur components (Chen et al., 2003; Kabe et al., 1997; Ma et al., 1994).

Extensive studies of the kinetic modeling and simulation of the hydrotreatment reactions have been made by Van Parys and Froment (1986), Van Parys et al. (1986), Froment et al. (1994, and 1997) and Vanrysselberghe and Froment (1996, and 1998b). Rigorous kinetics models have been introduced for the HDS of oil fractions (Froment et al. 1994). Rate equations for all reactions in the network for the HDS of DBT were developed on a commercial CoMo/Al₂O₃ catalyst under operating conditions significant to industrial applications (Vanrysselberghe and Froment 1996). Rate equations of the Hougen-Watson type were developed for the HDS of 4-Me-DBT and 4,6-DiMeDBT on the same catalyst and operating conditions (Vanrysselberghe et al. 1998a).

4.2 Reaction Network and Kinetic Modeling at the Molecular Level

Figure 4.1 shows a reaction scheme for the decomposition of dibenzothiophene. In this scheme the dibenzothiophene (DBT) like other sulfur-containing compounds are converted along two parallel routes. The first directly eliminates the S-atom by hydrogenolysis, which is a scission of the C-S bond. The second begins with hydrogenation whose products undergo a C-S scission. Hydrogenolysis and hydrogenation steps occur on different sites: σ sites for the first and τ sites for the last (Delmon, 1979; Gates et al., 1979; Vrinat, 1983; Van Parys and Froment, 1986; Edvinson and Irandoust, 1993; Froment 2004).

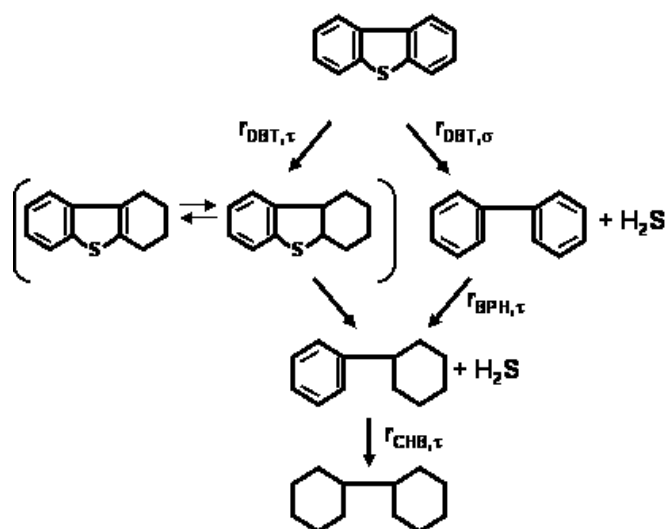


Figure 4.1 Reaction network for the HDS of dibenzothiophene into biphenyl (BPH), cyclohexylbenzene (CHB) and bicyclohexyl (BCH). (Houalla et al. 1978, Vanrysselberghe et al. 1996)

4.2.1 Rate Equations

The net production rates, R_i for biphenyl, cyclohexylbenzene and bicyclohexyl derived from the reaction scheme of DBT shown in Figure 4.1 are defined as

$$R_{BPH} = r_{DBT,\sigma} - r_{BPH,\tau} \quad (4.1)$$

$$R_{CHB} = r_{DBT,\tau} + r_{BPH,\tau} - r_{CHB,\tau} \quad (4.2)$$

$$R_{BCH} = r_{BCH,\tau} \quad (4.3)$$

The total rate of disappearance of DBT represented by the summation of the consumption of DBT by hydrogenolysis and hydrogenation is given by

$$R_{DBT} = r_{DBT,\sigma} + r_{DBT,\tau} \quad (4.4)$$

Several possible reaction mechanisms and corresponding Hougen-Watson rate equations were derived by Vanrysselberghe and Froment (1996). The various reaction mechanisms only differ by the way of adsorption of hydrogen. Table 4.1 shows the

different ways that hydrogen can be adsorbed. All these ways were considered by those researchers.

Table 4.1 Ways of Hydrogen Can be Adsorbed on the Active Sites of Catalyst.

Key	Way of adsorption
(A)	Atomic
(M)	Molecularly
(σ_c)	competitively in hydrogenolysis
(τ_c);	and hydrogenation
(σ_{nc} , τ_{nc});	Noncompetitively on a third type of active sites
(σ_τ)	Noncompetitively on the active sites for hydrogenation
(τ_σ)	or hydrogenolysis

The addition of the first H atom, the addition of the second H atom, and the simultaneous addition of two hydrogen atoms were considered for the adsorption of atomic hydrogen (A). Reaction with H₂ directly from the liquid phase was also considered.

The sulfur atom removed from DBT, THDBT, or HHDBT remains on the catalyst surface after reaction. Its removal occurs by means of reaction with H₂ directly from the liquid phase or via a mechanism corresponding with the mechanism of hydrogenolysis on the σ sites.

The discrimination between 174 rival models and parameter estimation led Vanrysselberghe and Froment (1996) to the following reaction mechanism

(A)(σ_c)(τ_c)(S_σ):

- a). Hydrogenolysis of DBT into BPH and H₂S on the σ sites. The rate-determining step (rds) was the surface reaction between the adsorbed species.
- b). Hydrogenation of DBT into THDBT and HHDBT on the τ sites followed by hydrogenolysis into CHB and H₂S on the σ sites. The rds was the surface reaction between the adsorbed species DBT and hydrogen.
- c). Hydrogenation of BPH into CHB on the τ sites. The rds was the surface reaction between the adsorbed species BPH and hydrogen.
- d). Hydrogenation of CHB into BCH on the τ sites. The rds was the surface reaction between the adsorbed species CHB and hydrogen.

The corresponding rate equations for dibenzothiophene (DBT) into biphenyl (BPH), which is further converted into bicyclohexylbenzene, can be written.

$$r_{DBT,\sigma} = \left[\frac{k_{DBT,\sigma} K_{DBT,\sigma} K_{H,\sigma} C_{DBT} C_{H_2}}{\left(1 + K_{DBT,\sigma} C_{DBT} + \sqrt{K_{H,\sigma} C_{H_2}} + K_{BPH,\sigma} C_{BPH} + K_{H_2S,\sigma} C_{H_2S}\right)^3} \right] \quad (4.5)$$

$$r_{DBT,\tau} = \left[\frac{k_{DBT,\tau} K_{DBT,\tau} K_{H,\tau} C_{DBT} C_{H_2}}{\left(1 + K_{DBT,\tau} C_{DBT} + \sqrt{K_{H,\tau} C_{H_2}} + K_{BPH,\tau} C_{BPH}\right)^3} \right] \quad (4.6)$$

$$r_{BPh,\tau} = \left[\frac{k_{BPh,\tau} K_{BPh,\tau} K_{H,\tau} C_{BPh} C_{H_2}}{\left(1 + K_{DBT,\tau} C_{DBT} + \sqrt{K_{H,\tau} C_{H_2}} + K_{BPh,\tau} C_{BPh}\right)^3} \right] \quad (4.7)$$

$$r_{CHB,\tau} = \left[\frac{k_{CHB,\tau} K_{CHB,\tau} K_{H,\tau} C_{CHB} C_{H_2}}{\left(1 + K_{DBT,\tau} C_{DBT} + \sqrt{K_{H,\tau} C_{H_2}} + K_{BPh,\tau} h_{BPh}\right)^3} \right] \quad (4.8)$$

The rate expressions for the HDS of the methyl substituted dibenzothiophenes are of the same functional form.

In the classical approach there are 215 rate equations for hydrogenolysis and 282 rate equations for the hydrogenations in the reaction networks of DBT and mono-, di-, and trisubstituted DBT. As shown in Table 4.2, these rate equations contain 497 kinetic coefficients and 635 adsorption equilibrium constants. (Froment et al. 1994)

Table 4.2 Total Number of Parameters for the Hydrodesulfurization of DBT and Methyl-Substituted Dibenzothiophene in the Classical Molecular Approach: 1132.

σ -Sites		
Adsorption (s)-DBT	$K_{\text{DBT},\sigma}(m;n;p)$	45
Hydrogenolysis (s)-DBT	$k_{\text{DBT},\sigma}(m;n;p)$	45
Adsorption (s)-BPH	$K_{\text{BPH},\sigma}(m;n;p)$	30
Adsorption (s)-THDBT	$K_{\text{THDBT},\sigma}(m;n;p)$	85
Hydrogenolysis (s)-THDBT	$k_{\text{THDBT},\sigma}(m;n;p)$	85
Adsorption (s)-HHDBT	$K_{\text{HHDBT},\sigma}(m;n;p)$	85
Hydrogenolysis (s)-HHDBT	$k_{\text{HHDBT},\sigma}(m;n;p)$	85
Adsorption (s)-CHB	$K_{\text{CHB},\sigma}(m;n;p)$	56
Adsorption H_2	$K_{\text{H}_2,\sigma}$	1
Adsorption H_2S	$K_{\text{H}_2\text{S},\sigma}$	1
τ -Sites		
Adsorption (s)-DBT	$K_{\text{DBT},\tau}(m;n;p)$	45
Hydrogenation (s)-DBT	$k_{\text{DBT},\tau}(m;n;p)$	85
Adsorption (s)-THDBT	$K_{\text{THDBT},\tau}(m;n;p)$	85
Hydrogenation (s)-THDBT	$k_{\text{THDBT},\tau}(m;n;p)$	85
Adsorption (s)-HHDBT	$K_{\text{HHDBT},\tau}(m;n;p)$	85
Adsorption (s)-BPH	$K_{\text{BPH},\tau}(m;n;p)$	30
Hydrogenation (s)-BPH	$k_{\text{BPH},\tau}(m;n;p)$	56
Adsorption (s)-CHB	$K_{\text{CHB},\tau}(m;n;p)$	56
Hydrogenation (s)-CHB	$k_{\text{CHB},\tau}(m;n;p)$	56
Adsorption (s)-BCH	$k_{\text{BCH},\tau}(m;n;p)$	30
Adsorption H_2	$K_{\text{H}_2,\tau}$	1

A kinetic model containing such a number of parameters is evidently not only impractical but it would be impossible to determine their value. Consequently a different modeling approach is required to reduce this number. In this development the kinetic modeling is based on structural contributions (Froment et al., 1994).

4.3 Kinetic Modeling Based Upon Structural Contributions

For reactions involving substituted sulfur components, the rates are related to those of a nonsubstituted reference component in terms of the electronic effects and the steric hindrance of the substituents on the adsorption equilibrium constants and the rate coefficients. (Froment et al., 1994)

Vanrysselberghe and Froment, (1998b) reported that the introduction of a methyl group in positions 1, 2, and/or 3 does not influence the rate of hydrogenolysis. These substituents are distant from the sulfur atom and do not cause steric hindrance on the vertical adsorption through the sulfur atom or on the surface reaction on the σ sites. Methyl groups in positions 4 and/or 6 cause a decrease in the rate of hydrogenolysis compared to that of dibenzothiophene. This is due to the steric hindrance of these methyl substituents.

4.3.1 Hydrogenolysis Reactions

The methodology of structural contributions comprises several assumptions which permit the reduction of the number of parameters for the hydrogenolysis steps as shown in Table 4.3.

Table 4.3 Assumptions Comprised in the Hydrogenolysis Step of Structural Contributions.

Assumption	Statement
1	In the adsorption electronic and steric effects are to be considered separately.
2	Methyl groups at a distance from the sulfur atom beyond the α -position only exert electronic effects on the adsorption.
3	Only methyl groups on the aromatic ring exert an electronic influence.
4	Methyl groups in the 4- and 6-positions also sterically obstruct the adsorption.
5	Once a molecule is adsorbed, only the electronic effects of the methyl groups are of importance.

The adsorption equilibrium constants for the various substituted dibenzothiophenes are related to that of DBT through five multiplying factors. Instead of 45 different parameters in the molecular approach, only 6 parameters appear in the approach based upon structural contributions: one adsorption equilibrium constant $K_{\text{DBT},\sigma}$ and 5 structural contributions.

$$K_{\text{DBT},\sigma}, K_{\text{EL}}^{\text{DBT}}(m;0;0), K_{\text{EL}}^{\text{DBT}}(m;n;0), K_{\text{EL}}^{\text{DBT}}(m;n;p), K_{\text{ST}}^{\text{DBT}}(4;0;0), \text{ and } K_{\text{ST}}^{\text{DBT}}(4;0;6)$$

The rate coefficient for the hydrogenolysis of (substituted) DBT into (substituted) biphenyl ((s)-BPH) depends only on the number of methyl groups. There are four rate coefficients:

$$\begin{aligned} k_{\text{DBT},\sigma}(0;0;0) & \quad \text{For DBT} \\ k_{\text{DBT},\sigma}(m;0;0) &= k_{\text{DBT},\sigma}(0;0;0) k_{\text{EL}}^{\text{DBT}}(m;0;0) \quad \text{For mono-Me-DBT} \\ k_{\text{DBT},\sigma}(m;n;0) &= k_{\text{DBT},\sigma}(0;0;0) k_{\text{EL}}^{\text{DBT}}(m;n;0) \quad \text{For di-Me-DBT} \\ k_{\text{DBT},\sigma}(m;n;p) &= k_{\text{DBT},\sigma}(0;0;0) k_{\text{EL}}^{\text{DBT}}(m;n;p) \quad \text{For tri-Me-DBT} \end{aligned}$$

The adsorption equilibrium constant for the product (substituted) biphenyl on the σ -sites is assumed to depend only on the total number of methyl groups:

$$\begin{aligned} K_{\text{BPH},\sigma}(0;0;0) & \quad \text{For biphenyl} \\ K_{\text{BPH},\sigma}(m;0;0) &= K_{\text{BPH},\sigma}(0;0;0) K_{\text{EL}+\text{ST}}^{\text{BPH}}(m;0;0) \quad \text{For mono-Me-biphenyl} \\ K_{\text{BPH},\sigma}(m;n;0) &= K_{\text{BPH},\sigma}(0;0;0) K_{\text{EL}+\text{ST}}^{\text{BPH}}(m;n;0) \quad \text{For di-Me-biphenyl} \\ K_{\text{BPH},\sigma}(m;n;p) &= K_{\text{BPH},\sigma}(0;0;0) K_{\text{EL}+\text{ST}}^{\text{BPH}}(m;n;p) \quad \text{For tri-Me-biphenyl} \end{aligned}$$

For the hydrogenolysis of substituted tetrahydrodibenzothiophene (s-THDBT), which contains a benzene ring and one thiophenic ring, the approach reduces the number of adsorption equilibrium constants from 85 to 6: one adsorption equilibrium constant $K_{\text{THDBT},\sigma}$ and 5 structural contributions.

$$K_{\text{THDBT},\sigma}, K_{\text{EL}}^{\text{THDBT}}(m;0;0), K_{\text{EL}}^{\text{THDBT}}(m;n;0), K_{\text{ST}}^{\text{THDBT}}(4;0;0), K_{\text{ST}}^{\text{THDBT}}(0;0;6), \text{ and } K_{\text{ST}}^{\text{THDBT}}(4;0;6)$$

For the rate coefficient for the hydrogenolysis of (substituted) tetrahydrodibenzothiophene into (substituted) cyclohexylbenzene ((s)-CHB), only the number of methyl groups on the aromatic ring has to be considered:

$$k_{\text{THDBT},\sigma}(0;0;0), k_{\text{THDBT},\sigma}(m;0;0) = k_{\text{THDBT},\sigma}(0;0;0)k_{\text{EL}}^{\text{THDBT}}(m;0;0)$$

$$k_{\text{THDBT},\sigma}(m;n;0) = k_{\text{THDBT},\sigma}(0;0;0)k_{\text{EL}}^{\text{THDBT}}(m;n;0)$$

The same has to be done for the hydrogenolysis of (substituted) hexahydrodibenzothiophene ((s)-HHDBT), which has only one benzene ring. Only methyl substituents on this ring are considered to have an electronic influence. Instead of 85 parameters, only the following 6 parameters have to be determined: one adsorption equilibrium constant $K_{\text{HHDBT},\sigma}$ and 5 structural contributions.

$$K_{\text{HHDBT},\sigma}, K_{\text{EL}}^{\text{HHDBT}}(m;0;0), K_{\text{EL}}^{\text{HHDBT}}(m;n;0), K_{\text{ST}}^{\text{HHDBT}}(4;0;0), K_{\text{ST}}^{\text{HHDBT}}(0;0;6), \text{ and } K_{\text{ST}}^{\text{HHDBT}}(4;0;6)$$

The rate coefficient for the hydrogenolysis of (substituted) hexahydrodibenzothiophene into (substituted) cyclohexylbenzene depends only on the number of methyl groups on the aromatic ring:

$$k_{\text{HHDBT},\sigma}(0;0;0),$$

$$k_{\text{HHDBT},\sigma}(m;0;0) = k_{\text{HHDBT},\sigma}(0;0;0) k_{\text{EL}}^{\text{HHDBT}}(m;0;0), \text{ and}$$

$$k_{\text{HHDBT},\sigma}(m;n;0) = k_{\text{HHDBT},\sigma}(0;0;0) k_{\text{EL}}^{\text{HHDBT}}(m;n;0).$$

The adsorption constant for (substituted) cyclohexylbenzene on the σ -sites, $K_{\text{CHB},\sigma}$ depends on the number of methyl groups on the phenyl and the cyclohexyl structures. In total there are 215 hydrogenolysis rate equations with 42 parameters which need to be determined from experimental data.

4.3.2 Effects of Methyl Substituents on the Rate of Hydrogenations

Hydrogenation reactions involve flat adsorption of the molecules on the τ -sites of the catalyst. This leads to the following assumption:

Assumption 6: Only the number of substituents and not their position relative to the sulfur atom has to be taken into account for the adsorption on the τ -sites and for the reaction between adsorbed species.

In total there are 282 hydrogenation rate equations containing 51 parameters which need to be determined from experimental data. However, when the structural contribution approach is applied, the total number of parameters for the complete

network can be reduced to 93. According to the rate equations derived for the HDS of DBT (Vanrysselberghe and Froment 1996) and assuming that the rate expressions for the HDS of the methyl substituted DBT's are of an identical form, this number can be further reduced to 34 (Froment 2004). Table 4.4 shows the number of parameters based on structural contribution.

Table 4.4 Total Number of Parameters for the HDS of DBT and MeDBTs Based on the Structural Contributions.

Reaction	Structural contributions sDBT	Adsorption and rate coefficient
σ-sites		
Adsorption of sDBT	5	1
Hydrogenolysis of sDBT	5	1
Adsorption of sBPH	3	1
Adsorption of H ₂	-	1
Adsorption of H ₂ S	-	1
τ sites		
Adsorption of sDBT	3	1
Hydrogenation of sDBT	3	1
Adsorption of sBPH	3	1
Hydrogenation of sBPH	2	1
Adsorption of H ₂	-	1
<i>Total</i>	24	10

4.4 Application of the Structural Contributions Approach to HDS of Complex Mixtures

In the HDS of complex mixtures it is also necessary to distinguish between hydrogenolysis and hydrogenation reactions. Further, the Hougen-Watson concept accounts for the adsorption of the reacting species. Also, it is logical to assume that the structure of the rate equations for substituted dibenzothiophenes is identical with that of the head of the family or parent molecule.

4.4.1 Hydrodesulfurization of Light Cycle Oil (LCO)

In agreement with the reaction network from Figure 4.1, the Hougen-Watson rate equation for the sulfur removal of DBT in the LCO can be written as

$$r_{DBT} = C_{DBT} C_{H_2} \left[\frac{k_{DBT,\sigma} K_{DBT,\sigma} K_{H,\sigma}}{DEN_{\sigma}} + \frac{k_{DBT,\tau} K_{DBT,\tau} K_{H,\tau}}{DEN_{\tau}} \right] \quad (4.9)$$

where the first term relates to hydrogenolysis and the second to hydrogenation. The denominators DEN_{σ} and DEN_{τ} are written more explicitly as

$$DEN_{\sigma} = \left(1 + \sum_i K_{i,\sigma} C_i + \sqrt{K_{H,\sigma} C_{H_2}} \right)^3 \quad (4.9.a)$$

$$DEN_{\tau} = \left(1 + \sum_i K_{i,\tau} C_i + \sqrt{K_{H,\tau} C_{H_2}} \right)^3 \quad (4.9.b)$$

The functional forms represented by DEN_{σ} and DEN_{τ} are identical to those determined in the study on the HDS of the model components DBT (Vanrysselberghe and Froment, 1996), 4-MeDBT, and 4,6-DiMeDBT (Vanrysselberghe et al., 1998a).

In the HDS of LCO the denominators DEN_{σ} and DEN_{τ} contain the concentrations of all adsorbing species of the LCO, multiplied by their respective adsorption equilibrium constant. Since not all adsorbing species and their corresponding adsorption equilibrium constants are identified, the denominators DEN_{σ} and DEN_{τ} are not directly accessible. The denominators DEN_{σ} and DEN_{τ} depend on the mixture composition and the temperature in the completely mixed reactor. A molar-averaged conversion has been used to express the variation of the liquid composition and both DEN_{σ} and DEN_{τ} denominators. Vanrysselberghe and Froment (1998b) defined that molar-averaged conversion as follows:

$$\bar{x} = \frac{1}{\sum_{i=1}^7 y_i} \sum_{i=1}^7 x_i y_i \quad (4.10)$$

with x_i the conversions of a set of selected components (BT, DBT, naphtho[2,1-b]thiophene, 4-MeDBT, 4,6-DiMeDBT, naphthalene, and phenanthrene) and y_i the corresponding mole fractions in the LCO feed.

According to Vanrysselberghe and Froment (1996) and for the model of HDS of LCO the net production rates, R_i for biphenyl, cyclohexylbenzene and bicyclohexyl derived from the reaction scheme of DBT shown in Figure 4.1 were defined in section 4.2.1 as

$$R_{BPH} = r_{DBT,\sigma} - r_{BPH,\tau} \quad (4.1)$$

$$R_{CHB} = r_{DBT,\tau} + r_{BPH,\tau} - r_{CHB,\tau} \quad (4.2)$$

$$R_{BCH} = r_{BCH,\tau} \quad (4.3)$$

The total rate of disappearance of DBT represented by the summation of the consumption of DBT by hydrogenolysis and hydrogenation is given by

$$R_{DBT} = r_{DBT,\sigma} + r_{DBT,\tau} \quad (4.4)$$

In the HDS of the LCO experimental values for R_i were obtained from the experimental conversions x_i at different W/F_{DBT}^0 in the perfectly mixed reactor:

$$R_i = \frac{x_i}{W/F_{DBT}^0} \quad (4.11)$$

For the disappearance of reactants, i.e. DBT, the concentration can be calculated as

$$C_{DBT} = C_{DBT}^0 (1 - x_{DBT}) \quad (4.12)$$

If one assumes constant liquid density, for the reaction products, BPH and CHB, the corresponding calculation is as follows

$$C_{BPH} = C_{DBT}^0 x_{BPH} \quad (4.13)$$

$$C_{CHB} = C_{DBT}^0 x_{CHB} \quad (4.14)$$

The concentration of hydrogen in the liquid phase (C_{H_2}) was obtained from calculations based on correlations proposed for petroleum fractions (Riazi and Vera, 2005; Korsten and Hoffmann, 1996). These calculations were applied for equations 4.15 to 4.17.

The expressions for the conversion of DBT, the conversion of DBT into biphenyl and the conversion of DBT into cyclohexylbenzene in a LCO in the completely mixed reactor become:

$$x_{DBT} = \frac{W}{F_{DBT}^0} C_{DBT} C_{H_2} \left[\frac{k_{DBT,\sigma} K_{DBT,\sigma} K_{H,\sigma}}{DEN_{\sigma}} + \frac{k_{DBT,\tau} K_{DBT,\tau} K_{H,\tau}}{DEN_{\tau}} \right] \quad (4.15)$$

$$x_{BPH} = \frac{W}{F_{DBT}^0} C_{H_2} \left[\frac{k_{DBT,\sigma} K_{DBT,\sigma} K_{H,\sigma} C_{DBT}}{DEN_{\sigma}} - \frac{k_{BPH,\tau} K_{BPH,\tau} K_{H,\tau} C_{BPH}}{DEN_{\tau}} \right] \quad (4.16)$$

$$x_{CHB} = \frac{W}{F_{DBT}^0} C_{H_2} \left[\frac{k_{DBT,\tau} K_{DBT,\tau} K_{H,\tau} C_{DBT}}{DEN_{\tau}} + \frac{k_{BPH,\tau} K_{BPH,\tau} K_{H,\tau} C_{BPH}}{DEN_{\tau}} - \frac{k_{CHB,\tau} K_{CHB,\tau} K_{H,\tau} C_{CHB}}{DEN_{\tau}} \right] \quad (4.17)$$

CHAPTER V

PARAMETER ESTIMATION

5.1 Determination of the Denominators DEN_{σ} and DEN_{τ}

In the LCO, as in all complex mixtures, the terms in the denominators DEN_{σ} and DEN_{τ} comprised in equations 4.12, 4.13 and 4.14 are not directly accessible, since not all adsorbing species and their corresponding adsorption equilibrium constants are known. Relating the rates of substituted dibenzothiophenes in the LCO to those of the unsubstituted parent molecule (DBT), requires the knowledge of both denominators DEN_{σ} and DEN_{τ} for each LCO experiment. These values differ for each LCO experiment, because of the evolution in the composition of the reacting mixture.

The denominators appearing in equations 4.12, 4.13, 4.14 can be calculated when kinetic equations are available for model components for which the products $k_i K_i K_H$, and $k_i K_i K_H$, appearing in the numerators, are known. In contrast to DEN_{σ} and DEN_{τ} these products do not vary with the mixture composition.

Since in this work, for various reasons, no experiments with model compounds were performed, the required products $k_{i,\sigma} K_{i,\sigma} K_{H,\sigma}$ and $k_{i,\tau} K_{i,\tau} K_{H,\tau}$ or the individual parameters in the HDS of DBT, 4-MDBT and 4,6-DMDBT were not available. The products $k_{DBT\sigma} K_{DBT\sigma} K_{H\sigma}$ were determined by Vanrysselberghe and Froment (1996, 1998b) for the hydrogenolysis of dibenzothiophene and $k_{DBT\tau} K_{DBT\tau} K_{H\tau}$ were determined for the hydrogenation of DBT at the same temperature range (i.e. 290-330°C in this work) on a

similar CoMo/Al₂O₃ catalyst. The properties of this catalyst and the catalyst used in the experiments with the LCO at Texas A&M University are shown in Table 5.1. It can be observed in this table that compositions of both catalysts are very close. Since the above products of parameters are not depending on the mixture composition, only on the catalyst and because the similarity on both catalysts the parameters $k_{DBT\sigma}K_{DBT\sigma}K_{H\sigma}$ and $k_{DBT\tau}K_{DBT\tau}K_{H\tau}$ previously determined for DBT pure, were accepted in this work.

Table 5.1 Properties of the Catalysts Used in the HDS of LCO.

Component	Units	AKZO Ketjenfine 742 ^(a)	HDS-1 ^(b)
MoO ₃	wt %	5-30	13.1-16.1
CoO	wt %	1-10	3.2-3.8
SiO ₂	wt %	0-6	NA
P ₂ O ₅	wt %	0-10	NA
Surface area	m ² _{cat} /g _{cat}	264	215
Pore volume	cm ³ /g _{cat}	0.52	0.50
Support		Al ₂ O ₃	Al ₂ O ₃

(a) Catalyst used by Vanrysselberghe and Froment (1996).

(b) Catalyst used in this work

NA= not available

In Table 5.2 are shown the expressions from Vanrysselberghe and Froment (1996) for the parameters in the numerator of equations 4.12 to 4.14 as a function of temperature. These parameters were considered for the estimation of DEN_σ and DEN_τ for each LCO experiment.

Table 5.2 Rate – and Adsorption Parameters for DBT Utilized in the Modeling of the HDS of the LCO (Taken from Vanrysselberghe and Froment (1996)).

Parameter	Units
$k_{DBT,\sigma} = 2.44336 \times 10^{10} \exp \left[\frac{-122.770 \times 10^3}{R_{gas} T} \right]$	kmol/kg _{cat} -h
$K_{H,\sigma} = 3.36312 \times 10^{-11} \exp \left[\frac{113.232 \times 10^3}{R_{gas} T} \right]$	m ³ /kmol
$K_{DBT,\sigma} = 7.56868 \times 10^1$	m ³ /kmol
$k_{DBT,\tau} = 2.86757 \times 10^{16} \exp \left[\frac{-186.190 \times 10^3}{R_{gas} T} \right]$	kmol/kg _{cat} -h
$k_{BPH,\tau} = 3.4112 \times 10^{23} \exp \left[\frac{255.714 \times 10^3}{R_{gas} T} \right]$	kmol/kg _{cat} -h
$K_{H,\tau} = 1.40255 \times 10^{-15} \exp \left[\frac{142.693 \times 10^3}{R_{gas} T} \right]$	m ³ /kmol
$K_{DBT,\tau} = 2.50395 \times 10^{-7} \exp \left[\frac{76.840 \times 10^3}{R_{gas} T} \right]$	m ³ /kmol
$K_{BPH,\tau} = 4.96685 \times 10^{-4} \exp \left[\frac{37.899 \times 10^3}{R_{gas} T} \right]$	m ³ /kmol
$k_{CHB,\tau} K_{CHB,\tau} (573K) = 3.38631 \times 10^{-1}$	m ³ /kg _{cat} -h

5.2 The Objective Function

The parameters DEN_{σ} and DEN_{τ} at temperature of 330, 310 and 290°C were obtained by minimization of the difference between the experimental and calculated conversions of DBT in the LCO as follows:

$$S = \sum_{j=1}^{n_{\text{exp}}} \sum_{i=1}^{i=3} (x_{ij} - \hat{x}_{ij})^2 \xrightarrow{DEN_{\sigma} \text{ and } DEN_{\tau}} \min \quad (5.1)$$

in which x_{ij} is the observed and \hat{x}_{ij} the predicted value of the dependent variable, i.e. the total conversion of DBT (x_{DBT}), conversion of DBT into BPH (x_{BPH}) and conversion of DBT into cyclohexylbenzene (x_{CHB}). The number of experiments (n_{exp}) was 7 for each temperature.

5.3 Levenberg-Marquardt Algorithm

The Levenberg-Marquardt (LM) algorithm is an iterative technique that locates the minimum of a multivariate function that is expressed as the sum of squares of non-linear real-valued functions (Lourakis 2005, Marquardt 1963). It has become a standard technique for non-linear least-squares problems (Mittelmann 2004). LM is a combination of steepest descent and the Gauss-Newton method. When the current set of parameters is far from the correct one, the algorithm behaves like a steepest descent

method: slow, but the convergence is guaranteed. When the current set of parameters is close to the optimal set of estimates it becomes a Gauss-Newton method. The parameters DEN_{σ} and DEN_{τ} have been estimated by means of this technique.

In this section a main program in FORTRAN to perform the estimation of DEN_{σ} and DEN_{τ} was written. The TWMARM and TWINVE subroutines were incorporated into the program to solve the non linear equations generated from the reaction network. The IMSL subroutines DNEQNF and FCN were applied in the solution of the equations 4.12 to 4.14 that represent the model of the HDS of LCO. The experimental data set corresponding to 3 responses (x_{DBT} , x_{BPH} and x_{CHB}), 7 experiments (W/F_{DBT}^0) and 2 parameters to be estimated (DEN_{σ} and DEN_{τ}) was considered in the minimization of the objective function.

5.4 Parameter Estimates and Comparison of Experimental and Calculated Conversions

The analysis of variance in Table 5.3 shows the output of the estimation of DEN_{σ} and DEN_{τ} at 330°C. The parameters DEN_{σ} and DEN_{τ} , their corresponding 95% confidence intervals and the calculated t-values at 330, 310 and 290°C are shown in Tables 5.4, 5.5 and 5.6 respectively. These results show that DEN_{σ} and DEN_{τ} are reliably estimated.

Table 5.3 Analysis of Variance on DEN_{σ} and DEN_{τ} at 330°C.

Source		D F	Mean square	F
Total sum of squares	2.769	21	0.1319	
Sum of squares due to regression	2.706	2	1.3529	1221
Residual sum of squares	0.021	19	0.0011	
Standard deviation	0.033			
Correlation coefficient	0.977			

Table 5.4 Parameter estimates, 95% Confidence Intervals and t-values at 330°C.

	Parameter estimate	lower limit	upper limit	t-value
DEN_{σ}	386.7	360.9	412.4	31.4
DEN_{τ}	11.0	9.0	13.0	11.5

Table 5.5 Parameter estimates, 95% Confidence Intervals and t-values at 310°C.

	Parameter estimate	lower limit	upper limit	t-value
DEN_{σ}	610.8	577.3	644.2	38.2
DEN_{τ}	7.6	6.8	8.3	21.1

Table 5.6 Parameter estimates, 95% Confidence Intervals and t-values at 290°C.

	Parameter estimate	lower limit	upper limit	t-value
DEN_{σ}	782.6	710.3	854.9	22.7
DEN_{τ}	7.7	5.5	9.9	7.4

The complete output of the estimation of DEN_{σ} and DEN_{τ} for all W/F_{DBT}^0 at 330°C is described in the Appendix F.

5.5 DEN_{σ} and DEN_{τ} as a Function of the Molar-Averaged Conversion

The values of the unknowns DEN_{σ} and DEN_{τ} were estimated for each LCO experiment. The variation of DEN_{σ} and DEN_{τ} with the mixture composition at 330°C in the completely mixed reactor is shown in Figures 5.1 and 5.2. The corresponding results for 310°C are shown in Figures 5.3 and 5.4 and for 290°C are illustrated in Figures 5.5 and 5.6. The mixture composition is expressed in terms of a molar-averaged conversion of the selected components in the HDS of the LCO in an identical manner as it was defined in section 3.5.2.2 (Vanrysselberghe and Froment, 1998b).

$$\bar{x} = \frac{1}{\sum_{i=1}^8 y_i^{LCO}} \sum_{i=1}^8 x_i y_i^{LCO} \quad (3.4)$$

with x_i the conversions of a set of the identified sulfur components in the LCO and reaction products DBT, 4-MeDBT, 3-MeDBT, 3-ethylDBT, 4,6-DiMeDBT, 3,6-DiMeDBT, 2,8-DiMeDBT, 4,9 DiMeNaphtho[2,3-b]thiophene, and y_i^{LCO} the corresponding mole fractions in the LCO. The values of DEN_{σ} and DEN_{τ} show that for a given temperature, the coverage of the σ -sites decreases and that of the τ -sites increases

with the molar-averaged conversion. Vanrysselberghe and Froment (1998b) reported different intervals of molar-averaged conversion, but nevertheless the results in figure 5.1 show a trend fairly similar to those reported by them. On the other hand, the DEN_{τ} calculated by those researchers was in the interval from 4 to 6 for molar-averaged conversions between 24 and 36 %. Figure 5.2 shows very close values of DEN_{τ} for the same interval considered in the preceding study, consequently the trend can also be accepted for the extended interval of molar-averaged conversions (>36%).

Figures 5.3 to 5.6 which illustrate the corresponding plots of DEN_{σ} and DEN_{τ} for 310 and 290°C cannot be compared because there are no reported data at these temperatures. Therefore it is assumed the trend obtained at these temperatures is correct.

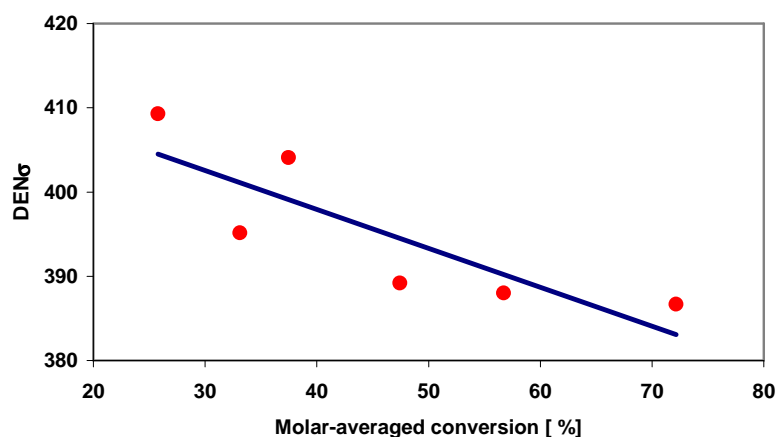


Figure 5.1 DEN_{σ} at 330°C as a function of the molar-averaged conversion of LCO. Line: Correlation obtained by least square fitting from the calculated DEN_{σ} .

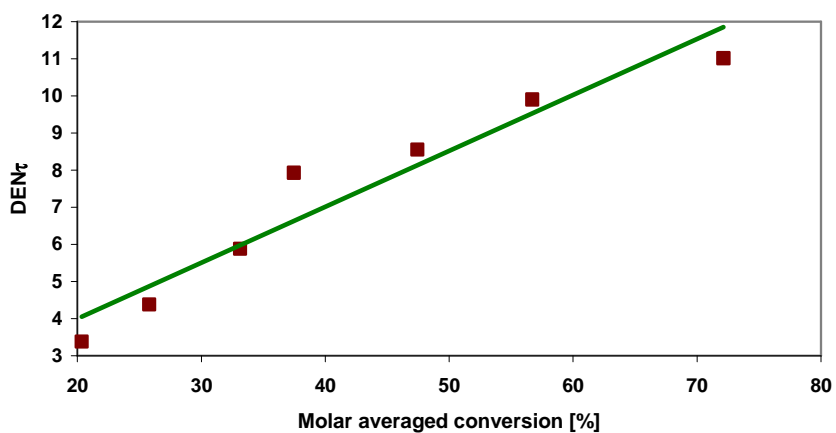


Figure 5.2 DEN_{τ} at 330°C as a function of the molar-averaged conversion of LCO. Line: Correlation obtained by least square fitting from the calculated DEN_{τ} .

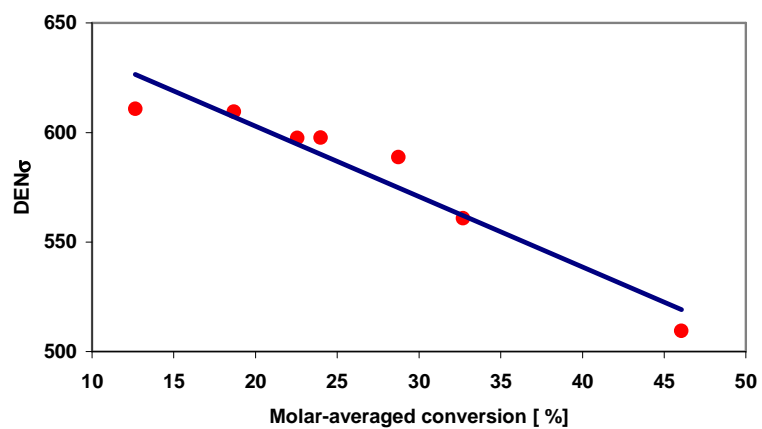


Figure 5.3 DEN_{σ} at 310°C as a function of the molar-averaged conversion of LCO. Line: Correlation obtained by least square fitting from the calculated DEN_{σ} .

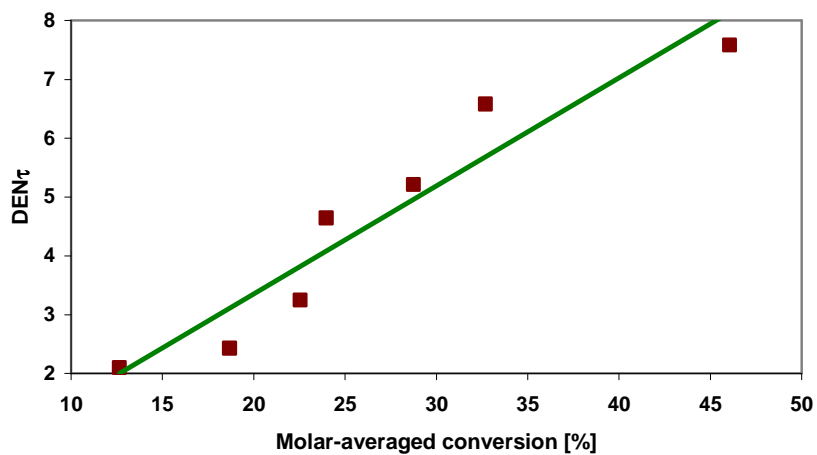


Figure 5.4 DEN_τ at 310°C as a function of the molar-averaged conversion of LCO. Line: Correlation obtained by least square fitting from the calculated DEN_τ.

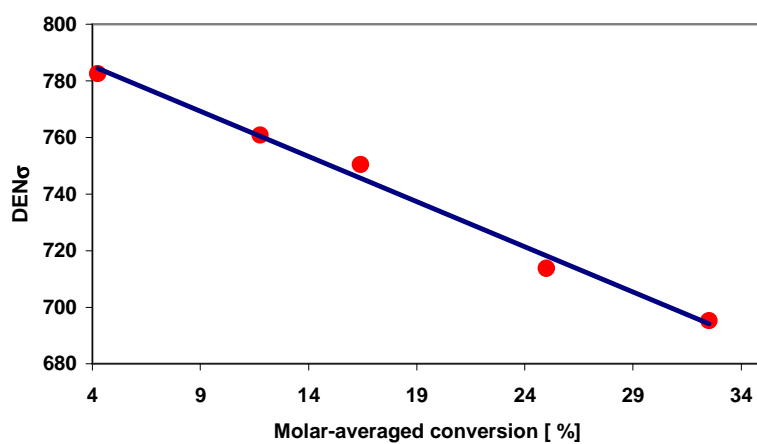


Figure 5.5 DEN_σ at 290°C as a function of the molar-averaged conversion of LCO. Line: Correlation obtained by least square fitting from the calculated DEN_σ.

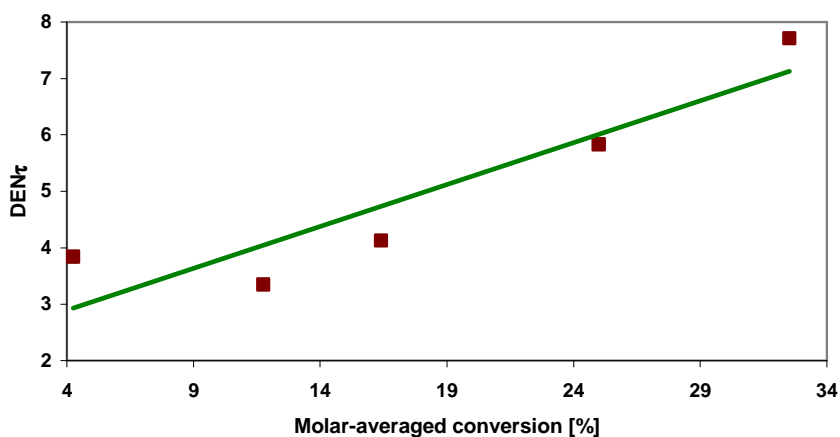


Figure 5.6 DEN_{τ} at 290°C as a function of the molar-averaged conversion of LCO. Line: Correlation obtained by least square fitting from the calculated DEN_{τ} .

Figures 5.7, 5.8 and 5.9 show how the calculated conversions based upon the rate equations 4.15 to 4.17 for the conversion of DBT, the conversion of DBT into biphenyl and the conversion of DBT into cyclohexylbenzene with the DEN values given above fit the experimental data with DEN_{σ} and DEN_{τ} estimated in this work at 330, 310 and 290°C respectively. The observed and the calculated conversions are plotted as a function of W/F_{DBT}^0 . The latter values were also acquired at $P= 65.5$ bar, $H_2/HC= 2.8$ mol ratio. Calculated data were obtained using values for the products in the numerator $k_{i,\sigma}K_{i,\sigma}K_{H,\sigma}$ and $k_{i,\tau}K_{i,\tau}K_{H,\tau}$ taken from Vanrysselberghe and Froment (1996).

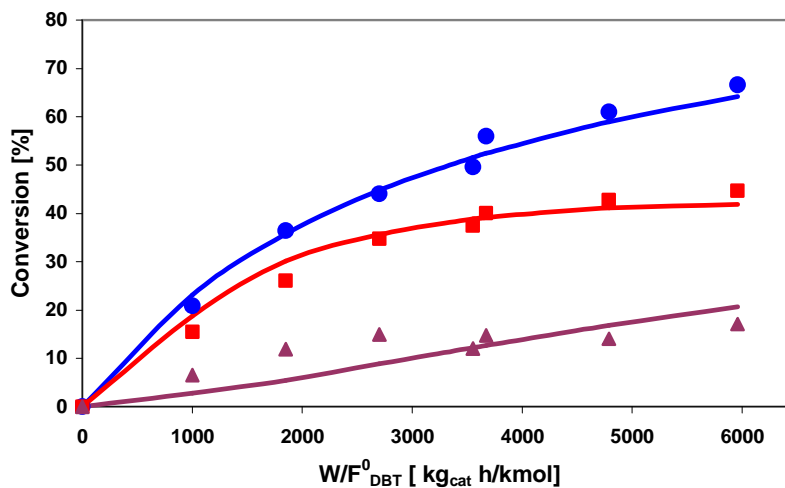


Figure 5.7 Comparison of experimental and calculated conversions as a function of W/F^0_{DBT} at 330°C. (●) Total conversion of DBT. (■) Conversion of DBT into biphenyl. (▲) Conversion of DBT into CHB. Full curves: calculated. Symbols: experimental.

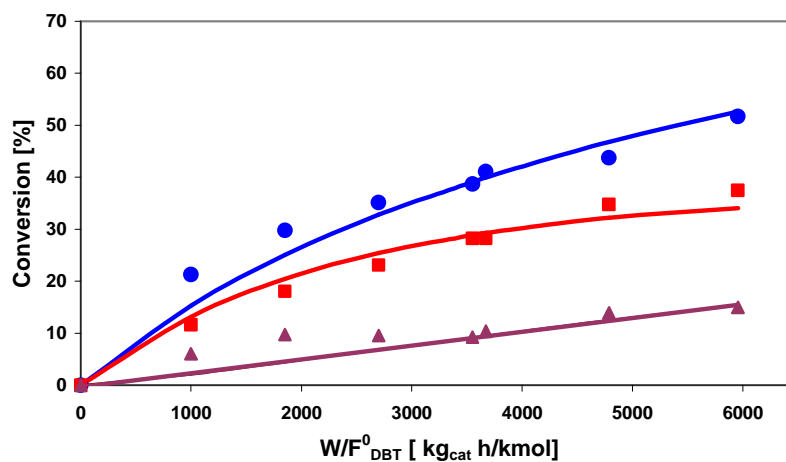


Figure 5.8 Comparison of experimental and calculated conversions as a function of W/F^0_{DBT} at 310°C. (●) Total conversion of DBT. (■) Conversion of DBT into biphenyl. (▲) Conversion of DBT into CHB. Full curves: calculated. Symbols: experimental.

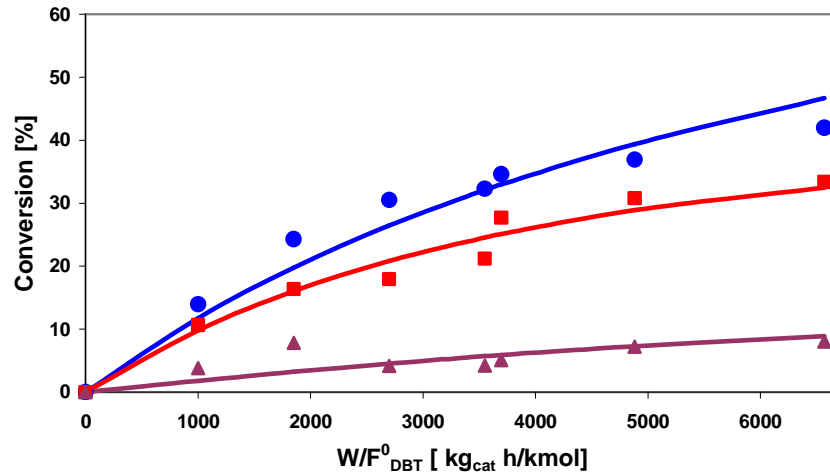


Figure 5.9 Comparison of experimental and calculated conversions as a function of W/F^0_{DBT} at 290°C. (●) Total conversion of DBT. (■) Conversion of DBT into biphenyl. (▲) Conversion of DBT into CHB. Full curves: calculated. Symbols: experimental.

5.6 Structural Contributions and Multiplication Factors for Substituted Dibenzothiophenes

The Hougen-Watson rate equation for hydrodesulfurization of a methyl substituted dibenzothiophene is related to that for non substituted DBT through structural contributions in the following way

$$r_{sDBT} = C_{sDBT} C_{H_2} \left[\frac{f_{sDBT,\sigma} k_{DBT,\sigma} K_{DBT,\sigma} K_{H,\sigma}}{DEN_{\sigma}} + \frac{f_{sDBT,\tau} k_{DBT,\tau} K_{DBT,\tau} K_{H,\tau}}{DEN_{\tau}} \right] \quad (5.2)$$

$$DEN_{\sigma} = \left(1 + \sum_i K_{i,\sigma} C_i + \sqrt{K_{H,\sigma} C_{H_2}} \right)^3$$

$$DEN_{\tau} = \left(1 + \sum_i K_{i,\tau} C_i + \sqrt{K_{H,\tau} C_{H_2}} \right)^3$$

$f_{sDBT,\sigma}$ represents the product of the structural contributions of electronic and steric hindrance effects of the substituents on the rates of hydrogenolysis taking place on the σ sites.

For substituted dibenzothiophenes the relation between $f_{sDBT,\sigma}$ and the structural contributions is given by:

MeDBT

a) No Me in 4 or 6

$$f_{sDBT,\sigma} = k_{EL,\sigma}^{sDBT}(m;0;0)K_{EL,\sigma}^{sDBT}(m;0;0) \quad (5.3)$$

b) 4-MeDBT

$$f_{sDBT,\sigma} = k_{EL,\sigma}^{sDBT}(m;0;0)K_{EL,\sigma}^{sDBT}(m;0;0)k_{ST,\sigma}^{sDBT}(4;0;0)K_{ST,\sigma}^{sDBT}(4;0;0) \quad (5.4)$$

DiMeDBT

a) No Me in 4 or 6

$$f_{sDBT,\sigma} = k_{EL,\sigma}^{sDBT}(m;n;0)K_{EL,\sigma}^{sDBT}(m;n;0) \quad (5.5)$$

b) 1 Me in 4 or 6

$$f_{sDBT,\sigma} = k_{EL,\sigma}^{sDBT}(m;n;0)K_{EL,\sigma}^{sDBT}(m;n;0)k_{ST,\sigma}^{sDBT}(4;0;0)K_{ST,\sigma}^{sDBT}(4;0;0) \quad (5.6)$$

c) 4,6-DiMeDBT

$$f_{sDBT,\sigma} = k_{EL,\sigma}^{sDBT}(m;n;0)K_{EL,\sigma}^{sDBT}(m;n;0)k_{ST,\sigma}^{sDBT}(4;6;0)K_{ST,\sigma}^{sDBT}(4;6;0) \quad (5.7)$$

TriMeDBT

a) No Me in 4 or 6

$$f_{sDBT,\sigma} = k_{EL,\sigma}^{sDBT}(m;n;p)K_{EL,\sigma}^{sDBT}(m;n;p) \quad (5.8)$$

b) 1 Me in 4 or 6

$$f_{sDBT,\sigma} = k_{EL,\sigma}^{sDBT}(m;n;p)K_{EL,\sigma}^{sDBT}(m;n;p)k_{ST,\sigma}^{sDBT}(4;0;0)K_{ST,\sigma}^{sDBT}(4;0;0) \quad (5.9)$$

c) 1 Me in 4 and 1 Me in 6

$$f_{sDBT,\sigma} = k_{EL,\sigma}^{sDBT}(m;n;p)K_{EL,\sigma}^{sDBT}(m;n;p)k_{EL,\sigma}^{sDBT}(4;6;0)K_{EL,\sigma}^{sDBT}(4;6;0) \quad (5.10)$$

and $f_{sDBT,\tau}$ the product of structural contributions of electronic and steric hindrance effects of the substituents on the rates of hydrogenation taking place on the τ sites

$$\mathbf{Me-DBT} \quad f_{sDBT,\tau} = k_{EL+ST,\tau}^{sDBT}(m;0;0)K_{EL+ST,\tau}^{sDBT}(m;0;0) \quad (5.11)$$

$$\mathbf{Di-MeDBT} \quad f_{sDBT,\tau} = k_{EL+ST,\tau}^{sDBT}(m;n;0)K_{EL+ST,\tau}^{sDBT}(m;n;0) \quad (5.12)$$

$$\mathbf{Tri-MeDBT} \quad f_{sDBT,\tau} = k_{EL+ST,\tau}^{sDBT}(m;n;p)K_{EL+ST,\tau}^{sDBT}(m;n;p) \quad (5.13)$$

The values of the products $k_{DBT,\sigma}K_{DBT,\sigma}K_{H,\sigma}$ and $k_{DBT,\tau}K_{DBT,\tau}K_{H,\tau}$ appearing in the numerators of equation 5.2 and other equations before (4.12, 4.13 and 4.14) are shown in Tables 5.7, 5.8 and 5.9.

Table 5.7 Value of the Products $k_{i,\sigma}K_{i,\sigma}K_{H,\sigma}$ and $k_{i,\tau}K_{i,\tau}K_{H,\tau}$ at 330°C. (Vanrysselberghe and Froment (1996)).

Component	Reaction	Numerator Group	Value
DBT	Hydrogenolysis	$k_{DBT,\sigma}K_{DBT,\sigma}K_{H,\sigma}$	9.28
DBT	Hydrogenation	$k_{DBT,\tau}K_{DBT,\tau}K_{H,\tau}$	0.0078
BPH	Hydrogenation	$k_{BPH,\tau}K_{BPH,\tau}K_{H,\tau}$	0.0742
CHB	Hydrogenation	$k_{CHB,\tau}K_{CHB,\tau}K_{H,\tau}$	0.0011

Table 5.8 Value of the Products $k_{i,\sigma}K_{i,\sigma}K_{H,\sigma}$ and $k_{i,\tau}K_{i,\tau}K_{H,\tau}$ at 310°C. (Vanrysselberghe and Froment (1996)).

Component	Reaction	Numerator Group	value
DBT	Hydrogenolysis	$k_{DBT,\sigma}K_{DBT,\sigma}K_{H,\sigma}$	8.70
DBT	Hydrogenation	$k_{DBT,\tau}K_{DBT,\tau}K_{H,\tau}$	0.0098
BPH	Hydrogenation	$k_{BPH,\tau}K_{BPH,\tau}K_{H,\tau}$	0.0444
CHB	Hydrogenation	$k_{CHB,\tau}K_{CHB,\tau}K_{H,\tau}$	0.0029

Table 5.9 Value of the Products $k_{i,\sigma}K_{i,\sigma}K_{H,\sigma}$ and $k_{i,\tau}K_{i,\tau}K_{H,\tau}$ at 290°C. (Vanrysselberghe and Froment (1996)).

Component	Reaction	Numerator Group	value
DBT	Hydrogenolysis	$k_{DBT,\sigma}K_{DBT,\sigma}K_{H,\sigma}$	8.11
DBT	Hydrogenation	$k_{DBT,\tau}K_{DBT,\tau}K_{H,\tau}$	0.0125
BPH	Hydrogenation	$k_{BPH,\tau}K_{BPH,\tau}K_{H,\tau}$	0.0256
CHB	Hydrogenation	$k_{CHB,\tau}K_{CHB,\tau}K_{H,\tau}$	0.0082

Vanrysselberghe and Froment (1998b) derived structural contributions for the hydrogenolysis reaction on the σ -sites of the various mono and dimethyldibenzothiophenes as follows:

$$K_{EL,\sigma}^{sDBT}(m;0;0)=K_{EL,\sigma}^{sDBT}(m;n;0)=k_{EL,\sigma}^{sDBT}(m;0;0)=k_{EL,\sigma}^{sDBT}(m;n;0) = 1 \quad (5.14)$$

for all m and n

In the present work the lack of experimental data on model sulfur-containing compounds such as DBT, 4-MDBT and 4,6 DMDBT led to acceptance of the preceding values, obtained by Vanrysselberghe and Froment (1996) and Vanrysselberghe et al., (1998a) on a very similar CoMo/Al₂O₃ catalyst to the HDS-1, and were used herein for the structural contributions for these substituted dibenzothiophenes. Accepting these values for the present work makes sense, even if the catalyst used is not the same. Indeed, what enter into the structural contributions are ratios of rate –and adsorption contributions and it is unlikely that these depend on the catalyst. Nevertheless, a confrontation with the experimental results is necessary, in particular with regard to accepting the values of the products $k_{DBT,\sigma}K_{DBT,\sigma}K_{H,\sigma}$ and $k_{DBT,\tau}K_{DBT,\tau}K_{H,\tau}$, which is a bolder policy.

$$K_{ST,\sigma}^{sDBT}(4;0;0) = \frac{K_{4-MeDBT,\sigma}}{K_{DBT,\sigma}} = 0.310 \quad (5.15)$$

$$K_{ST,\sigma}^{sDBT}(4;6;0) = \frac{K_{4,6-DiMeDBT,\sigma}}{K_{DBT,\sigma}} = 0.2384 \quad (5.16)$$

$$k_{ST,\sigma}^{sDBT}(4;0;0) = \frac{k_{4-MeDBT,\sigma}}{k_{DBT,\sigma}} = 5.3822 \exp\left[-\frac{10550}{R_{gas}T}\right] \quad (5.17)$$

$$k_{ST,\sigma}^{sDBT}(4;6;0) = \frac{k_{4,6-DiMeDBT,\sigma}}{k_{DBT,\sigma}} = 2638 \exp\left[\frac{16547}{R_{gas}T}\right] \quad (5.18)$$

At 603K (330°C), e.g. $k_{ST,\sigma}^{sDBT}(4;0;0) = 0.6566$ and $k_{ST,\sigma}^{sDBT}(4;6;0) = 0.0715$. The structural contributions $K_{ST,\sigma}^{sDBT}(4;0;0)$ and $K_{ST,\sigma}^{sDBT}(4;6;0)$ are temperature-independent since the adsorption equilibrium constants $K_{DBT,\sigma}$, $K_{4-MeDBT,\sigma}$, and $K_{4,6-DiMeDBT,\sigma}$ are weak function of temperature (Vanrysselberghe and Froment 1996).

Because of the flat adsorption on the τ sites, only the number of methyl groups and not their position relative to the sulfur atom has been taken into account for the adsorption and the reaction between the adsorbed species on the τ sites. On these sites the following structural contributions for hydrogenation of the mono and dimethyl DBT's can be obtained from the ratios of the adsorption equilibrium constant of each pure monomethyl or dimethyl substituted dibenzothiophene over the adsorption equilibrium constant of the pure DBT.

The values for calculating these ratios are

$$K_{4\text{-MeDBT},\tau} = 6.03699 \times 10^{-8} \exp\left[\frac{83802}{R_{\text{gas}}T}\right] \quad \text{m}^3/\text{kmol} \quad (5.19)$$

$$K_{\text{DBT},\tau} = 2.86757 \times 10^{16} \exp\left[\frac{-186.190 \times 10^3}{R_{\text{gas}}T}\right] \quad \text{m}^3/\text{kmol} \quad (5.20)$$

Therefore the structural contribution for this ratio is

$$K_{\text{EL+ST},\tau}^{\text{sDBT}}(m;0;0) = \frac{K_{4\text{-MeDBT},\tau}}{K_{\text{DBT},\tau}} = 2.41099 \times 10^{-1} \exp\left[\frac{6962}{R_{\text{gas}}T}\right] \quad (5.21)$$

The adsorption equilibrium constant for 4,6-DMDBT

$$K_{4,6\text{-DMDBT},\tau} = 1.58733 \times 10^{-8} \exp\left[\frac{90485}{R_{\text{gas}}T}\right] \quad (5.22)$$

in combination with the $K_{\text{DBT},\tau}$ lead to the following structural contribution

$$K_{\text{EL+ST},\tau}^{\text{sDBT}}(m;n;0) = \frac{K_{4,6\text{-DiMeDBT},\tau}}{K_{\text{DBT},\tau}} = 6.3393 \times 10^{-2} \exp\left[\frac{13645}{R_{\text{gas}}T}\right] \quad (5.23)$$

In a similar manner the rate coefficient of each substituted dibenzothiophene can be related to the corresponding rate coefficient of DBT to obtain the following structural contributions

$$k_{EL+ST,\tau}^{sDBT}(m;0;0) = \frac{k_{4-MeDBT,\tau}^1 + k_{4-MeDBT,\tau}^2}{k_{DBT,\tau}} = 1.48162 \times 10^8 \exp\left[-\frac{81078}{R_{gas}T}\right] \quad (5.24)$$

$$k_{EL+ST,\tau}^{sDBT}(m;n;0) = \frac{k_{4,6-DiMeDBT,\tau}}{k_{DBT,\tau}} = 1.28404 \times 10^{11} \exp\left[-\frac{112852}{R_{gas}T}\right] \quad (5.25)$$

Vanrysselberghe and Froment (1998b) also defined the structural contributions for the hydrogenolysis reaction of the trimethyldibenzothiophenes:

$$K_{EL,\sigma}^{sDBT}(m;n;p) = K_{EL,\sigma}^{sDBT}(m;n;p) = 1 \quad (5.26)$$

for all m and n

The $f_{sDBT,\sigma}$ and $f_{sDBT,\tau}$ can now be calculated by substituting the structural contributions in the corresponding equations for substituted dibenzothiophenes (5.3 to 5.13) and further both $f_{sDBT,\sigma}$ and $f_{sDBT,\tau}$ should be substituted in the equation 5.2.

$$r_{sDBT} = C_{sDBT} C_{H_2} \left[\frac{f_{sDBT,\sigma} k_{DBT,\sigma} K_{DBT,\sigma} K_{H,\sigma}}{DEN_{\sigma}} + \frac{f_{sDBT,\tau} k_{DBT,\tau} K_{DBT,\tau} K_{H,\tau}}{DEN_{\tau}} \right] \quad (5.2)$$

The products $k_{\text{DBT},\sigma}K_{\text{DBT},\sigma}K_{\text{H},\sigma}$ and $k_{\text{DBT},\tau}K_{\text{DBT},\tau}K_{\text{H},\tau}$ taken from Vanrysselberghe and Froment (1998b) in combination with the DEN_{σ} and DEN_{τ} estimated from the experimental data of the HDS of the LCO, (Tables 5.3 to 5.6) should also be substituted into equation 5.2. Finally, the rate of reaction of Hougen-Watson type (Equation 5.2) which represents the kinetic model based upon structural contributions approach of the Deep HDS of the LCO is completed.

Tables 5.10, 5.11 and 5.12 show the $f_{\text{sDBT},\sigma}$ and $f_{\text{sDBT},\tau}$ for the substituted dibenzothiophenes calculated from the structural contributions at 330, 310 and 290°C respectively.

Table 5.10 The Multiplication Factors $f_{\text{sDBT},\sigma}$ and $f_{\text{sDBT},\tau}$ for the Substituted Dibenzothiophenes Calculated from the Structural Contributions at 330°C.

	$f_{\text{sDBT},\sigma}$	$f_{\text{sDBT},\tau}$
MeDBT		13.63
a) No Me in 4 or 6	1	
b) 4-MeDBT	0.2036	
DiMeDBT		20.85
a) No Me in 4 or 6	1	
b) 1 Me in 4 or 6	0.2036	
c) 4,6-DiMeDBT	0.0170	
TriMeDBT		(&)
a) No Me in 4 or 6	1	
b) 1 Me in 4 or 6	0.2036	
c) 1 Me in 4 and 1 Me in 6	0.0170	

(&)Additional experiments with a trimethyl-DBT are required to obtain the structural contributions for the hydrogenation reaction (Vanrysselberghe and Froment, (1998b)).

Table 5.11 The Multiplication Factors $f_{sDBT,\sigma}$ and $f_{sDBT,\tau}$ for the Substituted Dibenzothiophenes Calculated from the Structural Contributions at 310°C.

	$f_{sDBT,\sigma}$	$f_{sDBT,\tau}$
MeDBT		8.21
a) No Me in 4 or 6	1	
b) 4-MeDBT	0.1894	
DiMeDBT		10.58
a) No Me in 4 or 6	1	
b) 1 Me in 4 or 6	0.1894	
c) 4,6-DiMeDBT	0.0191	
TriMeDBT		(&)
a) No Me in 4 or 6	1	
b) 1 Me in 4 or 6	0.1894	
c) 1 Me in 4 and 1 Me in 6	0.0191	

(&)Additional experiments with a trimethyl-DBT are required to obtain the structural contributions for the hydrogenation reaction (Vanrysselberghe and Froment, (1998b)).

Table 5.12 The Multiplication Factors $f_{sDBT,\sigma}$ and $f_{sDBT,\tau}$ for the Substituted Dibenzothiophenes Calculated from the Structural Contributions at 290°C.

	$f_{sDBT,\sigma}$	$f_{sDBT,\tau}$
MeDBT		4.77
a) No Me in 4 or 6	1	
b) 4-MeDBT	0.1753	
DiMeDBT		5.12
a) No Me in 4 or 6	1	
b) 1 Me in 4 or 6	0.1753	
c) 4,6-DiMeDBT	0.0215	
TriMeDBT		(&)
a) No Me in 4 or 6	1	
b) 1 Me in 4 or 6	0.1753	
c) 1 Me in 4 and 1 Me in 6	0.0215	

(&)Additional experiments with a trimethyl-DBT are required to obtain the structural contributions for the hydrogenation reaction (Vanrysselberghe and Froment, (1998)).

Figure 5.10 shows the comparison between the experimental R_i and the calculated values of R_i for a number of methyl- and dimethyl-dibenzothiophenes (s-DBT) in LCO.

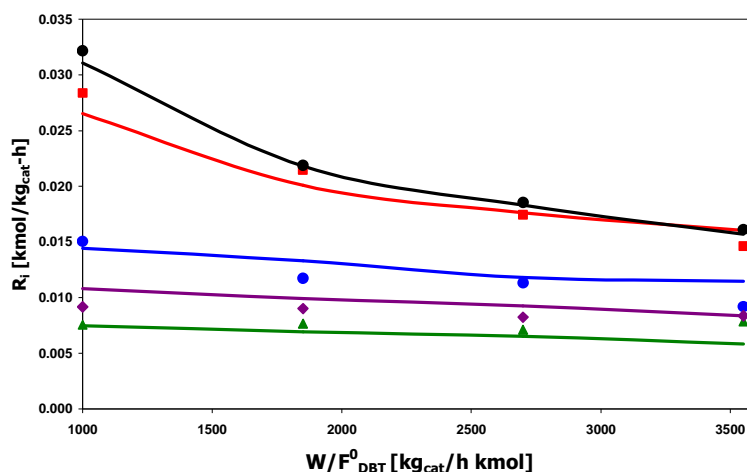


Figure 5.10 Comparison of experimental and calculated R_i as a function of W/F_{DBT}^0 for various s-DBT at 330°C. $P = 65.5$ bar, $H_2/HC = 2.8$ mol ratio. (●) 4-MeDBT. (■) 3-MeDBT. (▲) 4,6-DMDBT. (◆) 3,6-DMDBT. (●) 2,8-DMDBT. Full curves: calculated. Symbols: experimental.

The model reproduces very well the observed total conversions of DBT, conversions of DBT into BPH and conversions of DBT into CHB as a function of temperature.

Considering that the products $k_{DBT,\sigma}K_{DBT,\sigma}K_{H,\sigma}$ and $k_{DBT,\tau}K_{DBT,\tau}K_{H,\tau}$ and the structural contributions were taken from Vanrysselberghe and Froment (1998b) the agreement is remarkable. It illustrates the value of the structural contribution approach for the kinetic modeling of the hydrotreatment of petroleum fractions and of its application to various feedstocks and even catalysts providing, they belong to the same family.

CHAPTER VI

CONCLUSIONS AND RECOMENDATIONS FOR FUTURE WORK

In the present work an experimental setup was built for the investigation of the hydrotreatment of petroleum fractions. This equipment, the central part of which is a perfectly mixed flow reactor can be used for the hydrodesulfurization (HDS) of petroleum fractions such as Light Cycle Oil (LCO) or gasoil. Moreover, this equipment can be used to test not only industrial operating conditions of the HDS but also different catalysts and determine kinetic modeling as well.

In this development, a rigorous kinetic model was formulated to investigate the HDS of the LCO in the presence of a CoMo/ Al₂O₃ catalyst. A structural contribution methodology was applied to predict Hougen-Watson kinetics for HDS of methyl-substituted benzothiophenes and dibenzothiophenes in a complex feedstock such as LCO or diesel. The model was formulated with a significant reduction in the number of parameters to be estimated from 1132 to 34 for DBT as parent molecule in the HDS of the LCO.

The multiplication factors, f_{sDBT} , which are products of structural contributions for hydrogenolysis and hydrogenation of the mono- and dimethyl-dibenzothiophenes obtained from studies with pure DBT, 4-MeDBT and 4,6-DMDBT on a CoMo/Al₂O₃ catalyst (Vanrysselberghe and Froment, (1996)) can be used in the kinetic modeling of HDS of LCO or any other complex mixture upon a similar CoMo/Al₂O₃ catalyst.

The model reproduces very well the observed total conversions of DBT, conversions of DBT into biphenyl and conversions of DBT into cyclohexylbenzene as a function of temperature.

Since DEN_{σ} and DEN_{τ} in the Hougen-Watson expressions contain all the adsorbing species on the surface catalyst, the structural contribution approach can be used to formulate the corresponding kinetic model when experimental data for other model sulfur-containing compounds are available.

GC-MS was a good technique to identify the sulfur compounds in the feed and the reaction products; however, the exhausting task that needs to be followed recommends considering the inclusion of a more sensitive detector such as atomic emission detector (AED) or photometric flame detector (PFD).

NOMENCLATURE

A_i	peak-area of component i determined by Gas Chromatography
A_f	peak-area of fluorine determined by Gas Chromatography
BET	Brunauer-Emmett-Teller method
C_i	liquid concentration of component i , kmol/m _L ³
E_a	activation energy, KJ/kmol
F_{DBT}^0	molar feed flow rate of dibenzothiophene, kmol/h
$f_{sDBT,\sigma}$	products of the contributions of electronic and steric hindrance effects of the substituents on the rates of hydrogenolysis taking place on the σ sites
$f_{sDBT,\tau}$	products of the contributions of electronic and steric hindrance effects of the substituents on the rates of hydrogenolysis taking place on the τ sites
$k_{i,\sigma}$	rate coefficient for the reaction of component i on σ sites, kmol/(kgcat h)
$k_{i,\tau}$	rate coefficient for the reaction of component i on τ sites, kmol/(kgcat h)
$k_{EL,\sigma}^{sDBT}(m;0;0)$	electronic effect of one methyl group on the rate coefficient for the hydrogenolysis of a MeDBT on the σ sites
$k_{EL,\sigma}^{sDBT}(m;n;0)$,	electronic effect two methyl groups on the rate coefficient for the hydrogenolysis of a MeDBT on the σ sites
$k_{EL,\sigma}^{sDBT}(m;n;p)$	electronic effect of three methyl groups on the rate coefficient for the hydrogenolysis of a MeDBT on the σ sites
$k_{EL+ST,\tau}^{sDBT}(m;0;0)$	electronic and steric effect of one methyl group on the rate coefficient for the hydrogenation reaction of a MeDBT on the τ

sites

$k_{EL+ST,\tau}^{sDBT}(m;n;0)$	electronic and steric effect of two methyl groups on the rate coefficient for the hydrogenation reaction of a MeDBT on the τ sites
$k_{EL+ST,\tau}^{sDBT}(m;n;p)$	electronic and steric effect of three methyl groups on the rate coefficient for the hydrogenation reaction of a MeDBT on the τ sites
$k_{ST,\sigma}^{sDBT}(4;0;0)$	steric effect of a methyl group in positions 4 or 6 on the rate coefficient for the hydrogenolysis reaction of dibenzothiophenes on the σ sites
$k_{ST,\sigma}^{sDBT}(4;6;0)$	steric effect of two methyl groups in positions 4 and 6 on the rate coefficient for the hydrogenolysis reaction of dibenzothiophenes on the σ sites
$K_{i,\sigma}$	adsorption coefficient of component i on σ sites, $m_L^3/kmol$
$K_{EL,\sigma}^{sDBT}(m;0;0)$,	electronic effect of one methyl group on the adsorption of a MeDBT on the σ sites
$K_{EL,\sigma}^{sDBT}(m;n;0)$,	electronic effect of two methyl groups on the adsorption of a MeDBT on the σ sites
$K_{EL,\sigma}^{sDBT}(m;n;p)$	electronic effect of three methyl groups on the adsorption of a MeDBT on the σ sites
$K_{EL+ST,\tau}^{sDBT}(m;0;0)$,	electronic and steric effect of one methyl group on the adsorption of a MeDBT, DiMeDBT, and, TriMeDBT on the τ sites
$K_{EL+ST,\tau}^{sDBT}(m;n;0)$,	electronic and steric effect of two methyl groups on the adsorption of a MeDBT, DiMeDBT, and, TriMeDBT on the τ sites
$K_{EL+ST,\tau}^{sDBT}(m;n;p)$	electronic and steric effect of three methyl groups on the adsorption of a MeDBT, DiMeDBT, and, TriMeDBT on the τ sites
$K_{ST,\sigma}^{sDBT}(4;0;0)$	steric effect of a methyl group in position 4 or 6 on the adsorption of dibenzothiophenes on the σ sites
$K_{ST,\sigma}^{sDBT}(4;6;0)$	steric effect of two methyl groups in positions 4 and 6 on the

	adsorption of dibenzothiophenes on the σ sites
n_{exp}	number of experiments
R_{gas}	gas constant, kJ /kmol-K
r_i	total rate of disappearance of component i , kmol/(kg _{cat} h)
R_i	net production rate of component i , kmol/(kg _{cat} h)
S	objective function
T	temperature, K
V	reactor volume, m ³
W	total catalyst mass, kg _{cat}
x_A	conversion of component A
x_{A0}	initial conversion of component A
x_i	conversion of component i ;
\hat{x}_i	calculated conversion of component i
y_i	mole fraction of component i in LCO feed

Greek symbols

σ	with respect to the hydrogenolysis function
τ	with respect to the hydrogenation function

Subscripts

4,6-DiMeDBT	4,6-dimethyldibenzothiophene
4-MeDBT	4-methyldibenzothiophene
BT	benzothiophene

BPH	biphenyl
CHB	cyclohexylbenzene
DBT	dibenzothiophene
THDBT	tetrahydrodibenzothiophene
HHDBT	hexahydrodibenzothiophene
H	atomic hydrogen
H ₂	molecular hydrogen
s-DBT	methyl-substituted dibenzothiophene

LITERATURE CITED

- Altgelt, K. H.; Gouw, T. H. *Chromatography in Petroleum Analysis*; Marcel Dekker: New York, 1979.
- Castaneda, L. L. *Desarrollo de un Simulador Para Reactores de Oxidacion de Etileno en Lecho Fluidizado*, M.S. Thesis, Instituto Tecnológico de Ciudad Madero: México, 2000.
- Castaneda, L. L.; Alonso, M. F.; Centeno, N. G.; Ancheyta, J. J. *Estado del Arte de Tecnologías para el Hidroprocesamiento de Crudos Pesados*. Informe Técnico TCM-18.2, Instituto Mexicano del Petróleo: México, 1999.
- Chen, J.; Te, M.; Yang, H.; Ring, Z. Hydrodesulfurization of Dibenzothiophenic Compounds in a Light Cycle Oil. *Petroleum Science and Technology*. **2003**, *21*, (5&6), 911-935.
- Delmon, B. A New Hypothesis Explaining Synergy between Two Phases in Heterogeneous Catalysis. *Bull. Soc. Chim. Belg.* **1979**, *88*, 979.
- Depauw, G. A.; Froment, G. F. Molecular Analysis of the Sulphur Components in a Light Cycle Oil of a Catalytic Cracking Unit by GC-MS and GC-AED. *J. Chromatogr. A*. **1997**, *761* (1-2), 231.
- Diaz, R. R.; Mann, R. S.; Sambhi, I. S. Hydrotreatment of Athabasca Bitumen Derived Gas Oil over Ni-Mo and Co-Mo Catalysts. *Ind. Eng. Chem. Res.* **1993**, *32*, 1354-1358.
- DOE. Department of Energy, Energy Information Administration, *Annual Energy Review* **2004**, DOE/EIA-0384.
- Dzidic, I.; Petersen, H. A.; Wadsworth, P. A.; Hart, H. V. Townsend Discharge Nitric Oxide Chemical Ionization Gas Chromatography/Mass Spectrometry for Hydrocarbon Analysis of the Middle Distillates, *Anal. Chem.* **1992**, *64*, 2227-2232.

Edvinson, R.; Irandoust, S. Hydrodesulfurization of Dibenzothiophene in a Monolithic Catalyst Reactor. *Ind. Eng. Chem. Res.* **1993**, *32*, 391.

EPA. Air Toxics from Motor Vehicles; U.S. Environmental Protection Agency-Office of Mobile Sources. **2005** Document: EPA 400-F-2-004.

EPA. "Control of Air Pollution from New Motor Vehicles; Heavy-duty Engine and Vehicle Standards and Highway Diesel Fuel Sulfur Control Requirements." *Federal Register* **2001** *66*, 5101-5150.

Froment, G. F. Modeling in the Development of Hydrotreatment Processes. *International Symposium on Advances in Hydroprocessing of Oil Fractions, ISAHOF*, Oaxaca, Mexico, **2004**.

Froment, G. F.; Depauw, G. A.; Vanrysselberghe, V. Kinetics of the Catalytic Removal of the Sulphur Components from the Light Cycle Oil of a Catalytic Cracking Unit. Studies in Surface Science and Catalysis; *Proceedings of the 1st International Symposium/6th European Workshop on Hydrotreatment and Hydrocracking of Oil Fractions*, Oostende, Belgium, Feb 17-19, 1997; Amsterdam, The Netherlands, **1997**, *106*, 83.

Froment, G. F.; Depauw, G. A.; Vanrysselberghe, V. Kinetic Modeling and Reactor Simulation in Hydrodesulfurization of Oil Fractions. *Ind. Eng. Chem. Res.* **1994**, *33*, 2975.

Gates, B. C.; Katzer, J. R.; Schuit, G. C. A. *Chemistry of Catalytic Processes*; McGraw-Hill: New York, 1979.

Geneste, P.; Amblard, P.; Bonnet, M.; Graffin, P. Hydrodesulfurization of Oxidized Sulfur Compounds in Benzothiophene, Methylbenzothiophene and Dibenzothiophene Series over $\text{CoOMoO}_3\text{-Al}_2\text{O}_3$ Catalyst. *J. Catal.* **1980**, *61*, 115.

Girgis, M. J.; Gates, B. C. Reactivities, Reaction Networks, and Kinetics in High-Pressure Catalytic Hydroprocessing. *Ind. Eng. Chem. Res.* **1991**, *30*, 2021.

- Gonzalez, V. M.; Garcia I.; Beato B. Sizing Gas Cyclones for Efficiency. *Chemical Eng.* **1986**, *93*, 119.
- Houalla, M.; Broderick, D. H.; Sapre, A. V.; Nag, N. K.; De Beer, V. H. J.; Gates, B. C.; Kwart, H. Hydrodesulfurization of Methyl-Substituted Dibenzothiophenes Catalyzed by Sulfided Co-Mo/ γ -Al₂O₃. *J. Catal.* **1980**, *61*, 523.
- Houalla, M.; Nag, N. K.; Sapre, A. V.; Broderick, D. H.; Gates, B. C. Hydrodesulfurization of Dibenzothiophene Catalyzed by Sulfided CoO-MoO₃/ γ -Al₂O₃: The Reaction Network. *AIChE J.* **1978**, *24*, 1015.
- Hsu, C. S.; Drinkwater, D. Gas Chromatography-Mass Spectrometry for the Analysis of Complex Hydrocarbon Mixtures. *Chromatogr. Sci. Ser.*, **2001**, *86*, 55-94.
- Kabe, T.; Akamatsu, K., Ishihara, A.; Otsuki, S., Godo, M., Zhang, Q., Qian, W. Deep Hydrodesulphurization of Light Gas Oil. 1. Kinetics and Mechanisms of Dibenzothiophene Hydrodesulphurization. *Ind. Eng. Chem. Res.* **1997**, *36*, 5146-5152.
- Kabe, T.; Ishihara, A.; Tajima, H. Hydrodesulfurization of Sulfur-Containing Polyaromatic Compounds in Light Oil. *Ind. Eng. Chem. Res.* **1992**, *31*, 1577.
- Kilanowski, D. R.; Teeuwen, H.; De Beer, V. H. J.; Gates, B. C.; Schuit, G. C. A.; Kwart, H. Hydrodesulfurization of Thiophene, Benzothiophene, Dibenzothiophene, and Related Compounds Catalyzed by Sulfided CoO-MoO₃/ γ -Al₂O₃; Low-Pressure Reactivity Studies. *J. Catal.* **1978**, *55*, 129.
- Korsten, H.; Hoffmann, U. Three-Phase Reactor Model for Hydrotreating in Pilot Trickle-Bed Reactors. *AIChE J.*, **1996**, *42*, 1350.
- Kumar, V. R.; Balaraman, K. S.; Rao, V. S. R.; Ananth, M. S. Performance Study of Certain Commercial Catalysts in Hydrodesulphurization of Diesel Oils. *Petrol. Sci. and Tech.* **2001**, *19*, 1029-1038.

- Lecrenay, E., Sakanishi, K., Mochida, I. Catalytic Hydrodesulphurization of Gas Oil and Sulphur Compounds over Commercial and Laboratory-made CoMo and NiMo Catalysts: Activity and Reaction Scheme. *Catalysis Today*. **1997**, *39*, 13-20.
- Levache, D.; Guida, A.; Geneste, P. Hydrodesulfurization of Sulfided Polycyclic Aromatic Compounds over Ni-Mo/ γ -Al₂O₃ Catalyst. *Bull. Soc. Chim. Belg.* **1981**, *90*, 1285.
- Lourakis, M. I. *A Brief Description of the Levenberg-Marquardt Algorithm Implemented by Levmar*. Institute of Computer Science. Foundation for Research and Technology-Hellas (FORTH): Heraklion, Crete, Greece, 2005.
- Ma, X.; Sakanishi, K.; Mochida, I. Hydrodesulfurization Reactivities of Various Compounds in Vacuum Gasoil. *Ind. Eng. Chem. Res.* **1996**, *35*, 2487.
- Ma, X.; Sakanishi, K.; Isoda, T.; Mochida, I. Hydrodesulfurization Reactivities of Narrow-Cut Fractions in a Gas Oil. *Ind. Eng. Chem. Res.* **1995**, *34*, 748.
- Ma, X.; Sakanishi, K.; Mochida, I. Hydrodesulfurization Reactivities of Various Compounds in Diesel Fuel. *Ind. Eng. Chem. Res.* **1994**, *33*, 218.
- Marin R. C. *Middle Distillate Hydrotreatment Zeolite Catalysts Containing Pt/Pd or Ni*, Ph.D. Dissertation; Texas A&M University: College Station, 2006.
- Marquardt, D. An Algorithm for Least-Squares Estimation of Nonlinear Parameters. *SIAM J. Appl. Math.* **1963**, *11*, 431-441.
- Marroquin, G.; Ancheyta, J. Catalytic Hydrotreating of Middle Distillates Blends in a Fixed-bed Pilot Plant Reactor. *Applied Catalysis A: General*. **2001**, *207*, 407-420.
- Mittelman, H. D. The Least Squares Problem. [World Wide Web Site] <http://plato.asu.edu/topics/problems/nlolsq.html>. Jul. 2004. [Accessed on 26 Feb 2005]

- Nadkarni, R. A. Nuclear Activation Methods for the Characterization of Fossil Fuels. *Journal of Radioanalytical and Nuclear Chemistry*. **1984**, 84(1), 67-87.
- Nag, N. K.; Sapre, A. V.; Broderick, D. H.; Gates, B. C. Hydrodesulfurization of Polycyclic Aromatics Catalyzed by Sulfided CoOMoO₃/γ-Al₂O₃: The Relative Reactivities. *J. Catal.* **1979**, 57, 509.
- National Petroleum Refiners Association. *Hydroprocessing-Fuel Quality, 1998 Q&A Minutes*. National Petroleum Refiners Association (NPRA): Washington, D.C., 1998.
- Perry R. H.; Green D. W., *Perry's Chemical Engineers' Handbook*. McGraw-Hill: New York, 1995.
- Riazi, M. R.; Vera, J. H. Method to Calculate the Solubilities of Light Gases in Petroleum and Coal Liquid Fractions on the Basis of Their P/N/A Composition. *Ind. Eng. Chem. Res.* **2005**, 44, 186
- Schomburg, G. *Gas Chromatography*. VCH Publishers, Inc.: New York, NY, 1990.
- Song, C.; Hsu, C. S.; Mochida, I. *Chemistry of Diesel Fuels*. Taylor and Francis: New York, NY, 2000.
- Speight, J. G. *The Desulfurization of Heavy Oils and Residua*; Marcel Dekker: New York, 1981.
- Topsoe, H.; Clausen B. S.; Massoth F. E. *Hydrotreating Catalysis: Science and Technology*, Springer-Verlag: Berlin, 1996.
- Tsonopoulos, C.; Heidman, J. K.; Hwang, S. C. *Thermodynamic and Transport Properties of Coal Liquids*. John Wiley & Sons: New York, NY, 1986.
- Turaga, U. T.; Song, C.; MCM-41-Supported Co-Mo Catalysts for Deep Hydrodesulfurization of Light Cycle Oil. *Catalysis Today*, **2003**, 86, 129-140.

- Van Parys, I. A.; Froment, G. F. Kinetics of Hydrodesulfurization on a CoMo/ γ -Al₂O₃ Catalyst. 1. Kinetics of the Hydrogenolysis of Thiophene. *Ind. Eng. Chem. Prod. Res. Dev.* **1986**, 25, 431.
- Van Parys, I. A.; Hosten, L. H.; Froment, G. F. Kinetics of Hydrodesulfurization on a CoMo/ γ -Al₂O₃ Catalyst. 2. Kinetics of the Hydrogenolysis of Benzothiophene. *Ind. Eng. Chem. Prod. Res. Dev.* **1986**, 25, 437.
- Vanrysselberghe V., Froment G. F., *Hydrodesulfurization-Heterogeneous, Encyclopedia of Catalysis*, John Wiley & Sons, Inc.: New York, 2003.
- Vanrysselberghe, V.; Le Gall, R.; Froment, G. F. Hydrodesulfurization of 4-Methyldibenzothiophene and 4,6-Dimethyldibenzothiophene on a CoMo/Al₂O₃ Catalyst: Reaction Network and Kinetics. *Ind. Eng. Chem. Res.* **1998a**, 37, 1235.
- Vanrysselberghe, V.; Froment, G. F. Kinetic Modeling of Hydrodesulfurization of Oil Fractions: Light Cycle Oil. *Ind. Eng. Chem. Res.* **1998b**, 37, 4231.
- Vanrysselberghe, V.; Froment, G. F. Hydrodesulfurization of Dibenzothiophene on a CoMo/Al₂O₃ Catalyst: Reaction Network and Kinetics. *Ind. Eng. Chem. Res.* **1996**, 35, 3311.
- Vrinat, M. L.; The Kinetics of the Hydrodesulfurization Process: A Review. *Appl. Catal.* **1983**, 6, 137-158.
- Wadsworth, P. A.; Villalanti, D. C. Pinpoint Hydrocarbon Types. *Hydrocarbon Processing, International Edition*, **1992**, 71(5), 109-12.

APPENDIX A

GALLERY OF EXPERIMENTAL WORK IN THE HDS OF THE LCO



Figure A.1 Experimental setup in the service of the HDS of LCO. Room 608, Jack E. Brown Building. Artie McFerrin Department of Chemical Engineering.



Figure A.2 An experimental Robinson-Mahoney Stationary Basket Reactor used in the HDS of LCO. Front view.



Figure A.3 Robinson-Mahoney reactor assembly. Motor in the left and Agitator on the top.

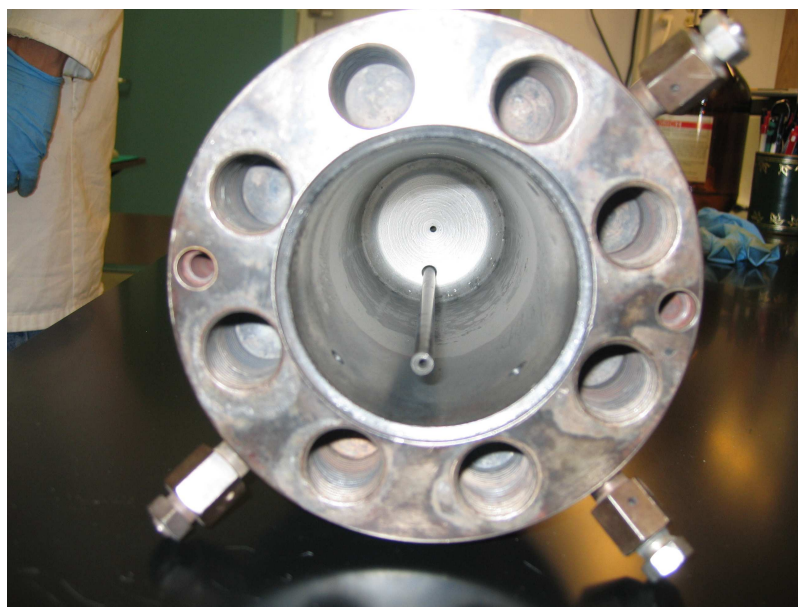


Figure A.4 Interior of Robinson-Mahoney reactor. Top view.



Figure A.5 Control Panel and GC-TCD. Operating variables in the setup were controlled with instruments on this board.



Figure A.6 GCD 1800 Gas chromatograph Mass spectrometer (GC-MS). Equipment used to analyze liquid samples in the HDS of the LCO.



Figure A.7 Coke formed in the HDS of LCO at H_2/HC molar ratio 2.4 or lower (insufficiency of H_2).



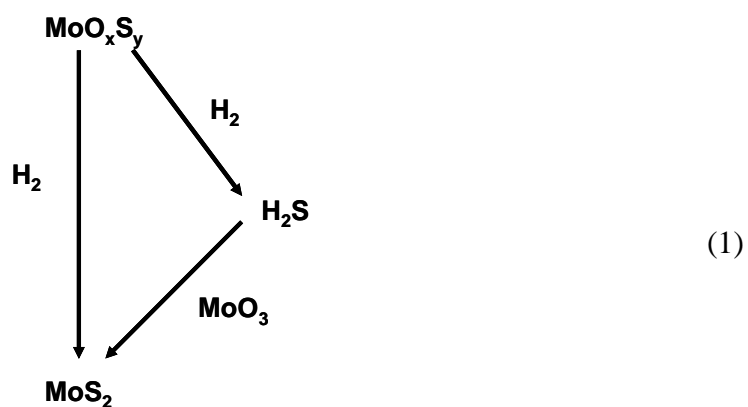
Figure A.8 Shaft assembly and stationary annular basket.

APPENDIX B

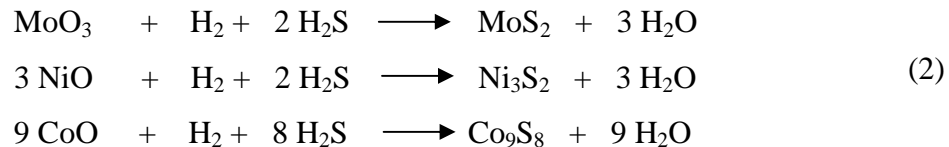
FUNDAMENTALS OF THE SULFIDING PROCESS

B.1 Reactions

In the ex-situ presulfurizing process, the catalytic metal oxides are converted to a range of complex metal oxysulfides. In addition, approximately one-third of the metals are completely converted to metal sulfides. When heated with hydrogen during the activation, the oxysulfides break down to form metal sulfides directly, or to form H_2S , which converts the metal oxides to metal sulfides. The reactions (1) and (2) are examples during the catalyst activation:



These reactions generate heat and water and consume hydrogen. Therefore, it is important to have the reactions take place in a controlled manner over several hours. The total required quantity of sulphur is determined for each catalyst based upon its promoter metals content. The following reactions show the stoichiometric amount of sulphur needed for successful sulphiding:



These sulfided metals are unstable components when they are exposed to air, then recommendations to store, handling, and loading the IMP-HDS presulfided catalyst in an industrial unit should be considered.

B.2 Storage, Handling, and Loading the Presulfided Catalyst in an Industrial Unit

1. The presulfided catalysts are classified as a self-heating substance and must be transported and stored in Department of Transportation (DOT) or International Maritime Dangerous Goods (IMDG) approved containers.
2. Avoid exposing the material to air for extended periods. Long-term exposure to air could cause the material to generate sulfur dioxide and heat. Keep the container sealed. During loading, open containers only as needed.
3. Material should be stored in a cool place and kept dry. The material may generate sulfur dioxide and heat if it is wetted. Exposure to air and water may also cause discoloration and agglomeration of the material. If the material does get wet or generate heat, the container should be purged with nitrogen or dry ice and resealed.

The material should be inspected for signs of degradation just before it is loaded into the reactor.

Note: Do not load oxidic (unsulfurized) CoMo or NiMo catalyst below the presulfurized catalyst in a reactor as it may be sensitive to early activation and subsequent exotherms as H₂S is generated during activation.

4. Presulfurized catalyst can be loaded into the reactor in either an air or inert environment. If loading in air, monitor SO₂ and reactor bed thermocouples. If the material begins to react, purge the reactor with nitrogen immediately.

Appropriate measures should be taken to protect personnel when a reactor is being purged or has been purged with nitrogen.

5. Personal protective equipment should be worn when the material is loaded. The sulfur and hydrocarbon dust from the material can be irritating to the eyes, skin, and respiratory system.
6. If the catalyst loading is interrupted, monitor SO₂ and reactor bed thermocouples closely for signs of reaction. If the loading will be interrupted for an extended period of time (more than 12 hours), purge the reactor with nitrogen.
7. Once the catalyst is loaded, blanket the reactor with nitrogen and seal the reactor. Avoid having air flow through the catalyst bed. If the catalyst bed begins to self-heat, purge the reactor with nitrogen immediately.

APPENDIX C

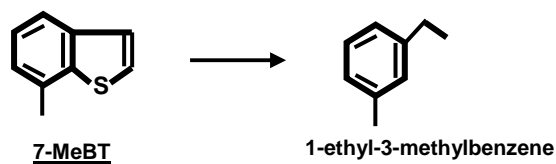
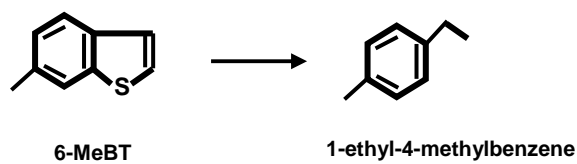
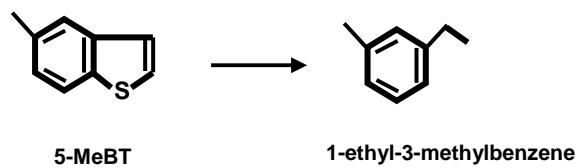
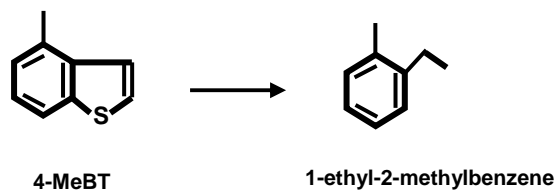
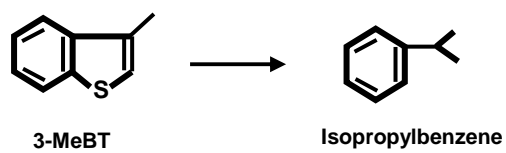
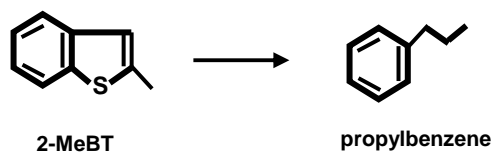
HP MANUAL INJECTION TECHNIQUE FOR THE GC-MS ANALYSIS OF LCO SAMPLES

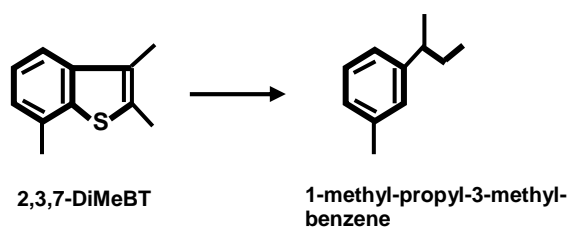
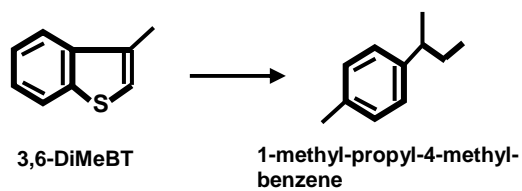
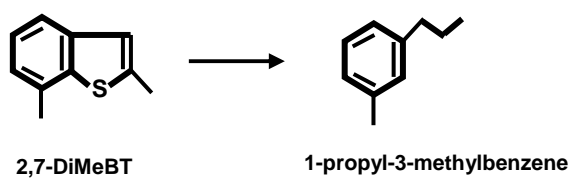
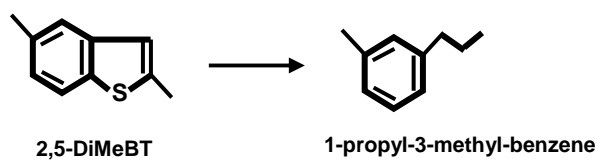
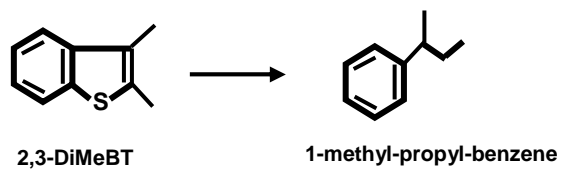
1. Flush out a clean 10 microliter syringe in the same solvent used for your sample. Pulling the solvent into the syringe, and then releasing it into a waste container. Repeat this process several times.
2. Draw air slowly into the syringe so that the tip of the plunger is at the 1.0 microliter mark.
3. With the needle in the sample solution, draw up the desired volume (1-2 microliters splitless), then remove the syringe.
4. Pull 2 more microliters of air into the syringe. The sample aliquot is now sandwiched between two air gaps.
5. Remove any excess sample from the needle by wiping the outside of the needle with a tissue.
6. Hold the plunger in place while you align the syringe over the injector. Inject the sample by inserting the syringe needle into the injector until the barrel of the syringe rests on the injector. Depress the plunger all the way into the syringe.
7. Press Start on the GCD front panel
8. Wait several seconds to allow all traces of sample to enter the system, and then remove the syringe from the injector.

APPENDIX D

REACTIONS OF SUBSTITUTED BENZO AND DIBENZO-THIOPHENES

D.1 Reactions of Methyl Substituted Benzothiophenes.



D.2 Reactions of di-, and tri-methyl Substituted Benzothiophenes.

APPENDIX E

SEPARATOR OF REACTION PRODUCT (CYCLONE)

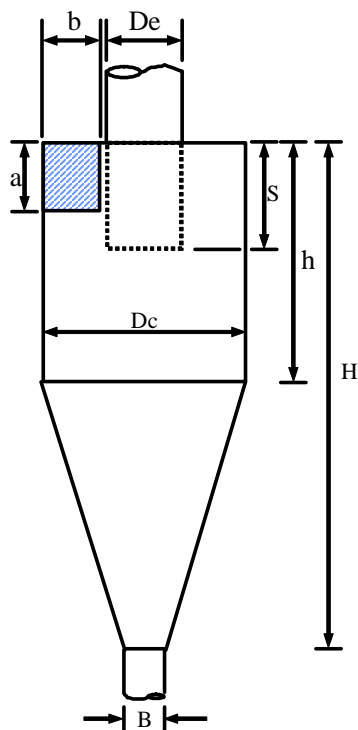
E.1 The cyclone was designed using the proposed method of Gonzalez V. M., and Perry. The Figure E1 presents the corresponding calculated dimensions.

E.2 Required Parameters

- a) Inlet flow
- b) Gas Density
- c) Liquid Density
- d) Gas Viscosity
- e) Pressure Drop
- f) f_1, f_2, f_3 (supposed based in literature)

E.3 Procedure

An iterative method is used to calculate the cyclone diameter (D_c), estimate saltation velocity of particles (V_s) and compare this value with inlet velocity (V_i). The (V_s/V_i) ratio is the control parameter to reach maximum efficiency. When the control condition is obtained, then with D_c found, the remaining dimensions are calculated according to the Stairmand proposed relations.



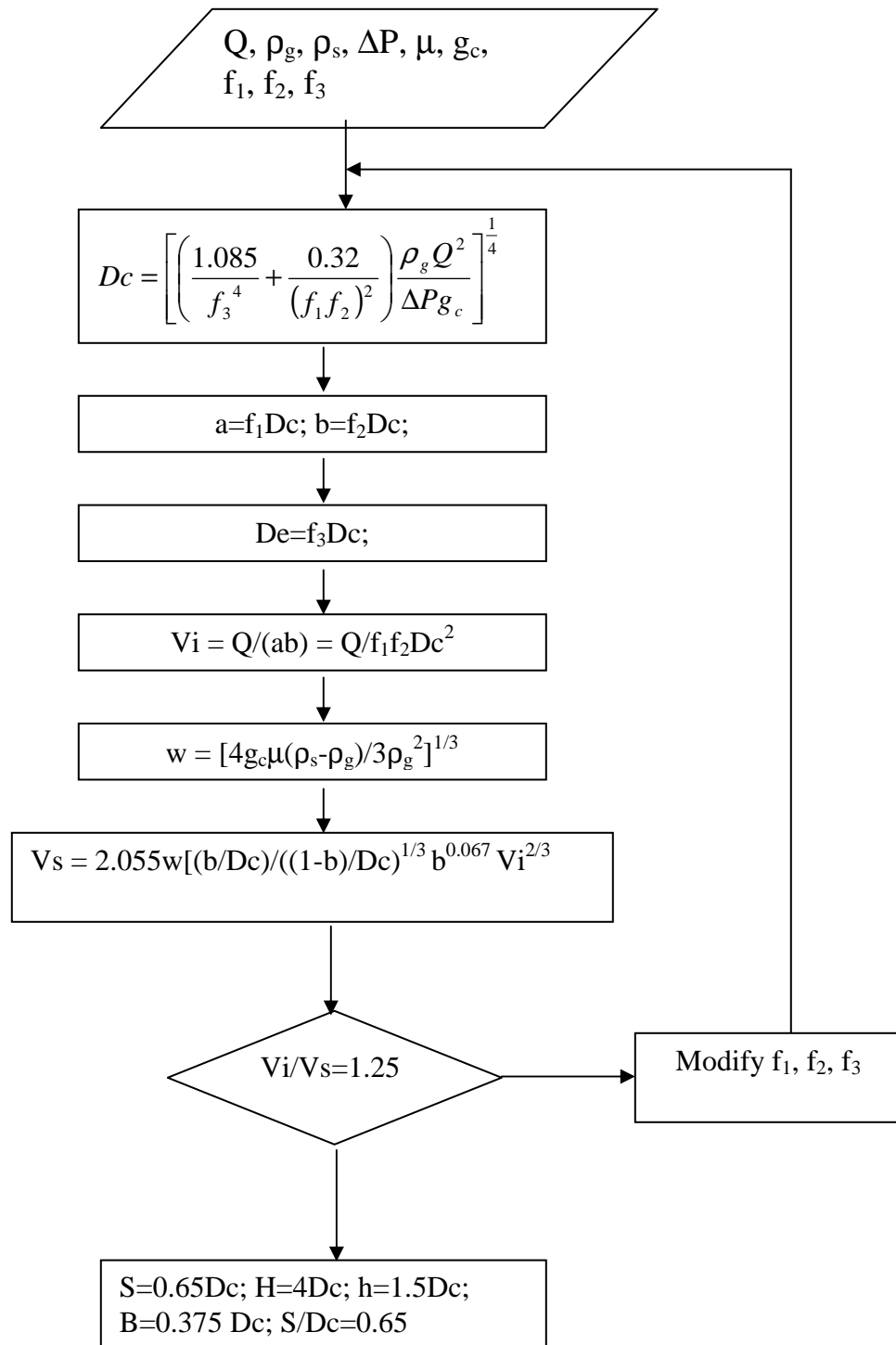
a	Inlet height, ft
B	Outlet diameter, ft
b	Inlet width, ft
Dc	Cyclone diameter., ft
De	Overflow outlet diameter, ft
Dg	Gas density, lbm/ft ³
DP	Cyclone pressure drop, in H ₂ O
Ds	Liquid-particles density, lbm/ft ³
f_1, f_2, f_3	Inlet height, width and outlet dia, factors, respectively.
G_c	Gravitational constant, ft/s ²
h	Cylinder height, ft
H	Overall height, ft
Q	Volumetric gas flow rate, ft ³ /s
S	Overflow outlet length, ft
u	Gas viscosity, lb/ft-s
V_i	Inlet velocity, ft/s
V_s	Saltation velocity, ft/s
w	Equivalent velocity, ft/s

Figure E.1 Dimensions of the separator

The actual dimensions for the separator used in the experimental setup are as follows:

Dimension	ft
a	0.019
B	0.024
b	0.019
Dc	0.062
De	0.019
h	0.144
H	0.271

E.4 Algorithm



APPENDIX F

TYPICAL OUTPUT GENERATED IN THE ESTIMATION OF PARAMETERS DEN_{σ} AND DEN_{τ} USING TWMARM AND TWINVE SUBROUTINES (MARQUARDT).

F.1 Output of the estimation. Experimental conditions: $T=330^{\circ}\text{C}$, $P=65.5$ bar and $W/F_{DBT}^0 = 1850$ $\text{kg}_{\text{cat}}\text{-h/kmol}$

USER SUPPLIED GUESS FOR ERROR COVARIANCE MATRIX

1.000D+00	0.000D+00	0.000D+00
0.000D+00	1.000D+00	0.000D+00
0.000D+00	0.000D+00	1.000D+00

INVERSE OF GUESS OF ERROR COVARIANCE MATRIX

1.000D+00	0.000D+00	0.000D+00
0.000D+00	1.000D+00	0.000D+00
0.000D+00	0.000D+00	1.000D+00

INITIAL SUM OF SQUARES 8.60803D-02
PRELIMINARY PARAMETER ESTIMATES
2.00000D+02 4.00000D+00

PRELIMINARY X-MATRICES

RESPONSE VERGELIJKING NR. 1

-1.120D-03	-2.261D-03
-1.200D-03	-2.422D-03

RESPONSE VERGELIJKING NR. 2

-9.346D-04	1.435D-02
-8.825D-04	2.772D-02

RESPONSE VERGELIJKING NR. 3

-1.825D-04	-1.640D-02
-3.095D-04	-2.943D-02

2.692D-06	5.436D-06
5.436D-06	1.098D-05

1.652D-06	-3.788D-05
-3.788D-05	9.744D-04

1.291D-07	1.210D-05
1.210D-05	1.135D-03

MATRIX SSSIJITXJ

4.474D-06 -2.034D-05
 -2.034D-05 2.120D-03

SCALING FACTORS E(I)

2.115D-03 4.605D-02

END OF MINIMISATION. RELATIVE CHANGE IN SUM OF SQUARES LESS THAN 1.0000D-06

6 ITERATIONS HAVE BEEN PERFORMED

FINAL PARAMETER ESTIMATES

4.20763395864D+02 3.25689744814D+00

FINAL MATRIX SSSIJITXJ

6.225D-07 -1.077D-06
 -1.077D-06 1.979D-03

DERIVATIVES OF THE SUM OF SQUARES FUNCTION WITH RESPECT TO THE PARAMETERS

-1.71092D-08 -2.99423D-08
 0LAMBDA= 1.562D-02 SUM OF SQUARES AFTER REGRESSION= 6.3924532D-04
 STEP= 1.00000D+00

INDEPENDENT VARIABLE NR. 1

1.000D+03 1.850D+03

OBSERVED VALUES OF RESPONSE VARIABLE NR. 1

2.093D-01 3.642D-01

OBSERVED VALUES OF RESPONSE VARIABLE NR. 2

1.548D-01 2.212D-01

OBSERVED VALUES OF RESPONSE VARIABLE NR. 3

6.540D-02 1.440D-01

CALCULATED VALUES OF RESPONSE VARIABLE NR. 1

2.281D-01 3.535D-01

CALCULATED VALUES OF RESPONSE VARIABLE NR. 2

1.619D-01 2.118D-01

CALCULATED VALUES OF RESPONSE VARIABLE NR. 3

6.544D-02 1.384D-01

RELIABILITY ANALYSIS

0 ANALYSIS OF VARIANCE TABLE

SOURCE		D.F.	MEAN SQUARE	F
TOTAL SUM OF SQUARES	0.27435376	6	0.45725627E-01	
SUM OF SQRS DUE TO REGRESSION	0.27150268	2	0.13575134E+00	0.8494E+03
RESIDUAL SUM OF SQUARES	0.63924532E-03	4	0.15981133E-03	
STANDARD DEVIATION =	0.12641651E-01			
CORRELATION COEFFICIENT =	0.98960800E+00			

UPDATED ESTIMATE OF ERROR COVARIANCE MATRIX

3.520D-04	1.750D-04	4.577D-05
1.750D-04	1.035D-04	3.999D-05
4.577D-05	3.999D-05	2.391D-05

ESTIMATED ERROR CORRELATION MATRIX

0.100D+01	0.917D+00	0.499D+00
0.917D+00	0.100D+01	0.804D+00
0.499D+00	0.804D+00	0.100D+01

INVERSE OF ESTIMATE OF ERROR COVARIANCE MATRIX

1.206D+19	-3.239D+19	3.109D+19
-3.239D+19	8.701D+19	-8.353D+19
3.109D+19	-8.353D+19	8.019D+19

COVARIANCE MATRIX OF PARAMETER ESTIMATES

2.095D-12	2.037D-15
2.037D-15	4.876D-18

BINARY CORRELATION COEFFICIENTS BETWEEN PARAMETER ESTIMATES

0.100D+01	0.637D+00
0.637D+00	0.100D+01

PAR NR	ESTIMATE	STANDARD DEVIATION	95%-CONFIDENCE LIMITS		T-VALUE
			LOWER	UPPER	
1	4.2076339586355994D+02	1.44736D-06	4.20763D+02	4.20763D+02	2.90710D+08
2	3.2568974481364035D+00	2.20815D-09	3.25690D+00	3.25690D+00	1.47494D+09

VITA

Luis Carlos Castañeda-Lopez was born in Parral Chihuahua, Mexico to Mr. Esteban Castaneda J. and Mrs. Maria Lopez S. He received a Bachelor of Science degree in Chemical Engineering from the Instituto Tecnológico de Chihuahua (ITCH), Mexico, in 1983, and he received his Master of Science in Petroleum Technology and Petrochemistry from Instituto Tecnológico de Madero, Tamps., Mexico in June 2000. He worked for Instituto Mexicano del Petróleo (IMP) for 18 years before obtaining an IMP scholarship to pursue his Ph.D. in Chemical Engineering at Texas A&M University.

The permanent address Mr. Castañeda-Lopez can be contacted is L. Cardenas M-7, L-17 Colonia Consejo Agrarista Mexicano, 09760, Iztapalapa Mexico, D.F., Mexico.